STRUCTURAL GEOMETRY OF THRUST FAULTING IN THE SUMMERFIELD AND LEFLORE SE 7.5-MINUTE QUADRANGLES, LEFLORE COUNTY, SE OKLAHOMA

BY

KRISTOPHER R. McPHAIL

Bachelor of Science
Oklahoma State University
Stillwater, Oklahoma
1998

Bachelor of Science
Oklahoma State University
Stillwater, Oklahoma
1999

Submitted to the Faculty of the
Graduate College of the
Oklahoma State University
in partial fulfillment of
the requirements for
the Degree of
MASTER OF SCIENCE
May, 2001

STRUCTURAL GEOMETRY OF THRUST FAULTING IN THE SUMMERFIELD AND LEFLORE SE 7.5-MINUTE QUADRANGLES, LEFLORE COUNTY, SE OKLAHOMA

Thesis Approved:

Ibrahim Cemen

Thesis Adviser

Zuhair al-Shaieb

Stanley T. Paxton

Dean of the Graduate College

ACKNOWLEDGEMENTS

I would like to extend thanks to my committee chair, Dr. Ibrahim Cemen, for his guidance, assistance and time throughout the coarse of this project. I would also like to think my other committee members, Dr. Al-Shaieb for his expertise and helpful hands, and to Dr. Stan Paxton for his unique way of approaching challenges in both geology and life. Special thanks to Dr. Jim Puckette for sharing his love for learning and helping me broaden my horizons in both school and career.

Thank you mother for all your support in this roller-coaster ride we call life. Your love has given me strength, always.

Thanks to my brothers, Kevin and Keith, and sister, Robin, for my perspectives on family and love for others.

To my lovely wife, Jennifer, thank you for all the sunsets. Your spirit, direction and loving support makes me a better man.

TABLE OF CONTENTS

LIST OF FIGURES

FIGURE PAGE

CHAPTER I

INTRODUCTION

The Arkoma Basin and Ouachita Mountains of southeastern Oklahoma and western Arkansas are a pair of genetically-related provinces created during the Late Paleozoic Ouachita Orogeny. The Arkoma Basin (Figure 1) is an elongate, foreland basin bound to the east by sediments of the Mississippi Embayment, to the west by the Arbuckle Mountains, to the northwest by the Cherokee Platform, to the northeast by the Ozark Uplift and to the south by the Ouachita Mountains (Johnson, 1988).

The Ouachita Mountains consist of three sub-provinces: the Frontal Ouachitas, the Central Ouachitas and the Broken Bow-Benton Uplift. The northernmost assemblage is the Frontal Ouachitas. This area is defined by imbricate thrust sheets contained between the Winding Stair Fault to the south and the Choctaw Fault to the north.

The Choctaw Fault has been defined as the structural boundary between the Ouachita Mountains and the Arkoma Basin. However, the

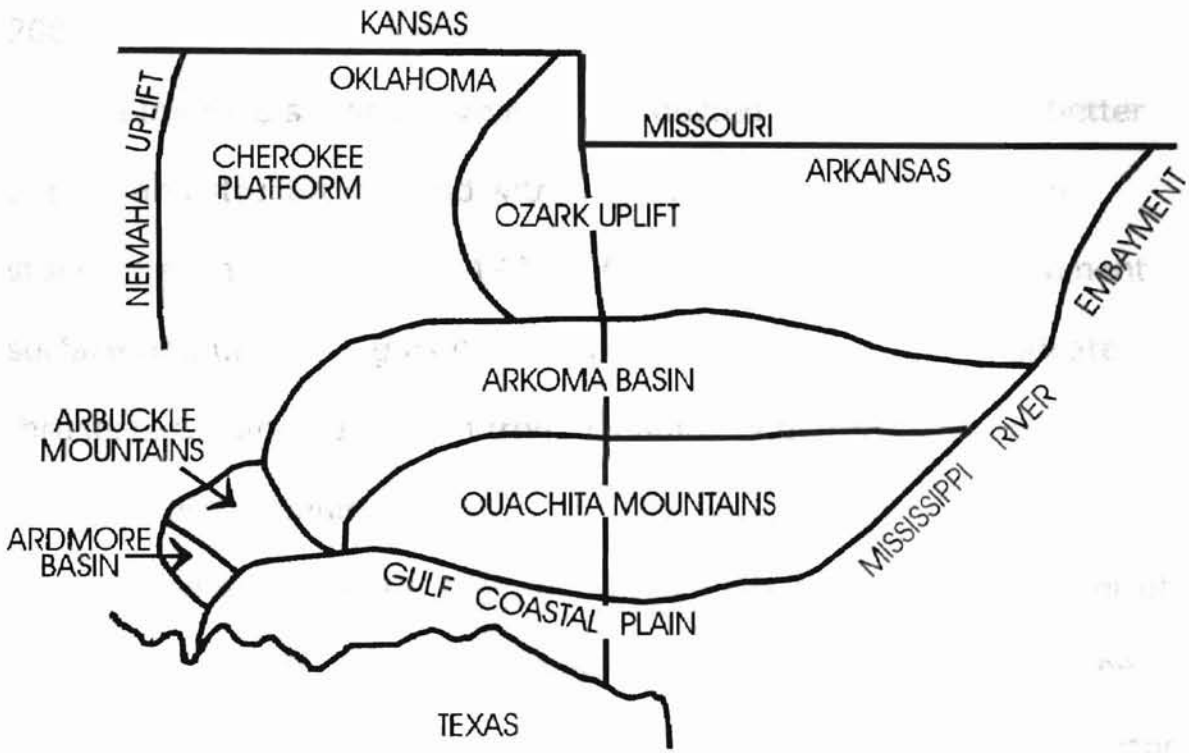

Figure 1. Major geologic provinces of eastern Oklahoma and western Arkansas. (Modified from Johnson, 1988)

overall change from one province to another is not abrupt. Imbricate thrust faults and tight to overturned folds characterize the dominant structures contained within the frontal Ouachitas. Whereas the Arkoma Basin contains broad, open folds with only minor evidence of faulting. The zone of gradation between these tectonic features is usually referred to as the transition zone (Cemen, Sagnak and Akthar, 2001).

Numerous studies have been conducted in this region to better understand structures found within this transition zone. Modern studies began with Arbenz (1984). His study revealed a decollement surface gradually rising as it propagated northward, blind imbricate thrusts extending basinward from a leading edge thrust and the presence of a triangle zone.

In the early 1990's, a project funded by the Oklahoma Center of Advancement of Science Technology (OCAST) began to evaluate the geometry of this triangle zone and underlying features in the Wilburton gas field area. Cemen and others (1994), Al-Shaieb and others (1995), Cemen and others (2001), and Cemen and others (in press) have delineated the Wilburton Triangle Zone from the Wilburton area extending past the Red Oak Field to the area adjacent to the Summerfield Quadrangle.

Statement of Purpose

The primary goal of this study is to delineate the structural geometry of the Late Paleozoic thrust system contained within the Arkoma Basin-Ouachita Mountain transition zone in Summerfield and LeFlore SE Quadrangles in LeFlore County, southeastern Oklahoma (T3N – T6N, R23E - R24E)(Figure 2). This includes:

1. defining and illustrating the main detachment surfaces;
2. depicting the structural geometry of thrust faulting along the frontal edge of the Ouachita fold-thrust belt;
3. establishing the geometry and structural position of the duplex contained within the footwall of the Choctaw fault zone;
4. determining the time constraints for the main structures;
5. characterizing the petrographic features of the lower Atokan Spiro sandstone, both in outcrop and subsurface; and
6. establishing the geometry of the Heavener anticline and Pine Mountain syncline and their spatial relationship with the Choctaw fault zone and underlying duplex structure.

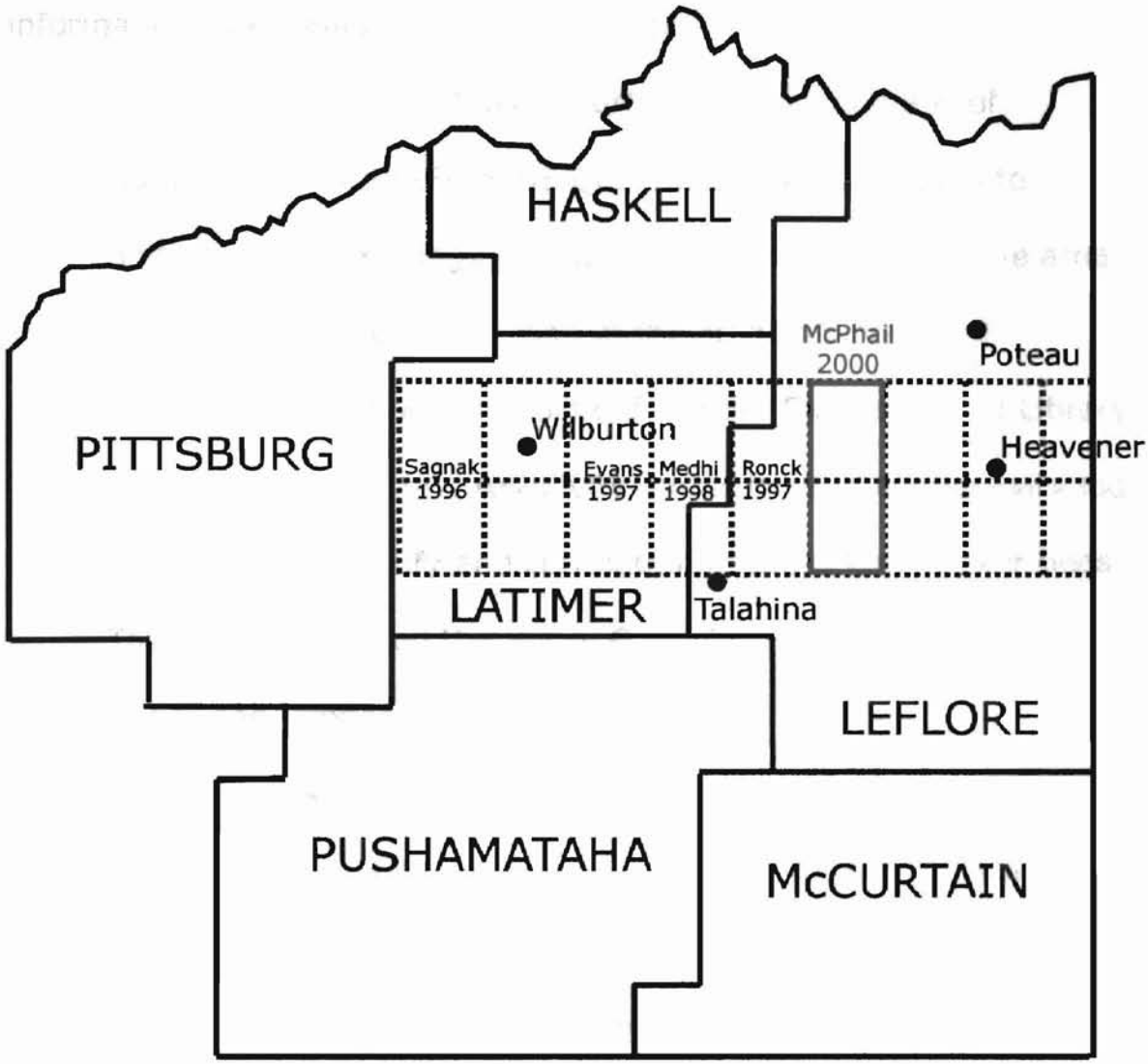

Figure 2. Location map of study area including southeastern Oklahoma counties and nearby towns.

Methodology

In order to accomplish the objectives stated above, the following information was compiled and integrated:

1. Oklahoma Geological Survey surface geological maps of Summerfield and LeFlore SE Quadrangles were studied to understand the geology and stratigraphic sequence of the area and a simplified geologic map of the area was prepared.
2. Wireline well logs were obtained from the Oklahoma Log Library in Tulsa. Gamma ray, resistivity, induction and conductivity logs were used to identify and correlate numerous key marker beds. These beds included the Spiro, Cecil, Brazil, Hartshorne and Booch sandstones.
3. Scout Tickets/Completion Cards were obtained from the Oklahoma Log Library and the Oklahoma State University Log Library and compared to wireline well log interpretations.
4. Reflection Seismic profiles donated by the former Amoco Production Company (now BP) were used to delineate major subsurface structural features.
5. Three balanced cross-sections were constructed in order to delineate structural geometry in the area.

6. Structural analysis of the Heavener anticline and Pine Mountain syncline was conducted using strike and dip data with programs such as RockWorks and GeoPlot.
7. Eleven thin-sections of the lower Atokan Spiro Sandstone, obtained from outcrop and core, were analyzed in order to delineate the petrographic signatures of hanging wall Spiro from footwall Spiro.

Incentives

Delineation of the structural features contained within the Summerfield and LeFlore SE Quadrangles has numerous implications to academia and industry alike. These include:

1. Delineation of eastward extent of structural features surrounding the Red Oak gas-field area
2. Determination of the presence and position of known hydrocarbon reservoirs such as the Spiro sandstone with regards to associated structural features (traps)
3. Explanation (full or partial) of why past drilling attempts were unsuccessful in deeper horizons within the area

CHAPTER II

GEOLOGIC SETTING

Introduction

The Arkoma Basin and Ouachita Mountains are tectonically related features that were created in the Early to Middle Pennsylvanian. The Arkoma Basin is one of seven major basins created during the Ouachita Orogeny. The other basins are Black Warrior, Sherman, Fort Worth, Kerr, Val Verda and Marfa. Now separated by basement uplifts, these foreland basins cover a distance spanning 1400 miles from eastern Alabama to Mexico (Meckel et al., 1992).

Numerous models have been created and debated with regards to the formation of the Ouachita orogenic belt. Morris, in 1974, suggested a northerly dipping subduction model, while others describe a subduction flip model (Roeder, 1973). However, the last 25 years have seen a convergence on the theory of a southerly-dipping subduction of an Atlantic-type continental margin beneath another land mass, be it an island arc, microcontinent, or a macrocontinent (Houseknecht, 1983). The later model is described below.

Tectonic Evolution of the Arkoma Basin and Ouachita Mountains

During the Late Precambrian-Early Cambrian, major rifting resulted in the creation of the proto-Atlantic (Iapetus) ocean basin along the southern margin of the North American Craton (Figure 3A). This rifting created a passive continental margin with a classic shelf-slope-rise geometry (Houseknecht, 1983). The depositional setting continued until the Middle Paleozoic (Figure 3B).

Sediments found on the shelf range in age from Cambrian to early Atokan. They consist of shallow water sandstones, shales and carbonates to the north and deepwater shales, sandstones, and carbonates to the south. Extensional faults were present during this time, allowing for an increase in accommodation space.

During the Late Devonian or Early Mississippian, a southerly dipping subduction zone began to consume oceanic crust under the southern landmass of Llanoria (Figure 3C). Evidence for this subduction zone is present within the Mississippian Stanley Formation, which includes volcaniclastics. South of the Ouachita province, other evidence includes Carboniferous volcanic rocks that are thought to be remnant vestiges of a magmatic arc complex (Houseknecht, 1986). The occurrence of these rock types suggest that the Ouachita

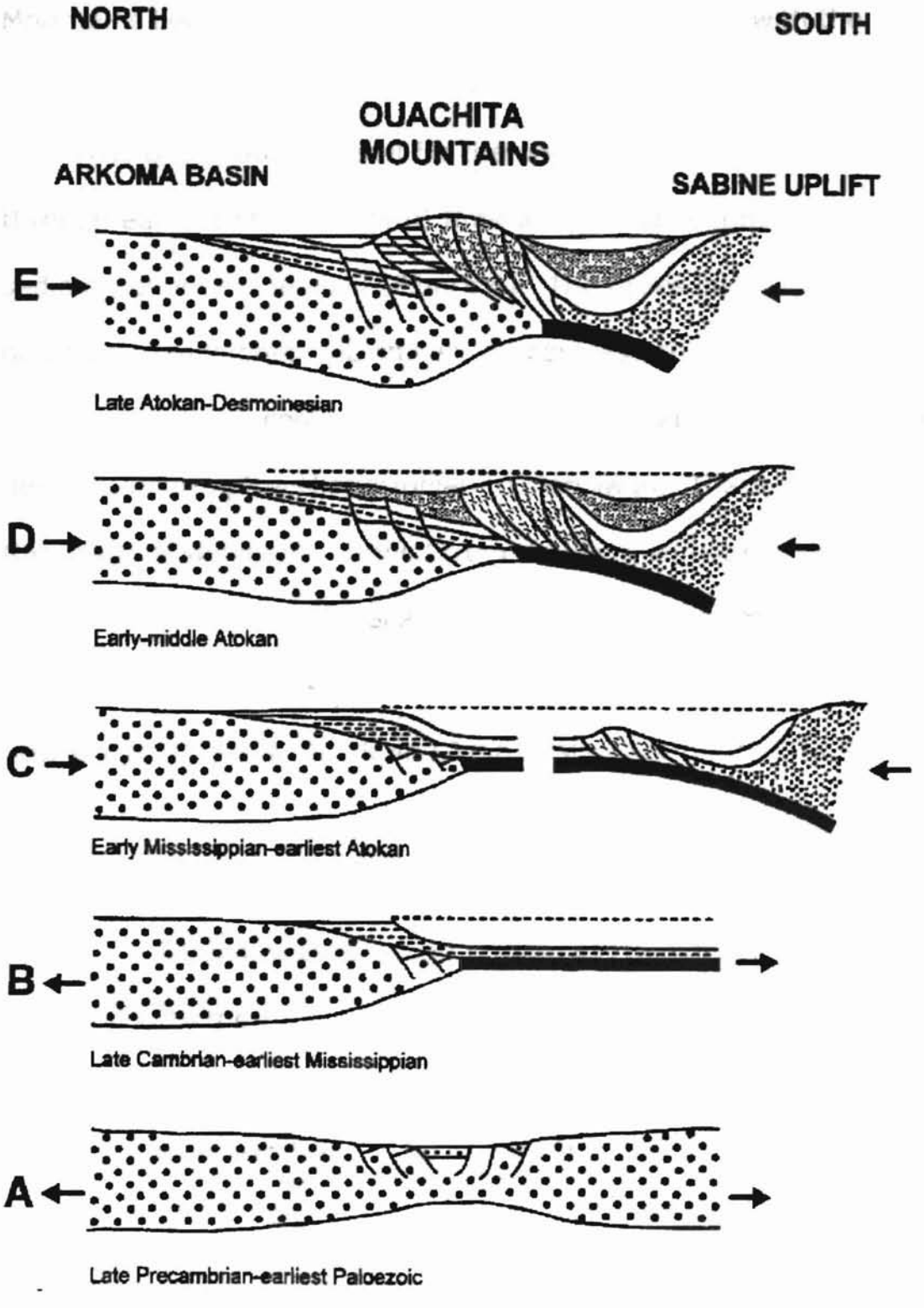

Figure 3. Tectonic model representing the evolution of the southern margin of the North America. (From Houseknecht, 1984)

Mountains began as an accretionary prism associated with the subduction complex along the northern margin of Llanoria.

The depositional model for the area during the Mississippian through earliest Atokan (Spiro) time was one of continued slow sedimentation on the shelf (Figure 4). The facies include carbonates, quartzose sandstones and shales. In contrast, the remnant ocean basin to the south contained relatively thick (5 km) flysch sediments deposited during the Mississippian to Morrowan. These deposits were the result of sediments derived from the east, where collision and uplift had already taken place (Figure 5). These sediments were then transported to the west and deposited in submarine fan complexes, now known as the Jackfork and Johns Valley Formation (Houseknecht, 1986).

After the deposition of the Spiro Sandstone, a dramatic change in the depositional setting began (Figure 6). Subduction in the area ceased due to the complete consumption of the remnant ocean basin and obduction of Llanoria had begun (Figure 3D). Obduction then created flexural bending on the 'stable' North American Craton, and created extensive basement-involved normal faulting (Ferguson and Suneson, 1988). These faults were primarily downthrown to the south and their overall trend paralleled that of the Ouachitas (Figure 7).

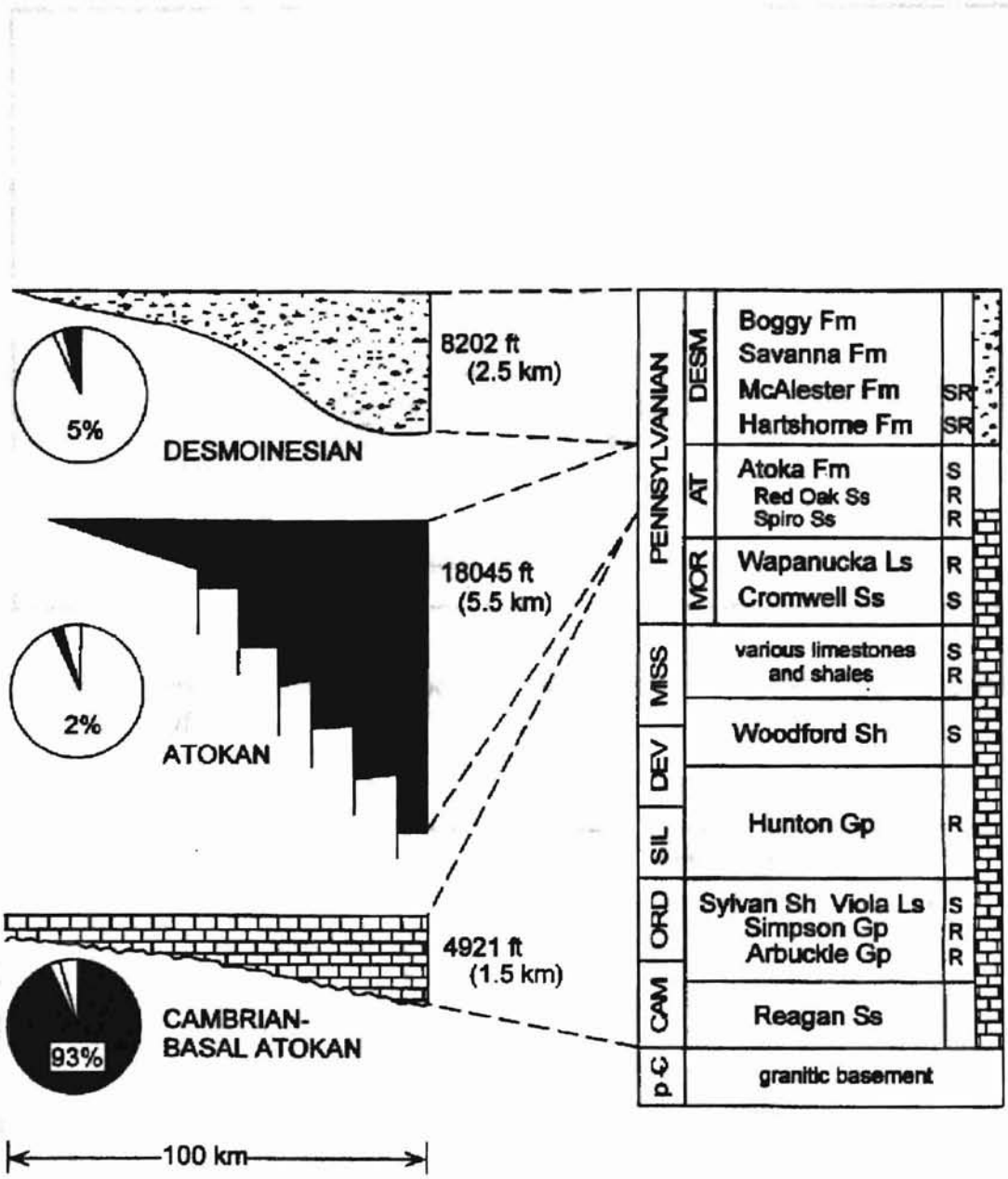

Figure 4. Stratigraphic framework of the Arkoma Basin with respect to total time of deposition during given time periods. (From Houseknecht and McGilvery, 1990)

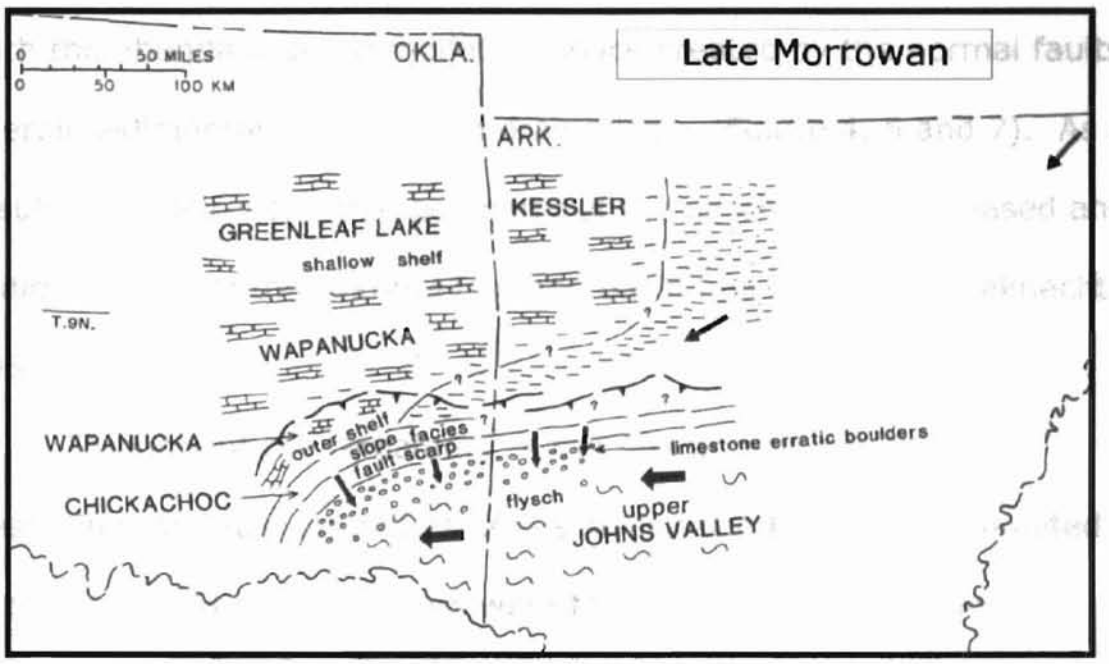

Figure 5. Late Morrowan depositional environment (from Sutherland, 1988).

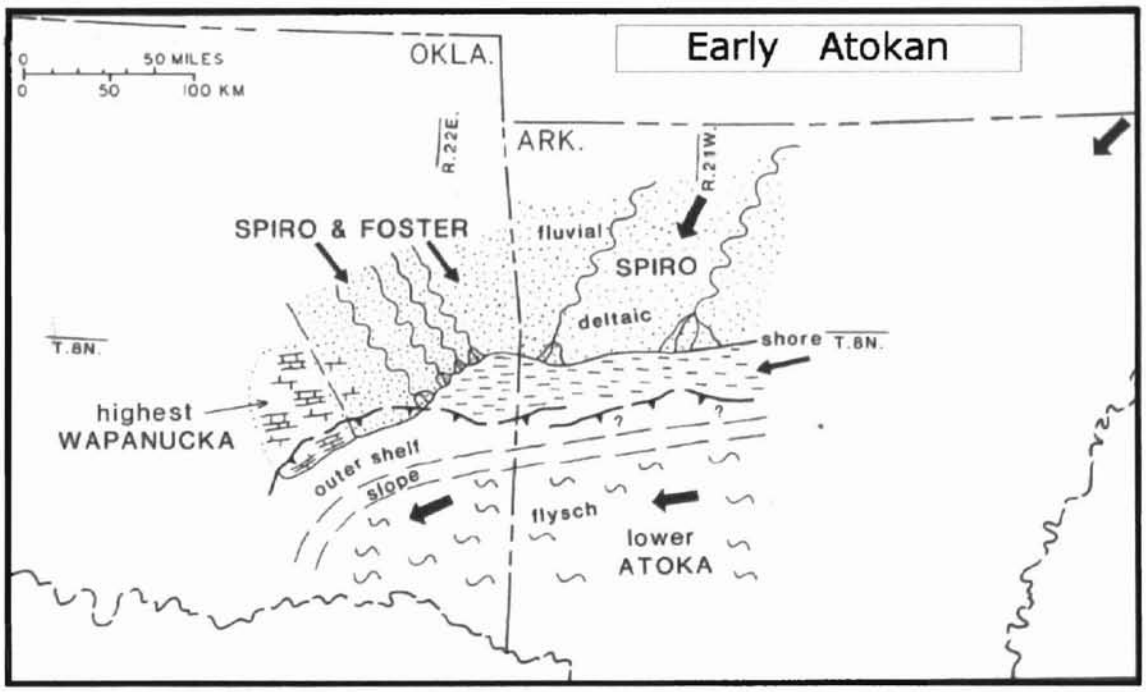

Figure 6. Early Atokan depositional environment (from Sutherland, 1988).

With the abundant accommodation space created by the normal faults, overall sedimentation increased dramatically (Figure 4, 6 and 7). As a result, the shelf-slope-rise geometry of the passive margin ceased and sedimentation of the Arkoma foreland basin had begun (Houseknecht, 1986).

Throughout the remainder of the Atokan and into the Desmoinseian, vast quantities of shales and sandstones accumulated in the basin. These sediments were the result of shallow marine, deltaic, and fluvial environments, which eventually filled the basin (Northcutt and Rottmann, 1995). Major deformation ceased in the Desmoinseian, leaving the subsurface units undisturbed through the present time.

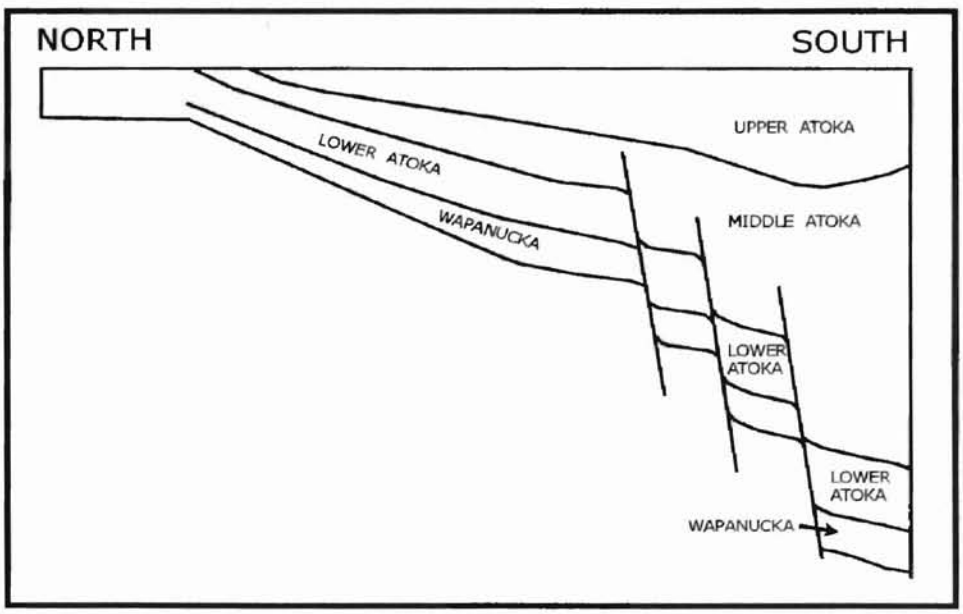

Figure 7. Diagram depicting syndepositional normal faults and their effects on surrounding units (from Sutherland, 1988).

CHAPTER III

STRATIGRAPHIC FRAMEWORK OF THE ARKOMA BASIN AND OUACHITA MOUNTAINS

The Arkoma Basin contains a thick assemblage of strata ranging in age from Cambrian to Pennsylvanian (Figure 8). The overall thickness within the basin increases to the south, with the overall thickness surpassing 25,000 feet in the transition zone of the Frontal Ouachitas. It is necessary to discuss the generalized framework of the area's stratigraphy in order to establish relationships between structural features and strata.

Proterozoic crystalline rocks comprise the basement of eastern Oklahoma (Figure 8). The modestly rugged surface of the basement is covered by the Cambrian Reagan Sandstone of the Timber Hills Group. This time-transgressive unit was deposited across much of the area, with the exception of local, topographic "highs" (Johnson, 1988). Completing the Timber Hills Group is the Honey Creek Limestone, which is the first in a series of shallow water-carbonates.

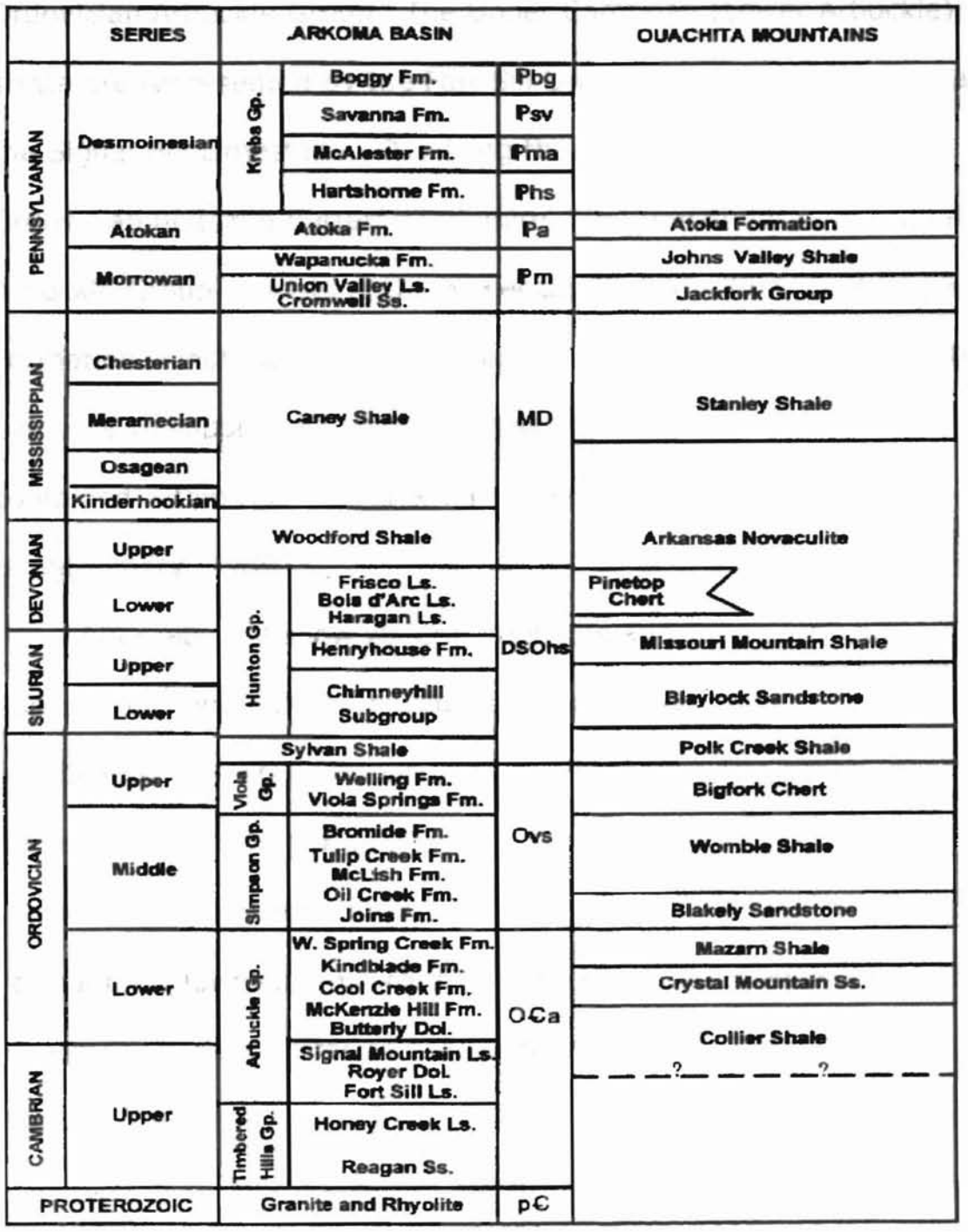

Figure 8. Stratigraphic chart for the Arkoma Basin and Ouachita Mountains provinces. (From Johnson, 1988)

Conformably overlying the Timber Hills Group is the Cambro-Ordovician Arbuckle Group. The Upper Cambrian (Lower Arbuckle) strata are represented by the Fort Sill Limestone, Royer Dolomite, and the Signal Hill Limestone. Overlying these limestones is the first Ordovician unit, the Butterfly Dolomite. The remainder of the Upper Arbuckle Group consists of the McKenzie Hill Formation, Cool Creek Formation, Kindblade Formation and the West Spring Creek Formation. Evidence to support the shallow water origin includes evaporites contained within the Cool Creek and West Spring Formations (Montgomery, 1989).

Alternating shallow water carbonates and sands continued to be deposited throughout the Middle and Upper Ordovician. Overlying the Arbuckle Group is the Simpson Group (Figure 8). The carbonate units present, in ascending order, are the Joins Formation, Oil Creek Formation, McLish Formation, Tulip Creek Formation and the Bromide Formation. However, toward their deep basin facies equivalents, these limestones undergo a facies change to the Blakely Sandstone and Womble Shale.

The Viola Group conformable overlies the Simpson (Figure 8). It is comprised of the Viola Springs Formation and the Willing Formation. These formations contain numerous limestone facies, which include nodular chert-rich packstones, mudstones, porous grainstones,

wackestones and some dolomitized wackestones (Sikes, 1995). Unconformably overlying the Viola Group is the Upper Ordovician Sylvan Shale, which is a gray to green shale with well-developed laminations. This unit appears to mark a high point of marine incursion (Montgomery, 1989).

Following in stratigraphic succession is the conformable Lower Silurian to Lower Devonian Hunton Group (Figure 8). Within the basin, an oolitic bed marks the base (Montgomery, 1989) of the Chimneyhill Subgroup. Completing the Hunton group, in ascending order, is the Henryhouse Formation, Haragan Limestone, Bois d'Arc Limestone and the Frisco Limestone.

Following the deposition of the Frisco, an extensive erosional period occurred before the deposition of the overlying Woodford Shale. The Woodford is primarily a black, pyritic, chert-bearing shale that ranges in thickness from 150 to 250 feet within the basin.

The Mississippian Caney Shale conformably overlies the Woodford. It is Chesterian in age, based upon macrofossils taken from isolated exposures (Southerland, 1979). Deposited above the Caney is the informal Springer Shale. Depending on the source, it ranges in age from Chesterian (Ham, 1978) to Morrowan (Southerland, 1979).

Shallow, shelf-like sedimentation continued into the Pennsylvanian (Morrowan). However, there was an abundant increase

in sand content within the facies (Johnson, 1988). Within the basin, overall thickness of Morrowan strata ranges from a few hundred feet in the north to about a thousand feet on the southern margin. At this margin, the units grade into flysch sediments up to 6000 feet thick in the Ouachita trough. In ascending order, Morrowan units in the Arkoma Basin are the Cromwell Sandstone, Union Valley Limestone and the Wapanucka Limestone. Their correlatable units in the Ouachita Mountains are the Jackfork Group and Johns Valley Shale (Figure 8).

Overlying the Wapanucka Formation is the Atokan Formation (Figure 9). Total thickness of the Atokan Formation increases to the south, and along the southern edge of the Arkoma Basin it exceeds 18,000 feet (Houseknecht and McGilvery, 1990). The Atokan Formation is about seventy percent shale (Johnson, 1988) and can be subdivided into three major units: Lower, Middle and Upper Atokan. These distinctions are based on the effects of syndepositional normal faults within the basin (Johnson, 1988). The remainder of the lithologies found within the Atokan are sandstones, siltstones and thin coal beds.

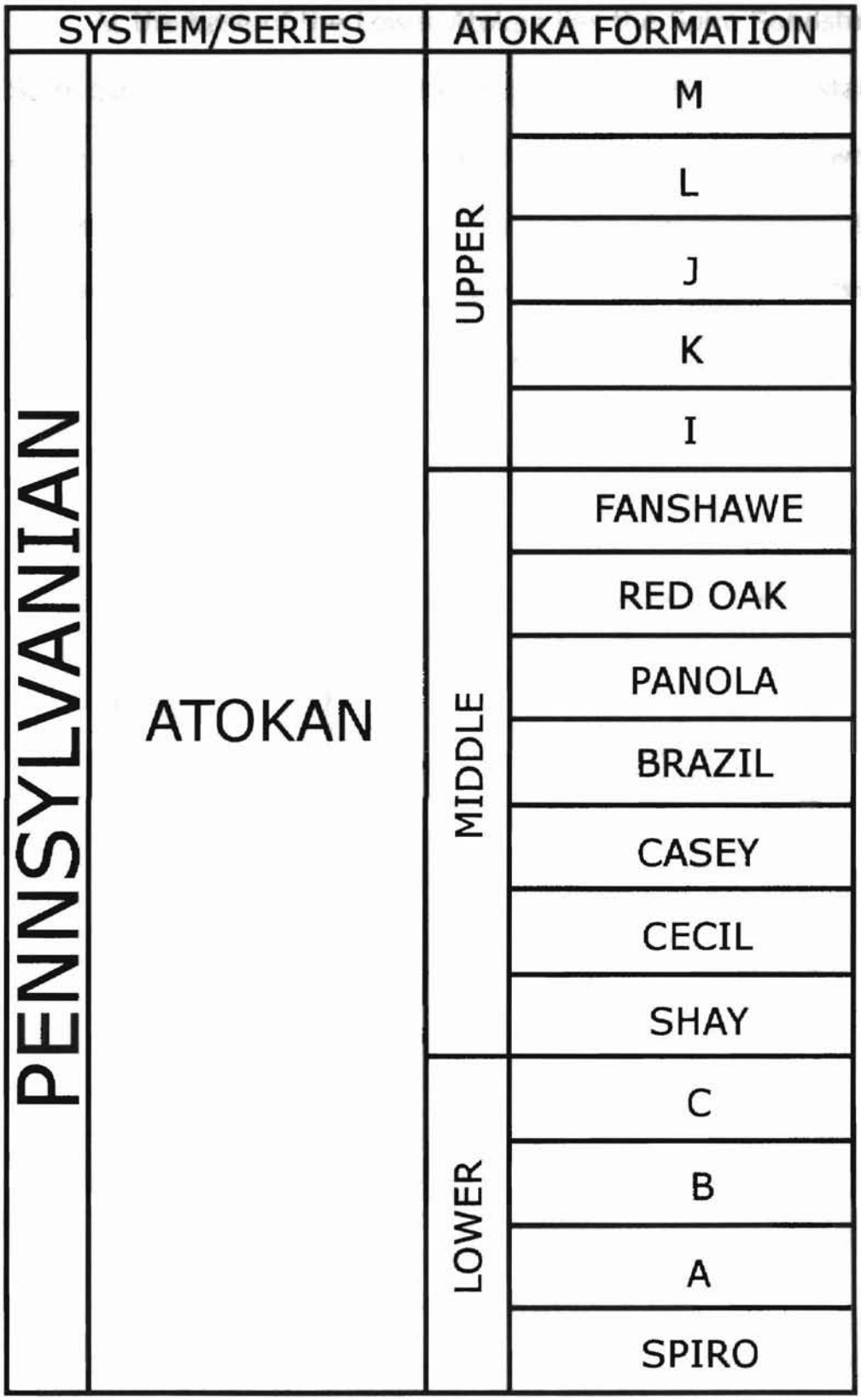

Figure 9. Stratigraphic chart of Atokan strata, Arkoma Basin.

At the base of the Lower Atokan lies the Spiro Sandstone. The Spiro Sandstone represents the final element of the long stable shelf along the southern margin of the North American Craton, which had persisted since the Cambrian (Houseknecht and McGilvery, 1990). A detailed analysis of its lithology and depositional history follows in Chapter 4. A representative log signature can be seen in Figure 10.

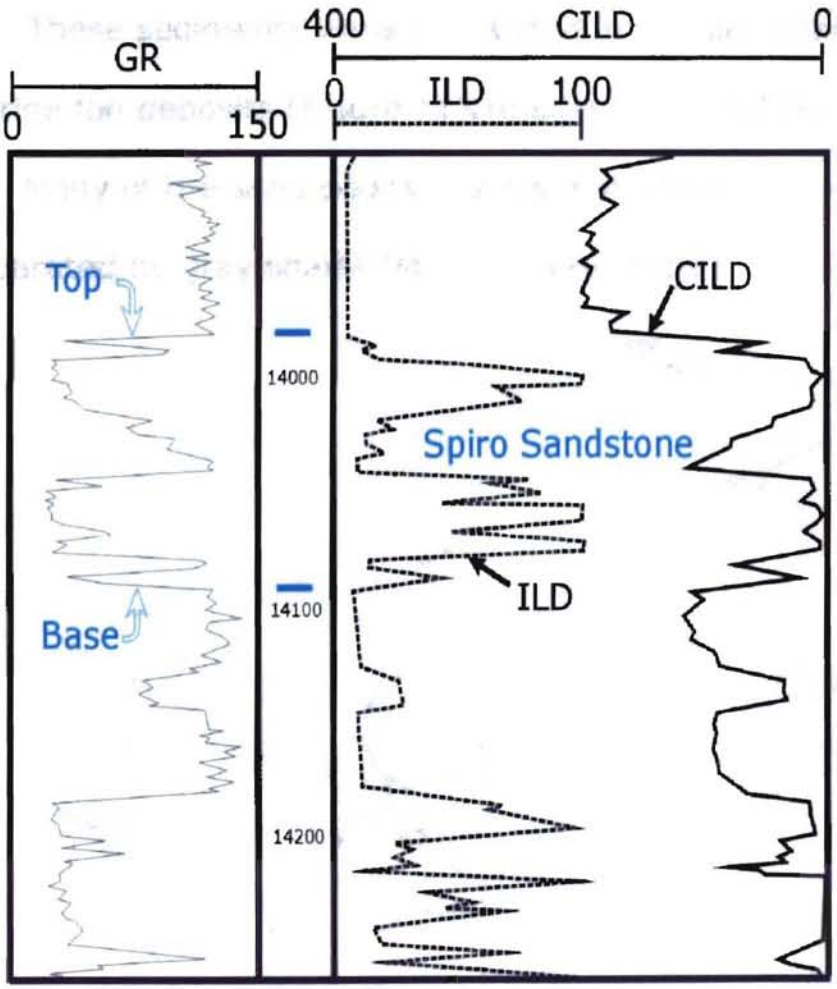

Figure 10. Log signature of Spiro Sandstone. (AnSon Corporation, #1-21 Nevil, Sec. 21, T5N, R23E)

Following the deposition of the Lower Atokan (Spiro) units, the depositional environment changed from the stable shelf into a tectonically active foredeep (Houseknecht and McGilvery, 1990). Sedimentation rates increased dramatically, with sediments primarily originating from the emerging eastern portions of the Ouachita orogenic belt. Syndepositional normal faults within the area show a substantial increase in bed thickness in the southerly, downthrown blocks. These sediments were distributed in deltaic, slope and submarine fan deposits (Figure 11)(Houseknecht and McGilvery, 1990). Many of the sand deposits show a shoestring geometry and are separated by gray shales (Montgomery, 1989).

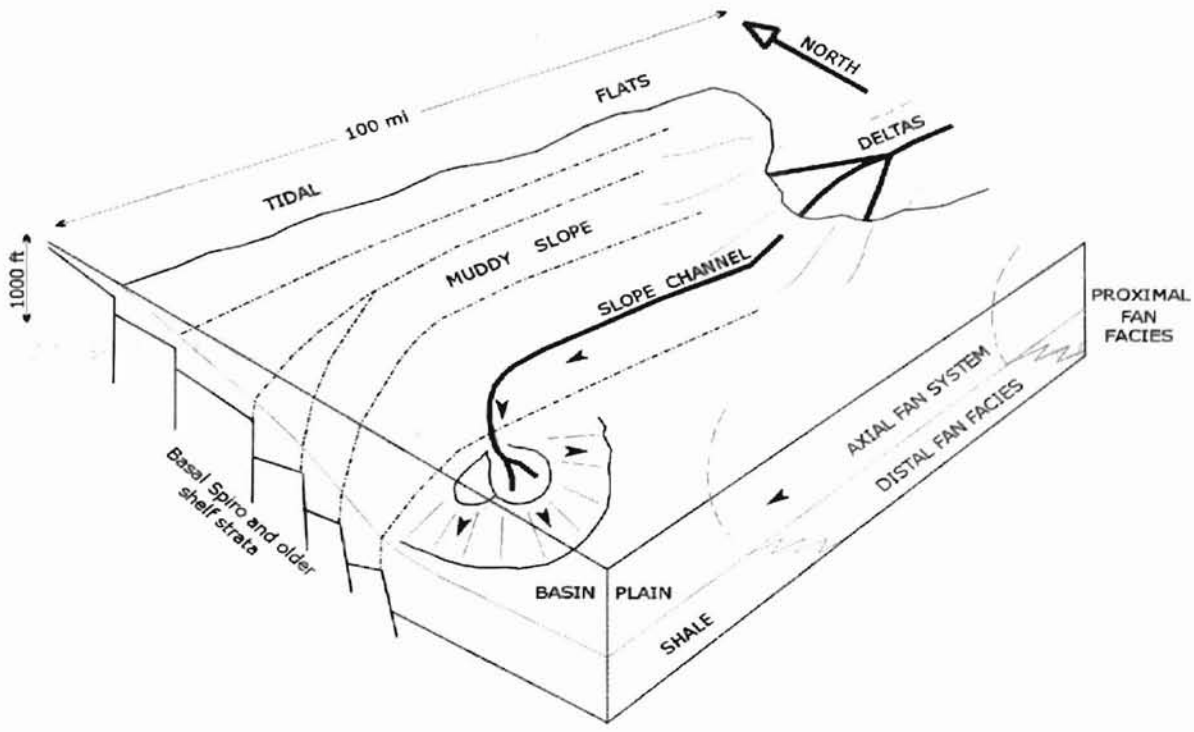

Figure 11. Depositional reconstruction of Atokan strata in Arkoma Basin. (Modified from Houseknecht, 1986)

The middle Atokan sandstones include the Shay, Cecil, Brazil, Panola, Red Oak and Fanshawe. Well-log signatures of the Cecil are represented in Figure 12. Within this area, numerous wells penetrated two Cecil horizons. Both Cecil A and Cecil B are comprised of thin sand bodies intermixed with shale. Figure 13 illustrates the typical log signature of the Brazil. Overall thickness of the Brazil is approximately 900 feet within the area. Thick accumulations of sand can be found within the Brazil, however, most sand bodies are relatively thin and intertwined by shales.

For correlation purposes, Marker Y was used when previously listed signatures, primarily Red Oak, were undetectable. The stratigraphic position of Marker A is in such a place to represent parts or all of the Panola, Red Oak and Fanshawe Sandstones. A log signature of Marker Y is shown in Figure 14.

The Upper Atokan Strata is comprised primarily of shales and a few small, discontinuous sandstone bodies. The prevailing growth faults in the Middle Atokan do not appear to be present in the Upper Atokan. If faulting was present, dewatering and compaction of underlying shales could have absorbed any significant displacement. As a result, the Upper Atokan appears virtually unfaulted (Southerland 1988).

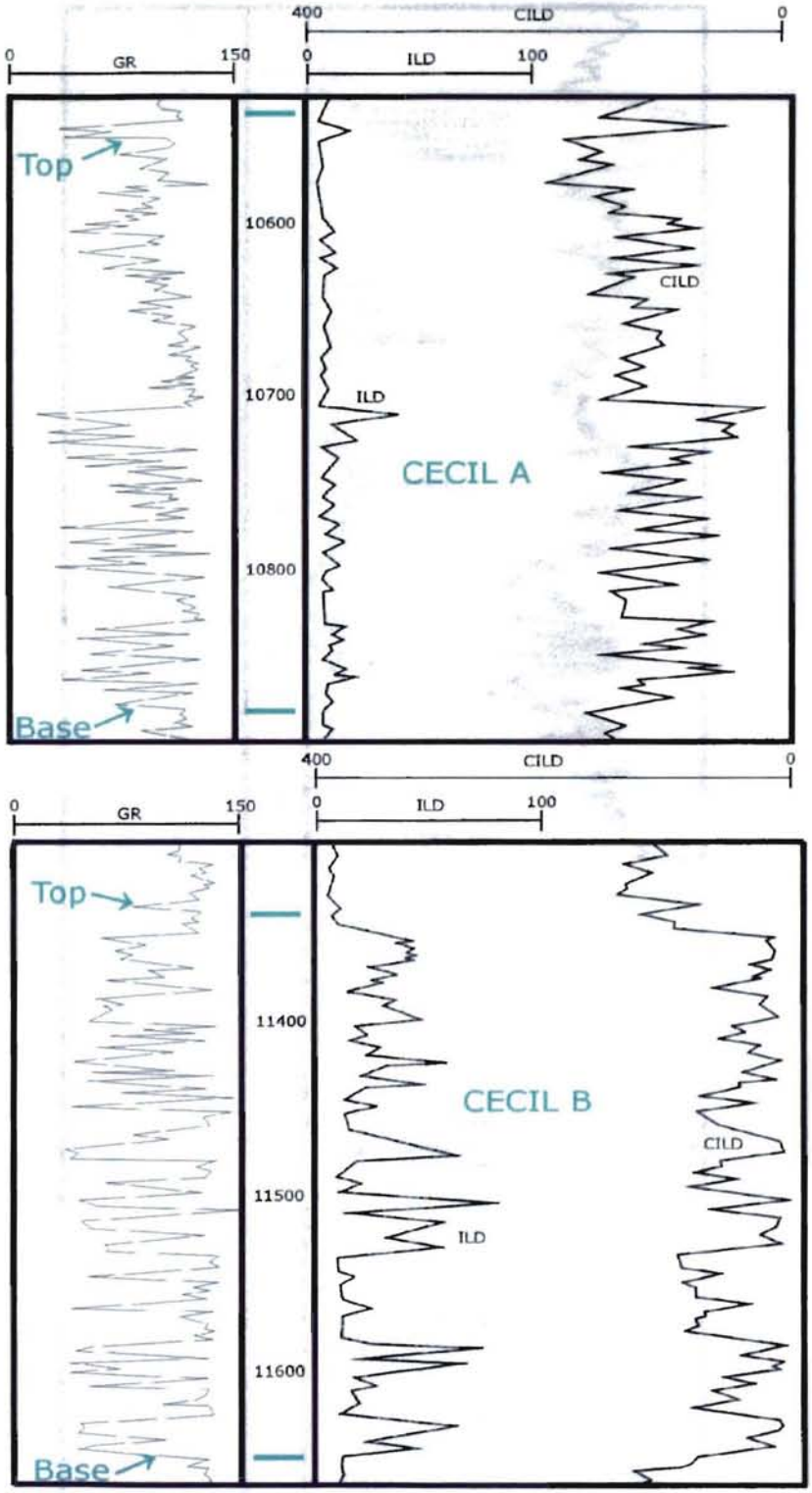

Figure 12. Log signature of Cecil A (Top) and Cecil B (Bottom) from JV-P Hollan #1 (Sec. 20, 5N, 23E).

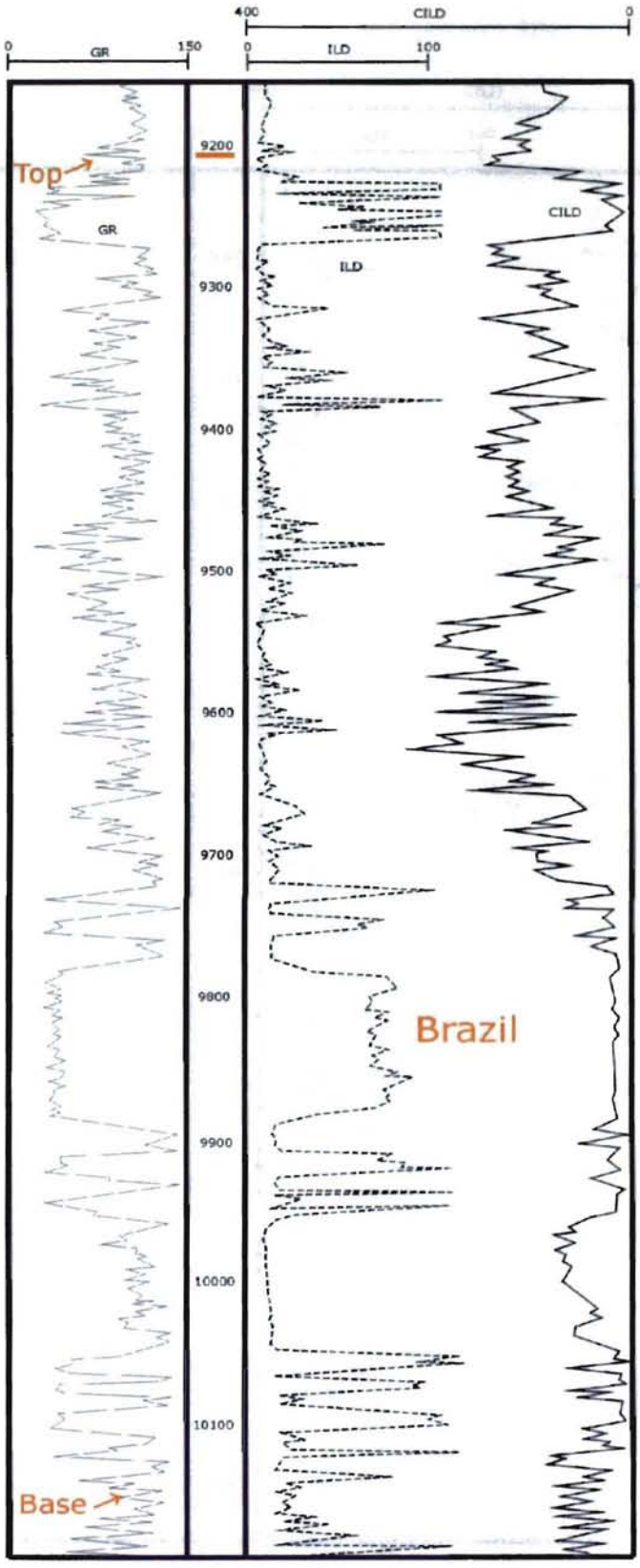

Figure 13. Log signature of Brazil Sandstone from Buttrill No. 1-34 (Sec. 34, T6N, R23E)

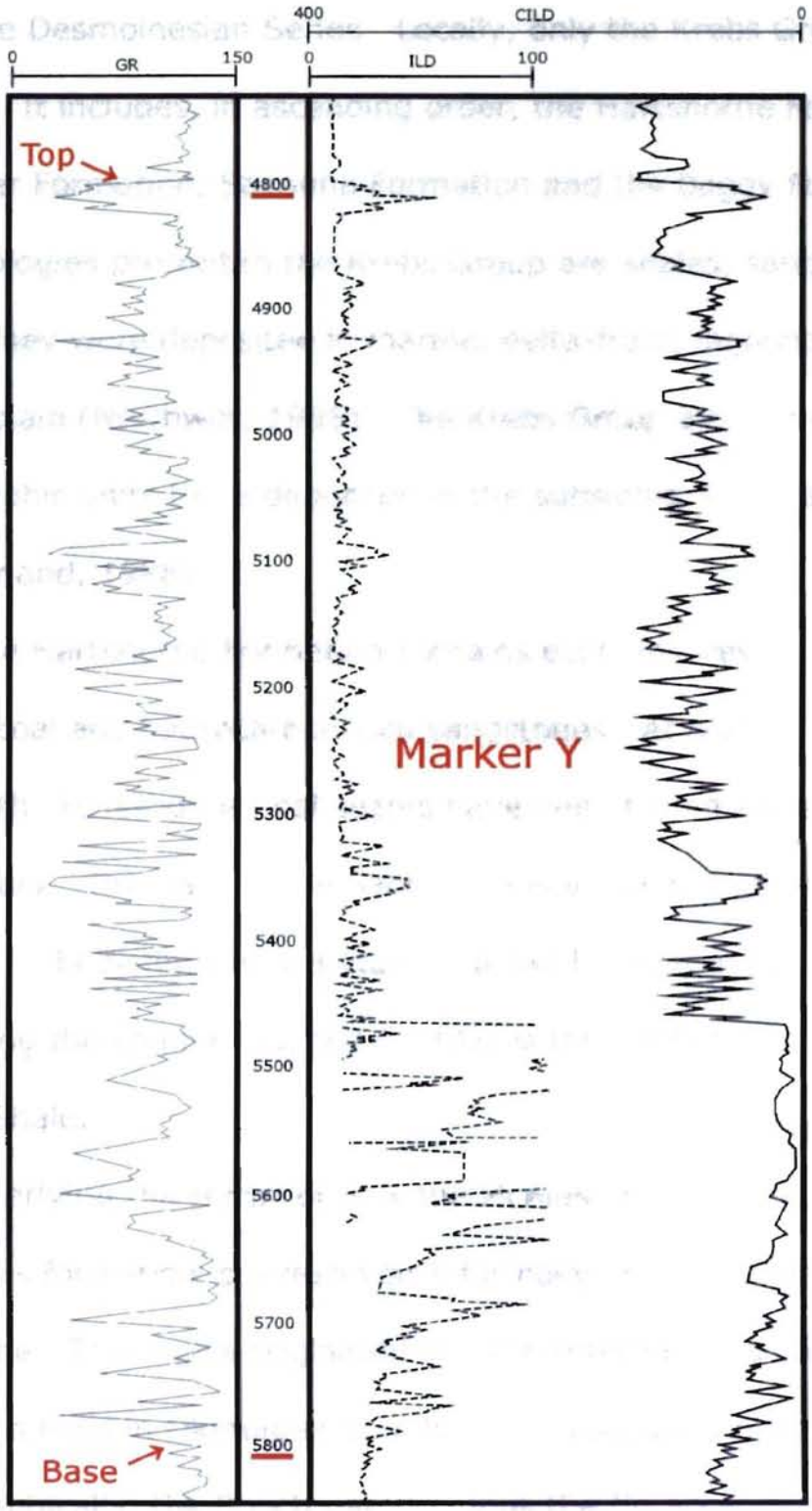

Figure 14. Representative log of Marker Y from U.S.A. Unit #1 (Sec. 7, T5N, R24E).

The youngest rock units found within this area of the Arkoma Basin are Desmoinesian Series. Locally, only the Krebs Group is present. It includes, in ascending order, the Hartshorne Formation, McAlester Formation, Savanna Formation and the Boggy Formation. The lithologies present in the Krebs Group are shales, sandstones and coals. They were deposited in marine, delta-front, lagoonal, and coastal plain (Northwitt, 1995). The Krebs Group also signifies the last stratigraphic units to be deposited in the subsiding Arkoma Basin (Southerland, 1988).

The Hartshorne Formation contains economic resources in the form of coal and hydrocarbon-rich sandstones. At surficial and shallow depths, the Hartshorne Coal seams have been mined since the turn of the century. The Hartshorne Sandstone is an oil and gas producing reservoir. Its distinctive signature and can be seen in Figure 15. Underlying the channel deposit (-4492) is the contact of the Upper Atokan Shale.

Overlying the Hartshorne is the McAlester Formation. Contained within this formation is a reservoir informally known as the Booch Sandstone. This name originated in 1906 referring to a sand unit in the Morris Field in Okmulgee County (Northcutt and Rottmann, 1995). Stratigraphically, the Booch name groups the (in ascending order) Warner, Lequire, Cameron, Tamaha and Keota Sandstones into the

Lower, Middle and Upper Booch. Attempts to correlate these subsurface units to the surface have been unsuccessful at best. This is partially due to the discontinuous nature of the unit. Due to the fluvial-deltaic nature of the Booch, some areas contain only one sand body, while other areas contain three or more. In this area, one to two distinctive sand bodies have been identified. Figure 16 shows a typical log signature of the Upper and Lower Booch.

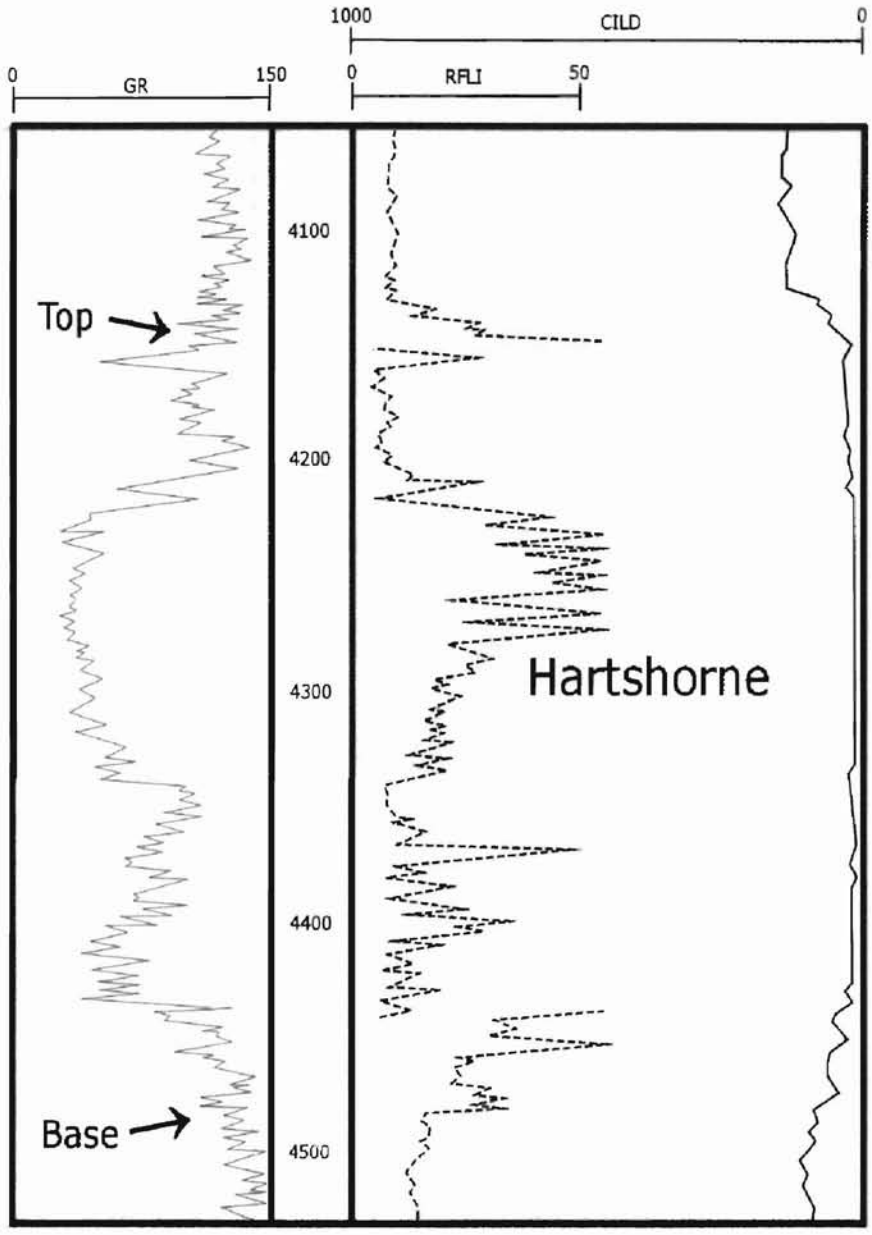

Figure 15. Representative log signature of the Hartshorne Sandstone from J.L. Sheffler Ranch #1 (Sec. 14, T6N, R23E).

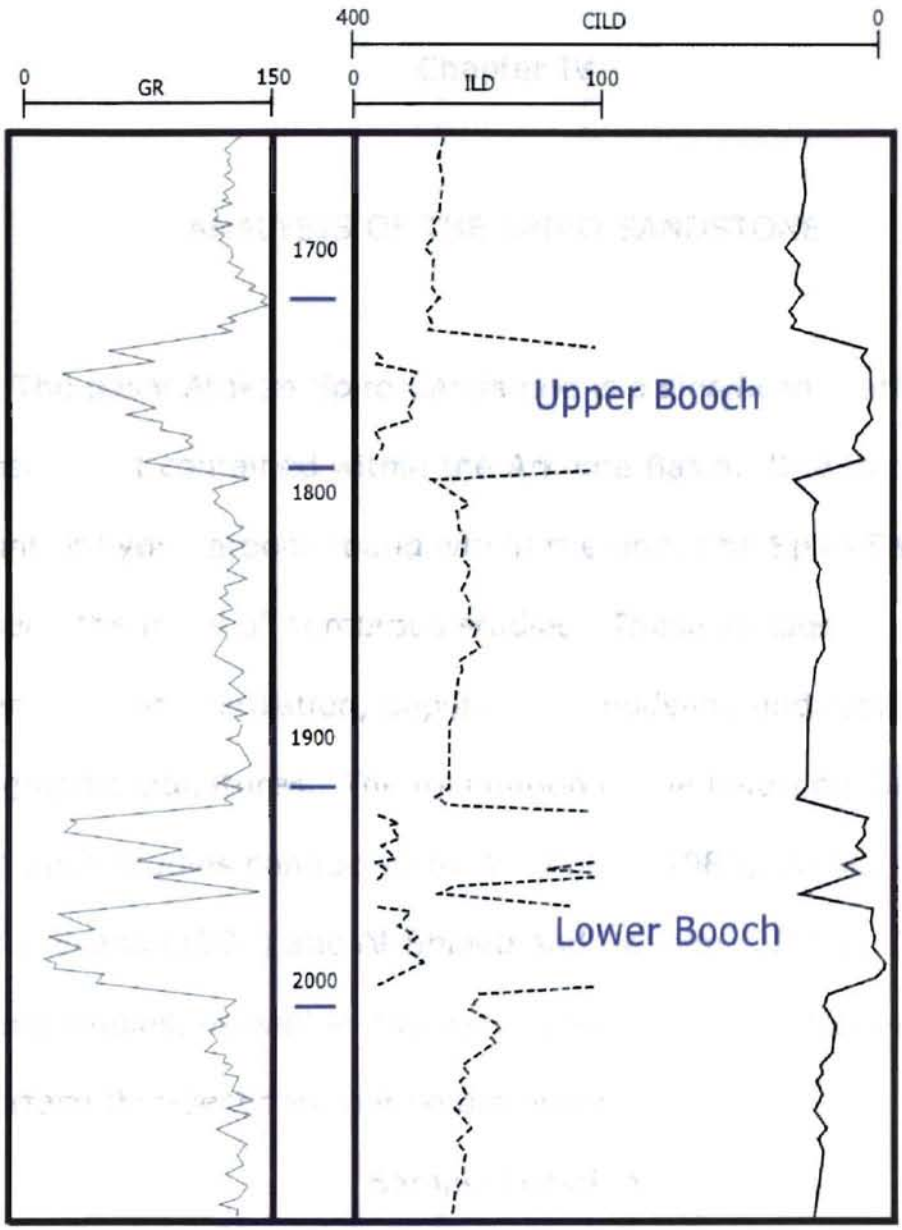

Figure 16. Representative log signature of the Upper and Lower Booch Sandstones from LeFlore #1-27A (Sec. 27, T6N, R23E).

Chapter IV

ANALYSIS OF THE SPIRO SANDSTONE

The basal Atokan Spiro Sandstone is a significant, laterally extensive unit contained within the Arkoma Basin. Due to the vast amount of hydrocarbons found within the unit, The Spiro Sandstone has been the focus of numerous studies. These studies include diagenetic characterization, depositional modeling and type casting of petrographic signatures. The foundation of the following discussion is based upon studies conducted by Al-Shaieb (1989), Al-Shaieb et al. (1994), Evans (1997) and Al-Shaieb and Deyhim (2000). The results of these studies, as well as the data collected from surface and subsurface thin-sections, will be discussed.

Sample Location

Samples of overthrusted, hanging wall Spiro were taken from an outcrop one-half mile south of the town of Red Oak in Latimer County, along State Highway 82 in Section 23, section 5 North, Range 21 East (Figure 17). Here the Spiro is observed to be overturned and steeply dipping to the south. The underlying Sub-Spiro shale and sand can

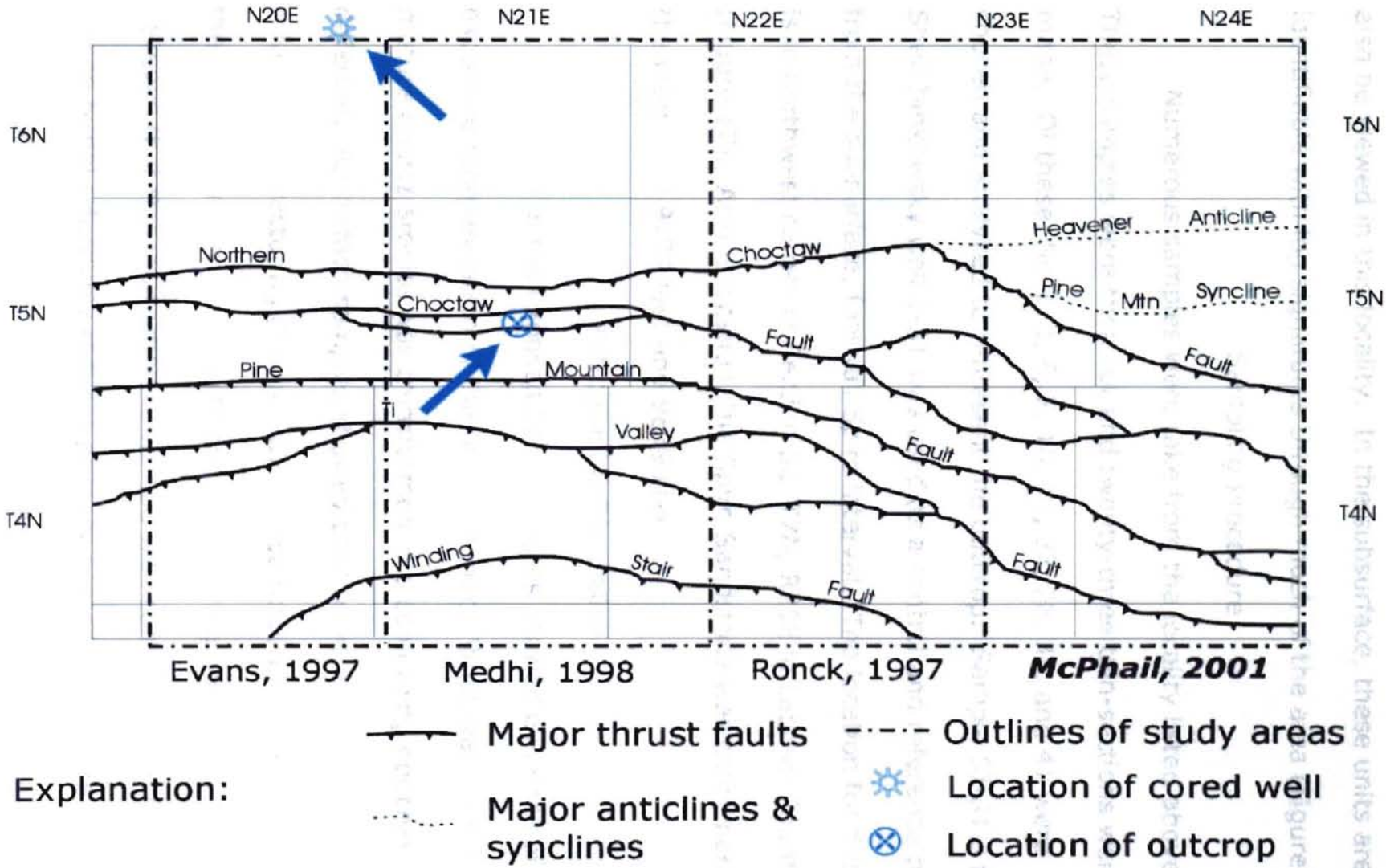

Figure 17. Regional base map depicting core and outcrop locations.

also be viewed in this locality. In the subsurface, these units are identifiable with log signatures through much of the area (Figure 10).

Sampling Procedure

Numerous samples were take from the locality listed above. These samples were then cut and twenty-three thin-sections were made. Of these, Sp-1, 3, 6, 7, 10, 11, 23, 28, 38, and 41 were chosen and analyzed to represent the outcrop. Sample SJ-31.3 from Shell Jankowsky well 1-31 was used as a control and reference point from the subsurface, footwall Spiro interval. The location for this well is in northwest corner of Section 32, T7N, R20E in Latimer County (Figure 17). At this location, the Spiro Sandstone was cored between the interval of 9799 feet and 9839 feet.

Petrographic Discussion

Analysis of the exposed Spiro samples showed evidence of extensive reorganization of the original fabric. What was once a mature quartz arenite was transformed into something noticeably different. All surface samples showed conclusive evidence of grain rotation and fracturing (Figure 18). These features were obtained by the units interaction with faults and folds during thrusting. It is also believed that this interaction combined with compressional forces during burial effectively reduces primary porosity by ductile deformation of malleable grains. As a whole, the composition of the

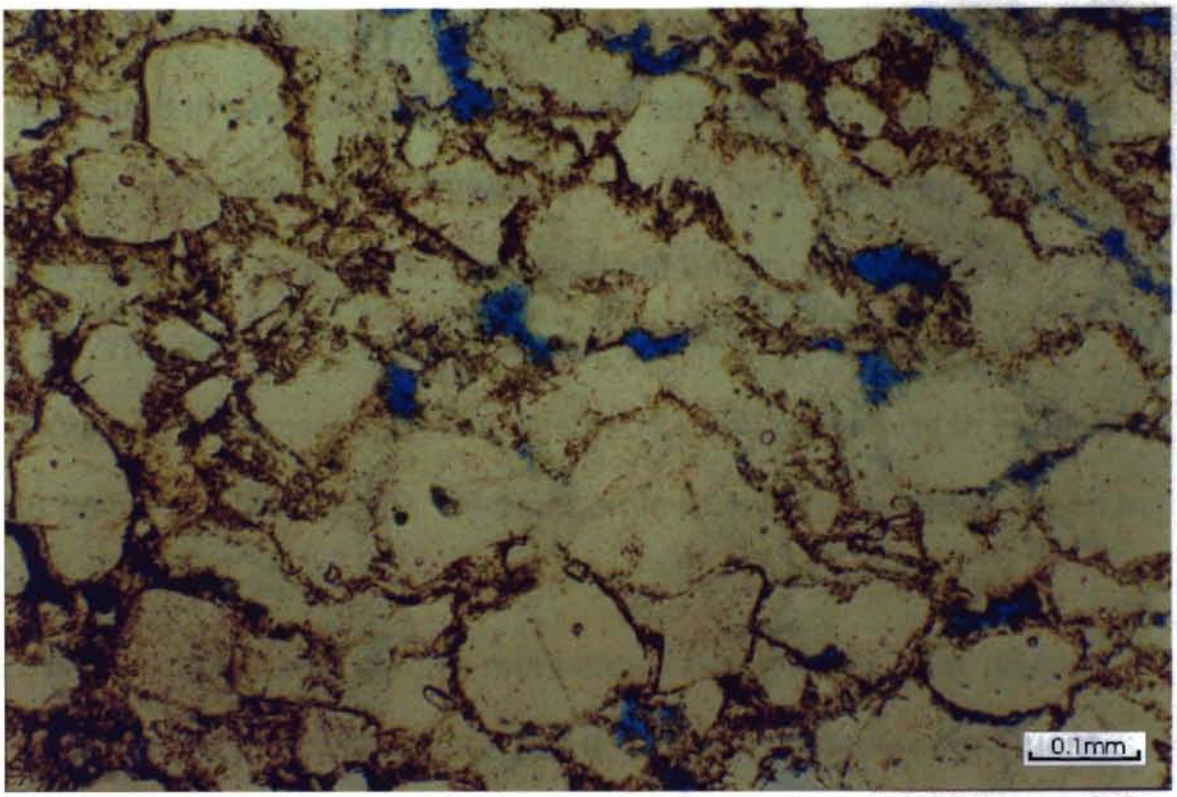

Figure 18. Photomicrograph showing grain rotation, fracturing and the abundant hematite staining between grains. (10x-PPL)

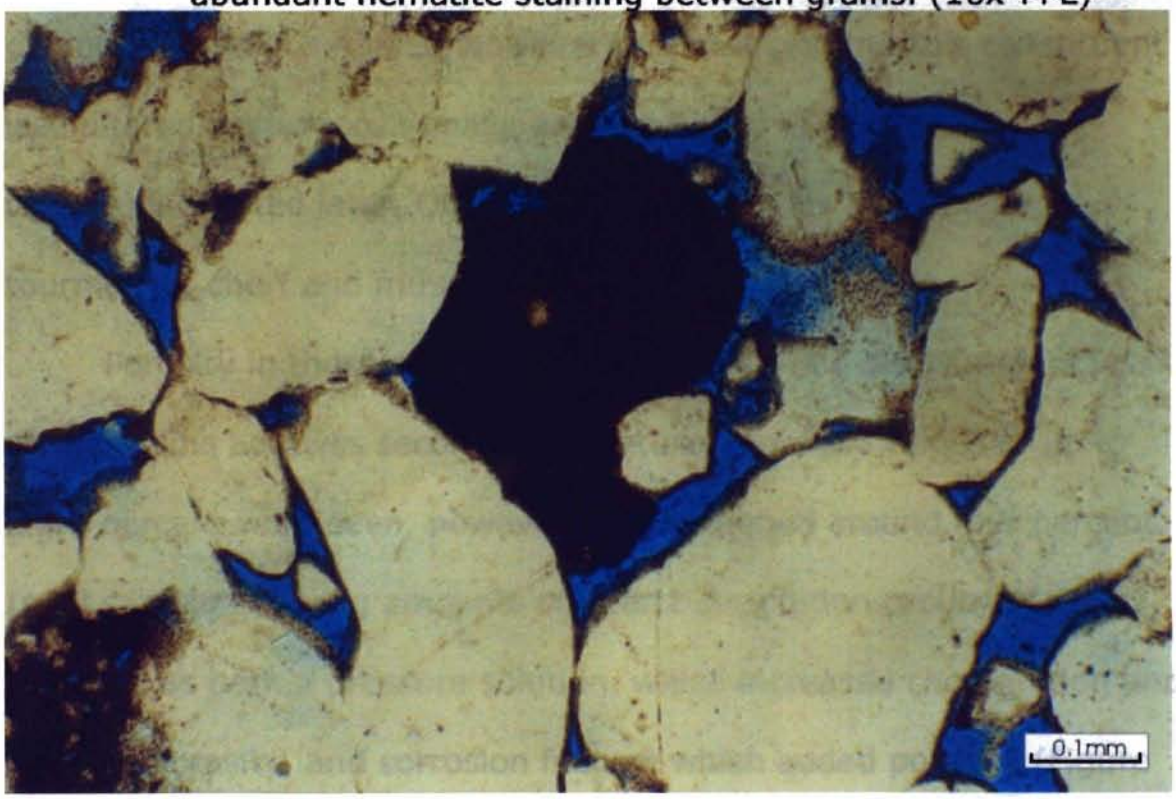

Figure 19. Photomicrograph showing dominant quartz grains coated by clays, which preserves porosity. (10x-PPL)

ten samples are relatively uniform in constituents. The one exception was found in sample Sp-23. The area between the grains contained significant amounts of hematite, which can be seem under plain, polarized light (Figure 18) and identified under reflected light.

The only major detrital constituent in all samples is quartz (Figure 19). Percentage-wise, their corrected range was in excess of 95 percent in all samples. Metamorphic rock fragments were seen in all samples except in Sp-1 and Sp-38. In these samples, grain rotation and fracturing were more extensive, showing that physical and chemical processes destroyed this rather unstable constituent. Another constituent altered is glauconite. Only small amounts were distinguishable in samples, however it is believed that this constituent was altered post-depositionally and converted to diagenetic constituents listed later. Other accessory minerals included zircon, tourmaline, chert and muscovite (Figure 20).

Porosity in these samples was derived by the dissolution of less stable grains and was secondary in nature. Porosity values of up to eight percent were seen, however they averaged around four percent. In all samples varying amounts of quartz dissolution occurred. This occurred as both a pressure solution, which increased cementation and reduced porosity, and corrosion feature which added porosity (Figure 19). Closer examination of this corrosion feature yields abundant

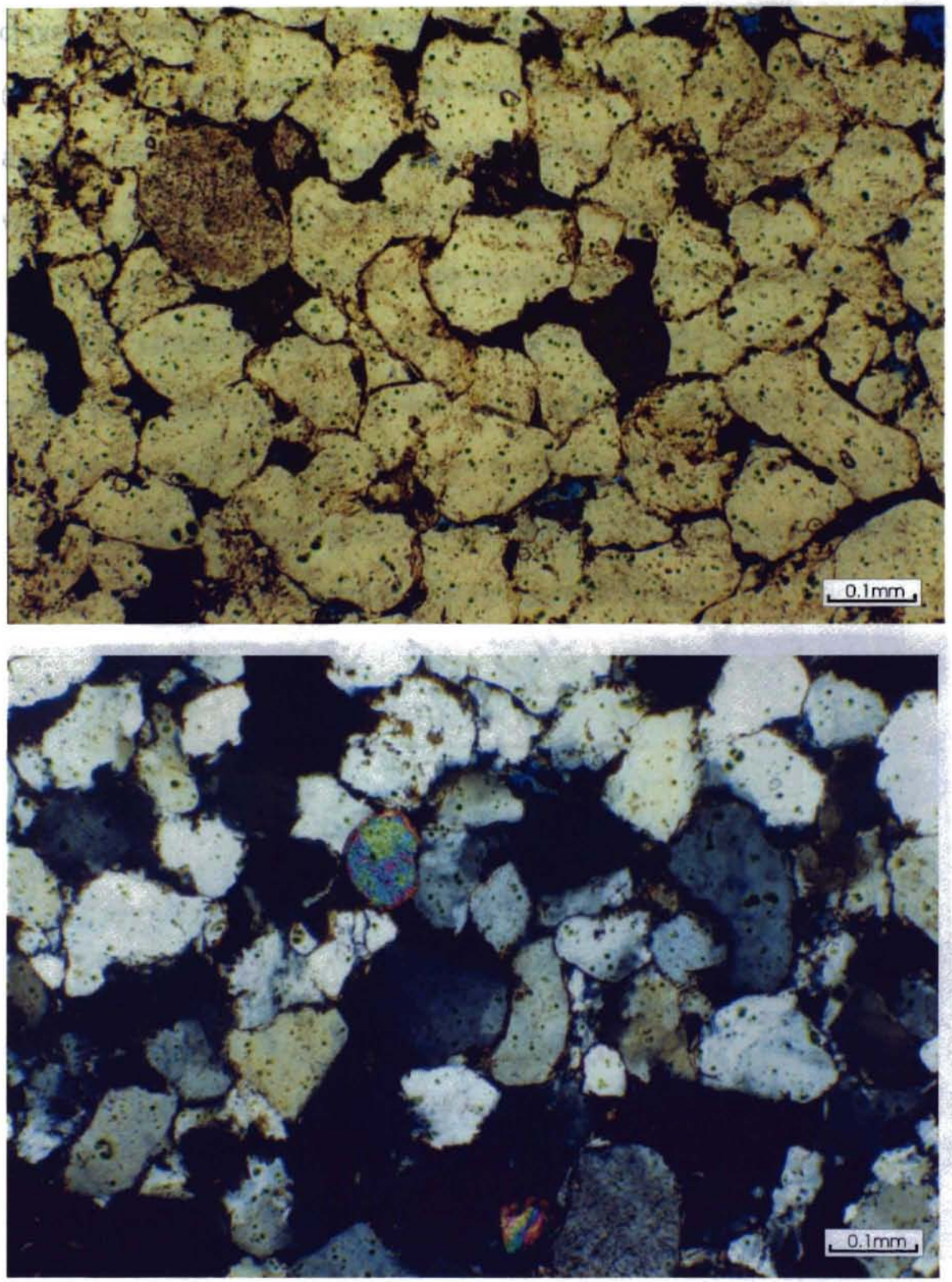

Figure 20. Photomicrograph showing abundant clays (top-PPL) and zircon grains (bottom-XNL) from Spiro Sandstone outcrop.

clays. Alteration and dissolution of metamorphic rock fragments (MRF's) and glauconite altered the pore space on a microscale, altering the pH enough to allow quartz dissolution. A similar feature was also noted in the subsurface Spiro Sandstone sample.

Diagenetic constituents were significant in the overall fabric of the rock. Limonite and hematite were present in most samples. These elements were derived from the dissolution of unstable grains like glauconite and MRF's. The dissolution of these grains also gave rise to authigenic clays, predominately illite. The presence of illite (Figure 21) inhibited quartz overgrowth, were present.

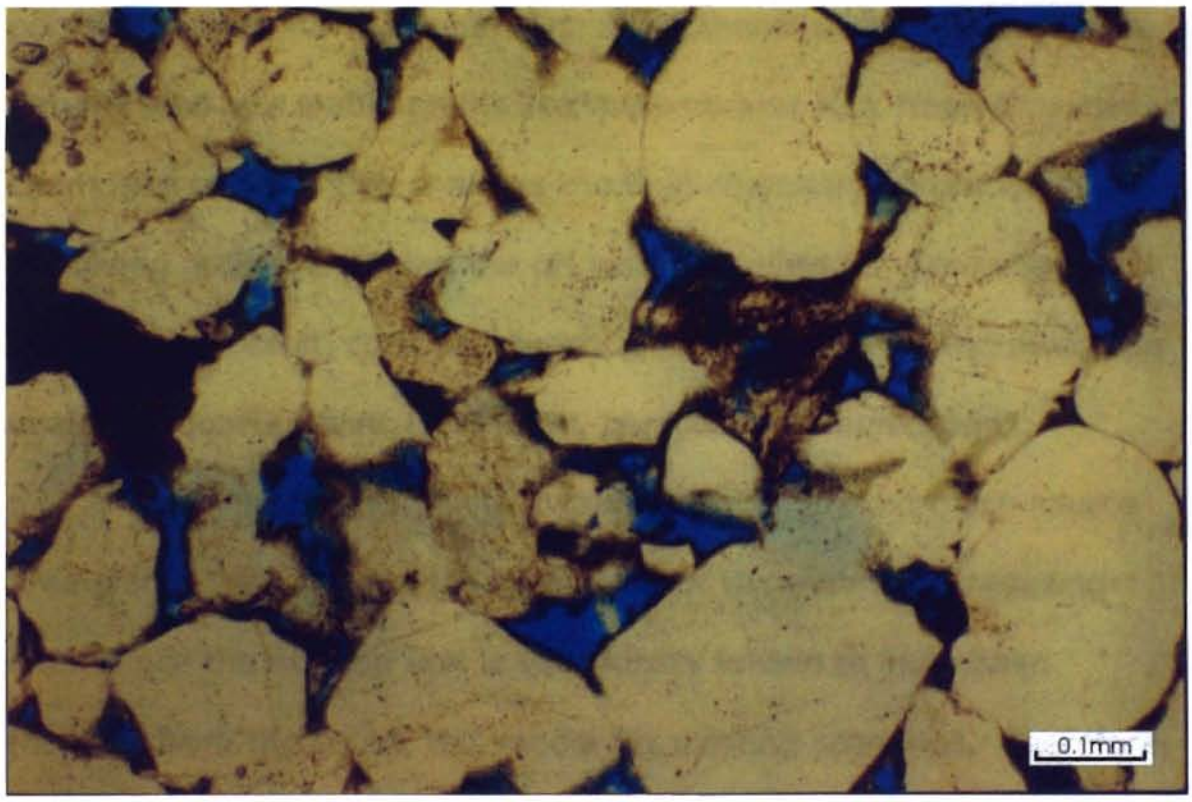

Figure 21. Photomicrograph with abundant illite coating and increased secondary porosity with the dissolution of MRF's.

Application of Findings

Comparison of surface and subsurface slides show significant differences. Where surface samples showed examples of glauconite and altered derivatives, subsurface samples showed abundant chamosite. This distinctive feature shows distinctive differences in their depositional environments. Chamosite is known to form in reducing marine environments, wereas glauconite forms in a normal, agitated open marine environment. The significance of this feature is its effect on porosity. In the sample containing chamosite, primary porosity was very well preserved. This preservation of primary porosity allowed for the generation of additional porosity. Pore fluids deteriorated less stable grains like metamorphic rock fragments and chamosite pellets. This changed the fluid chemistry surrounding these dissolving grains, changing the pH locally to allow for dissolution of quartz. As a result, corroded quartz grains could be viewed alongside unaltered quartz grains (Al-Shaieb, personal communication).

Placement of these units in comparison to the northern source area places the open marine area south of the restricted, reducing one. Since the outcrop unit is structurally known to have been thrusted from the south, this model fits existing scenarios. Therefore, the two Spiro units are not petrographically the same, having been formed in slightly different, adjoining environments (Figure 22).

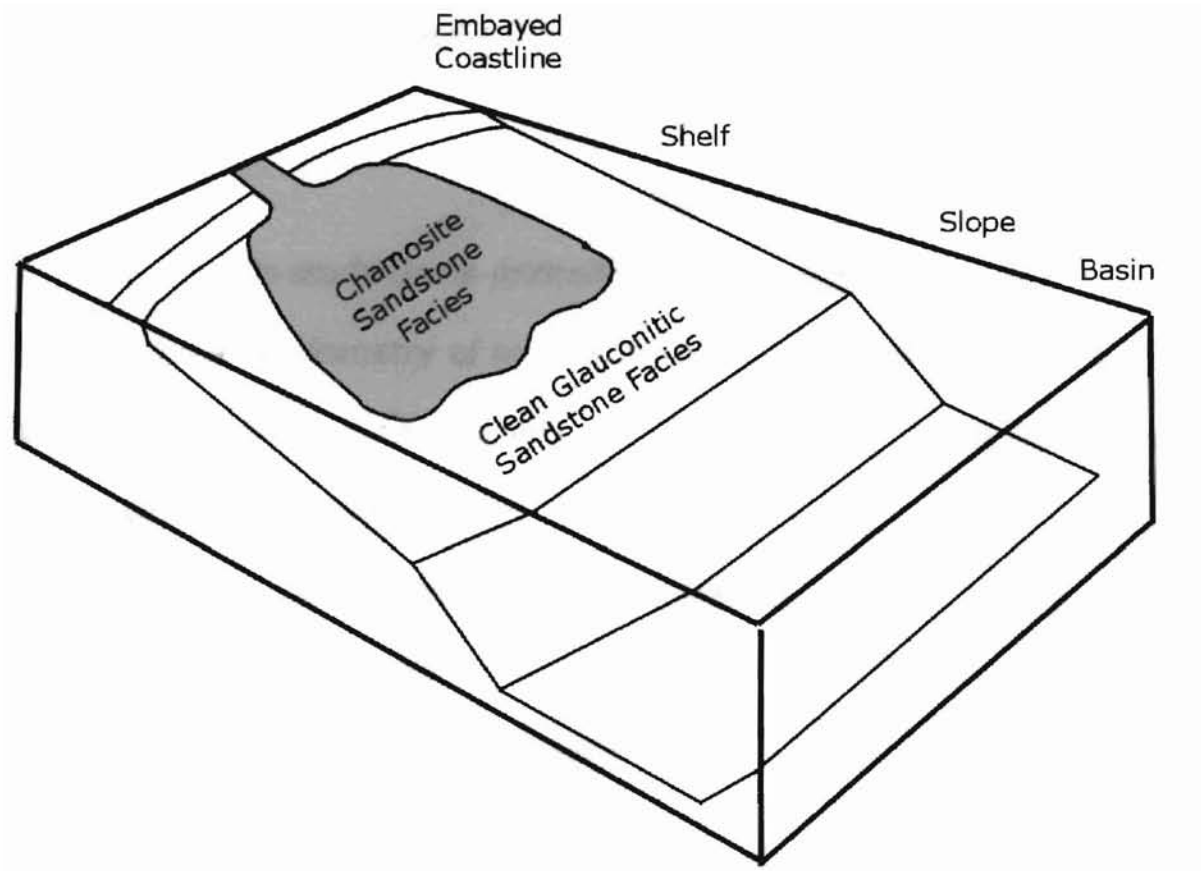

Figure 22. Schematic block diagram representing depositional model of chamosite and glauconite within the Spiro Sandstone. (Modified from Al-Shaieb and Deyhim, 2000)

CHAPTER V

KINEMATICS AND GEOMETRY OF THRUST FAULTS

Introduction

Since this study deals primarily with thrust faulting, the kinematics and geometry of several structural features associated with thrusting will be described briefly. A thrust system is an assemblage of related thrust sheets contained within a given area (Boyer and Elliot, 1982). Thrust sheets (Figure 23) are volumes of rock displaced by movements of an underlying fault (Boyer and Elliot, 1982). Due to this relationship, names for overlying thrust sheets are typically derived from their orogenic thrust faults.

When a thrust fault intersects a stratigraphic horizon, it is called a cutoff line. If this cutoff line, or edge, is created by the trailing thrust, the thrust on the hinterland side, it is a trailing cutoff line. On the other hand, if the cutoff line is created by the leading thrust (the thrust on the foreland side) then it is termed the leading cutoff line. If a given thrust propagates to the synorogenic ground surface, it is

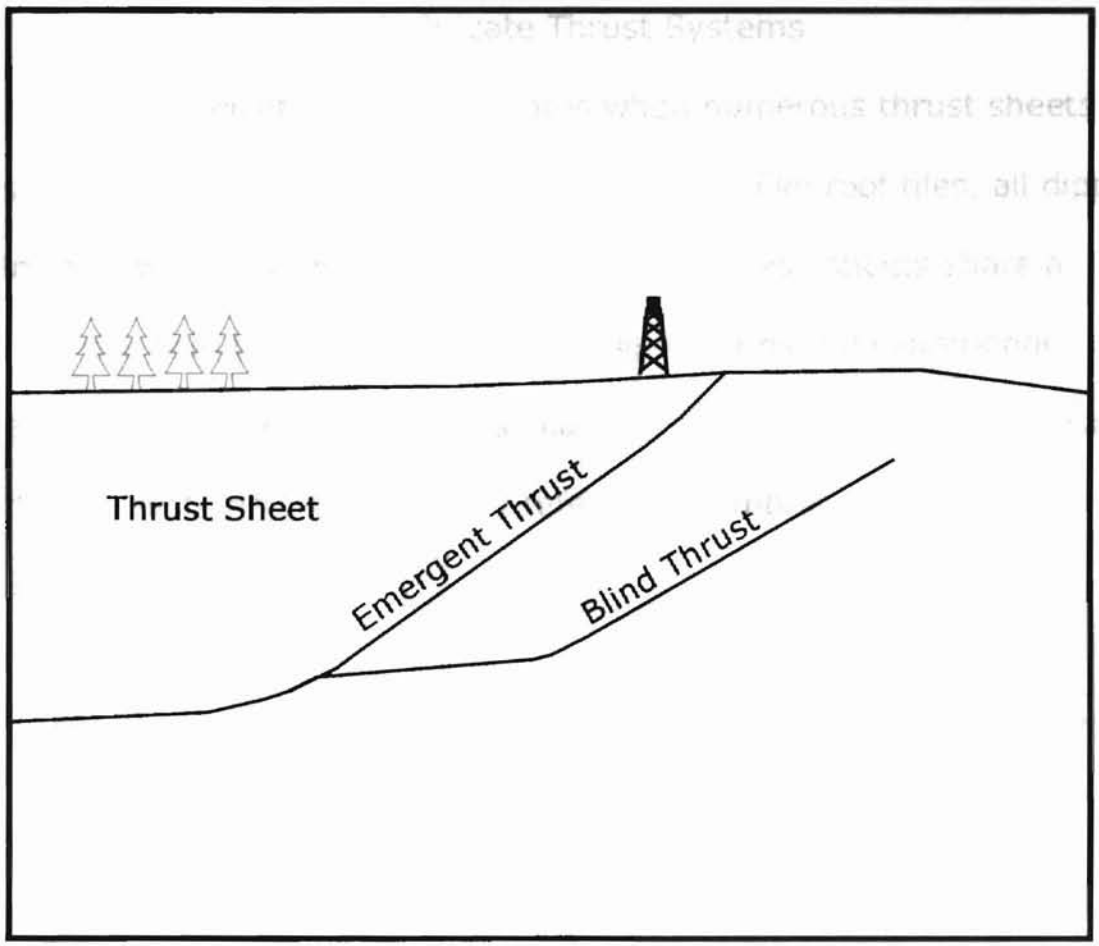

Figure 23. Illustration depicting elements of a thrust system.

called an emergent thrust, whereas a blind thrust is a thrust sheet that does not reach the ground surface (Figure 23).

Thrust faults arise from branch lines stemming from detachment surfaces. It is possible for a unit of rock to be surrounded by branch lines. This occurs when a fault diverges after splitting and later converges upon the initial surface. In this case, the body of rock is classified as a horse (Boyer and Elliot, 1982).

Imbricate Thrust Systems

An imbricate thrust originates when numerous thrust sheets of similar shape and size stack upon each other like roof tiles, all dipping in the same general direction (Figure 24). These sheets share a common sole thrust and increase in dip towards the synorogenic erosional surface. Due to these curved triangular wedges, imbricate thrusts systems are commonly referred as 'imbricate fans' (Boyer and Elliot, 1982).

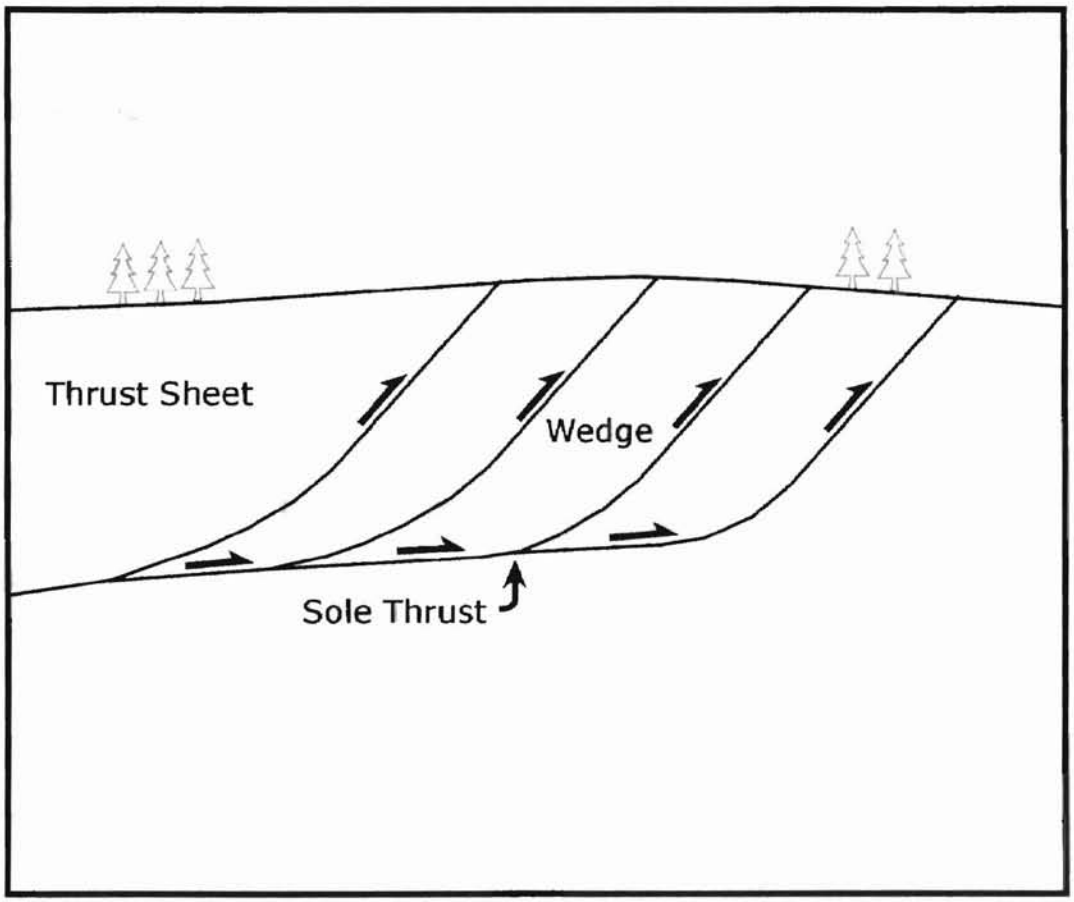

Figure 24. Illustration of Imbricate fan depicting geometry and components.

Imbricate fans can propagate in one of two ways (Figure 25). If an imbricate thrust system has maximum slip in a direction towards the foreland, it is termed a leading imbricate fan. If maximum slip is towards the hinterland, then it is called a trailing imbricate fan. Due to the nature of these systems, imbricate fans illustrate an effective way to shorten and thicken a given sequence (Boyer and Elliot, 1982).

Duplex Structures

Duplexes are composed of numerous horses stacked one on top of another (Figure 25). Their overall shape and size is variable, depending on the overall magnitude of the displacement and the spatial relationship between branching lines (ramps). Equally variable is the ability of individual horses to change into splays along strike. These variations within the duplex can result from oblique and lateral ramping (Figure 26). Therefore, fault surfaces meeting along two branch lines (C-C') can resemble a horse in cross-section (Figure 26, B-B') and a splay in map view (Figure 26, A-A') (Boyer and Elliot, 1982).

Even with all of this variability, there are common features observed within many duplexes. Commonly, the overriding thrusts' inflection point nearly parallels that of the underlying thrust surface and within a given horse, beds often form anticline-syncline pairs. In

addition, these folded pairs maintain their general size and shape from horse to horse within a duplex.

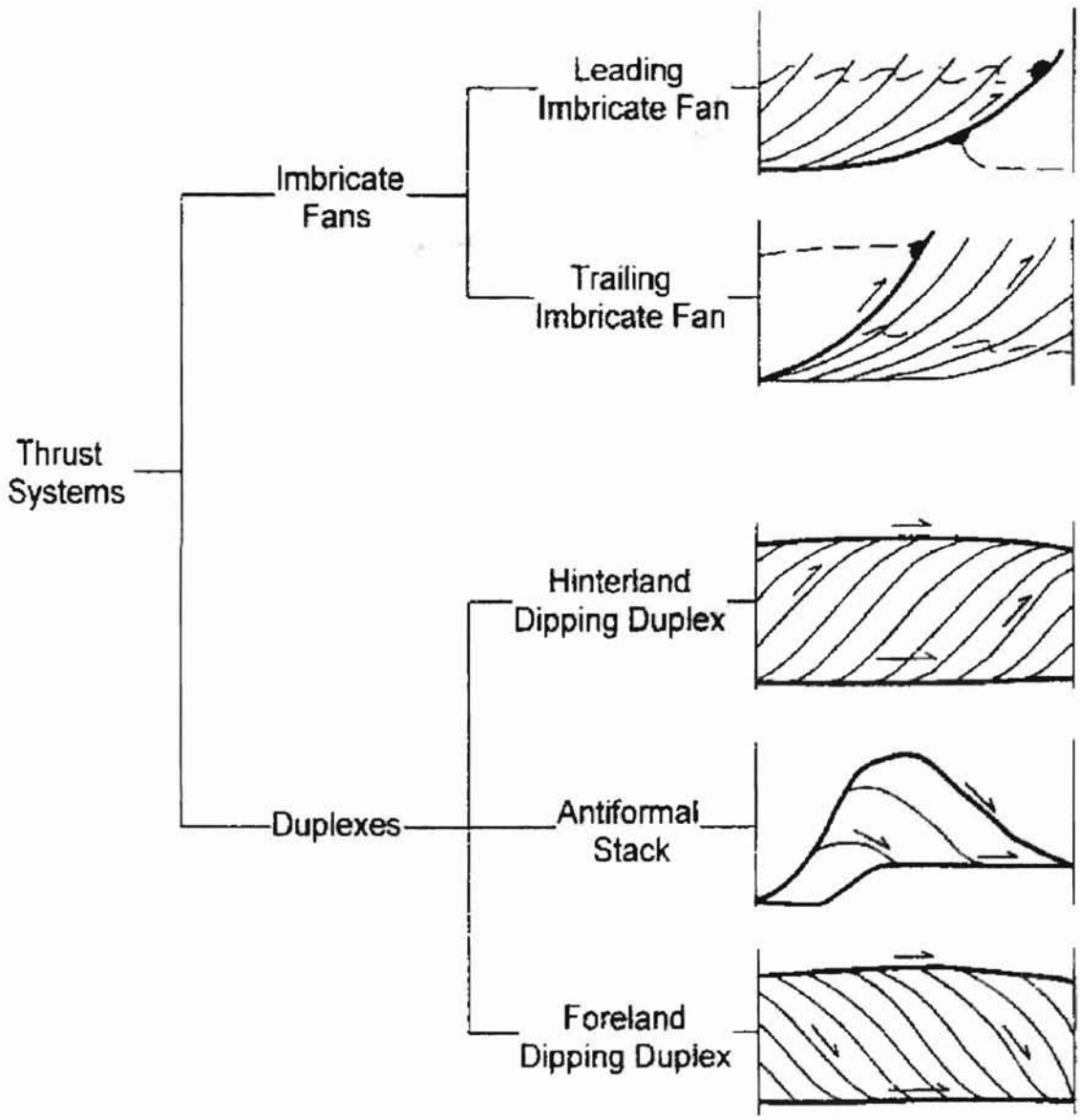

Figure 25. Classification of thrust systems (from Boyer and Elliot, 1982).

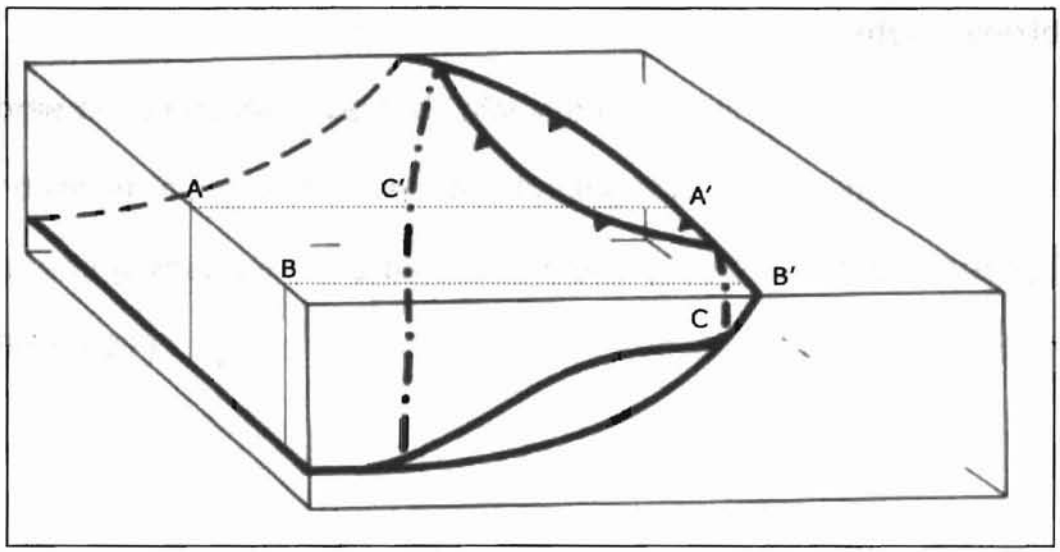

Figure 26. Illustration of variation within a solitary splay (modified form Boyer and Elliot, 1982).

Hinterland-Dipping Duplexes

Hinterland-dipping duplexes are also known as break forward thrust sequences. They form when displacement is "transferred onto a new fault surface generated in the footwall of the previously active zone" (Butler, 1987). This displacement is generally less than the distance between ramps. These structures originate as a leading thrust travels roughly horizontally through incompetent units (shales, etc.) and increasing updip ($\pm$ 30 degrees) through component units (sandstones, etc.), creating a ramp (Figure 27). After the ramp, the thrust will level off, back to horizontal, when it reaches another incompetent bed. When the frictional forces increase to overcome the

driving force of the thrusting, a new fault is initiated at the base of the ramp, creating a new trailing branch line. This new branch line occurs on the same initial detachment, or sole thrust. The older, overriding horse becomes inactive and "piggy-backs" upon the newer horse. The end result is a set of hinterland-dipping thrusts with horse sequences becoming younger towards the foreland (Boyer and Elliot, 1982) (Figure 27).

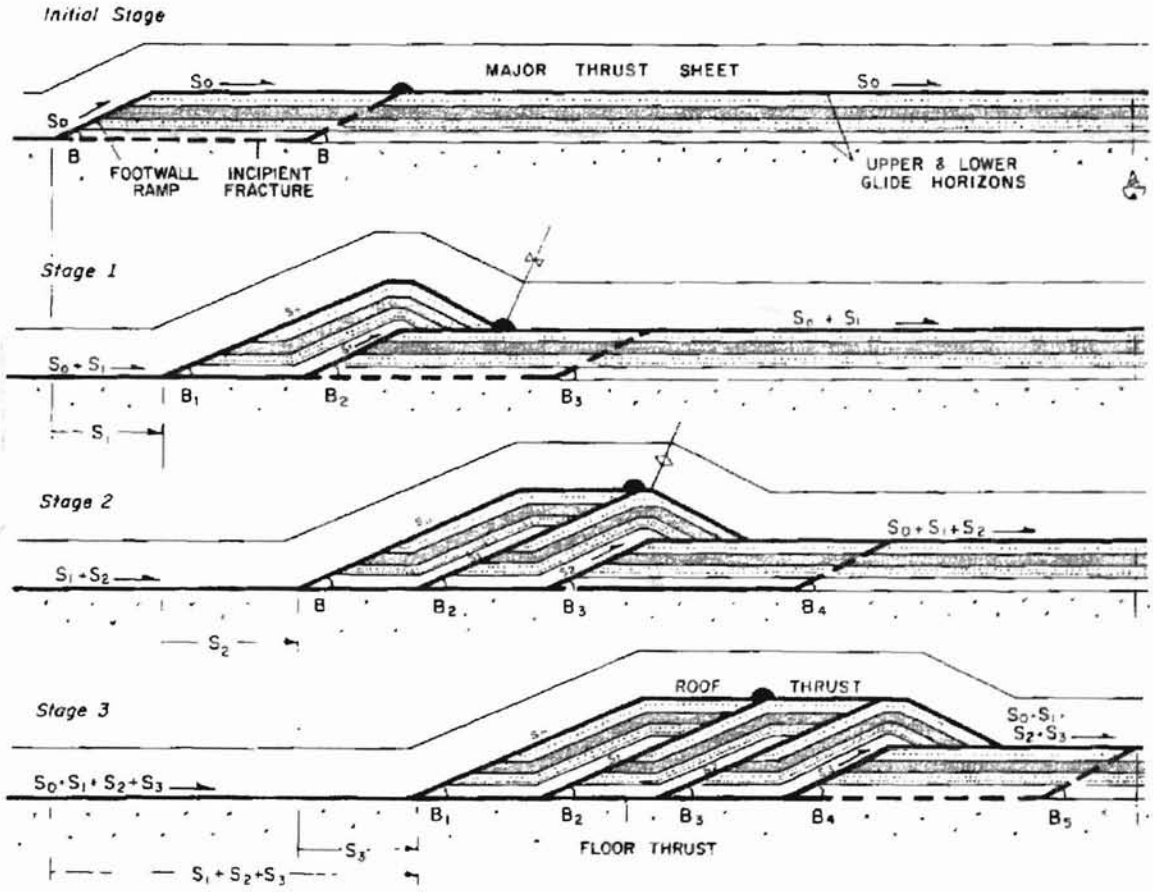

Figure 27. Formation of a duplex structure assuming plane strain and kink folding (from Butler, 1987).

Antiformal Stack

The formation of an antiformal stack is similar to the previously stated "piggy-back" sequence. In this structure, however, the displacement and the distance between the ramps are roughly equal. As a result, the trailing branch lines juxtapose one another, building the horses vertically (Figure 28). As they build, the older horses within the structure rotate towards the hinterland. With the addition of more horses, the pitch of the older horses increases (Figure 28, C-D) (Boyer and Elliot, 1982).

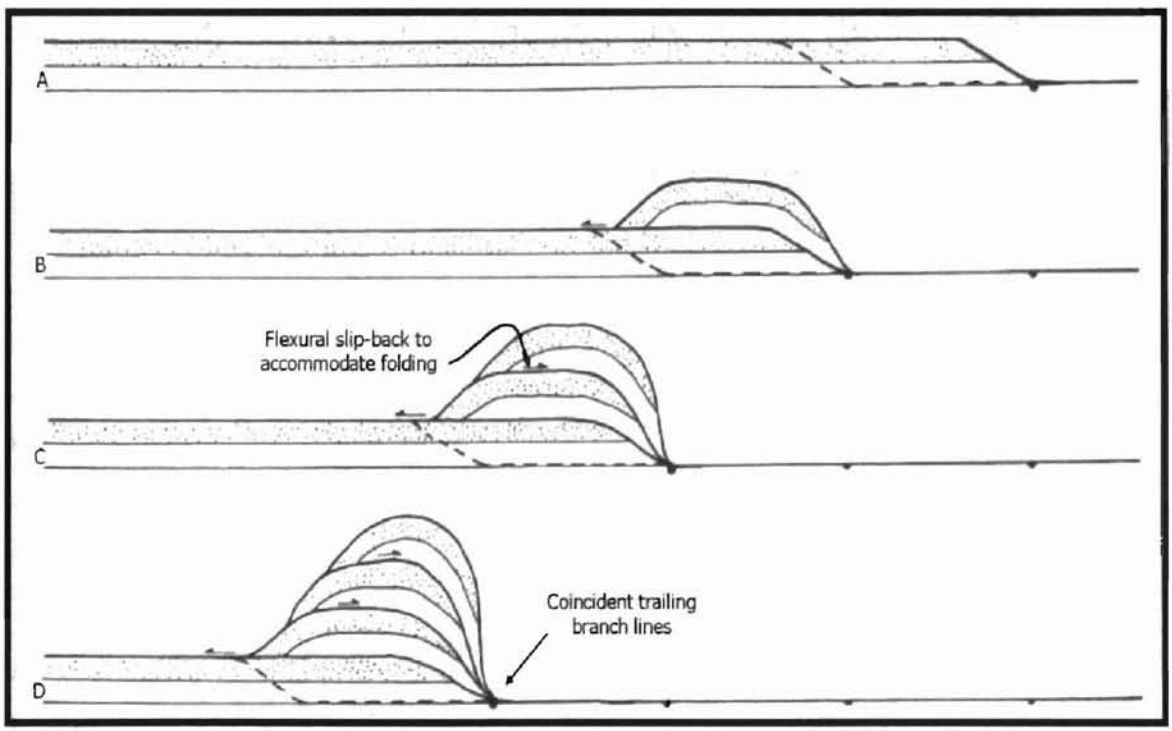

Figure 28. Formation (a-d in time) of an antiformal stack duplex (modified from Butler, 1987).

Foreland-dipping Duplex

If the displacement of a given thrust is greater than the distance between individual ramps, then a foreland-dipping duplex occurs. In this example, the frictional forces surmount quicker than in the hinterland-dipping duplex, offsetting the branch lines towards the hinterland direction. As a result, the horse features dip towards the foreland, with the older horses near the foreland and the younger horses towards the hinterland (Figure 29). When the section is restored, trailing lines appear in the usual order as preceeding duplexes. Evidence of this type of duplex has yet to be well documented, however, it is kinematically correct (Butler, 1982).

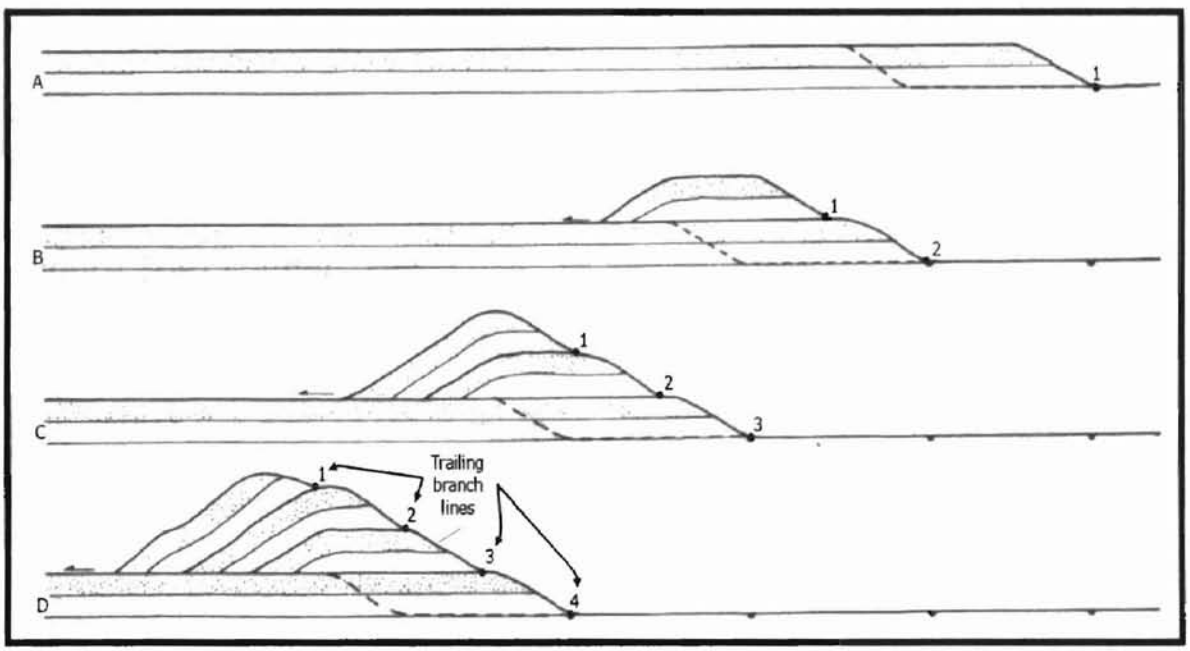

Figure 29. Formation (a-d in time) of a foreland-dipping duplex (modified from Butler, 1987).

Break-backward Thrust Sequences

With all of the previously described examples, fault propagation moves forward in the foreland direction, originating in and around the previous thrusts' footwall. However, when this forward propagation is inhibited due to hindrance, a break-back thrust sequence occurs. In this example of deformation, the roof thrust becomes inactive and all displacement is transferred along the sole thrust (Butler, 1987). The result is the forward propagation of the displacement front by the development of internal break-backward sequences (Figure 30b). If the displacement front is fixed (Figure 30c, point w), the displacement on the back-thrusts are determined by the length of the lower thrust segment (Butler, 1987). The resulting structure is a piggyback sequence resembling an antiformal stack. However, if the displacement front is not fixed, the resulting structure continues to develop break-backward sequences in the direction of the foreland (Figure 30e) (Butler, 1987).

Triangle Zones

Near the end of the evolution process of a fold-thrust belt, opposing forces can create a back-thrust. Unlike the previously cited examples, propagation and movement of the hanging wall is towards the hinterland. Therefore, the overall direction of the back-thrust is

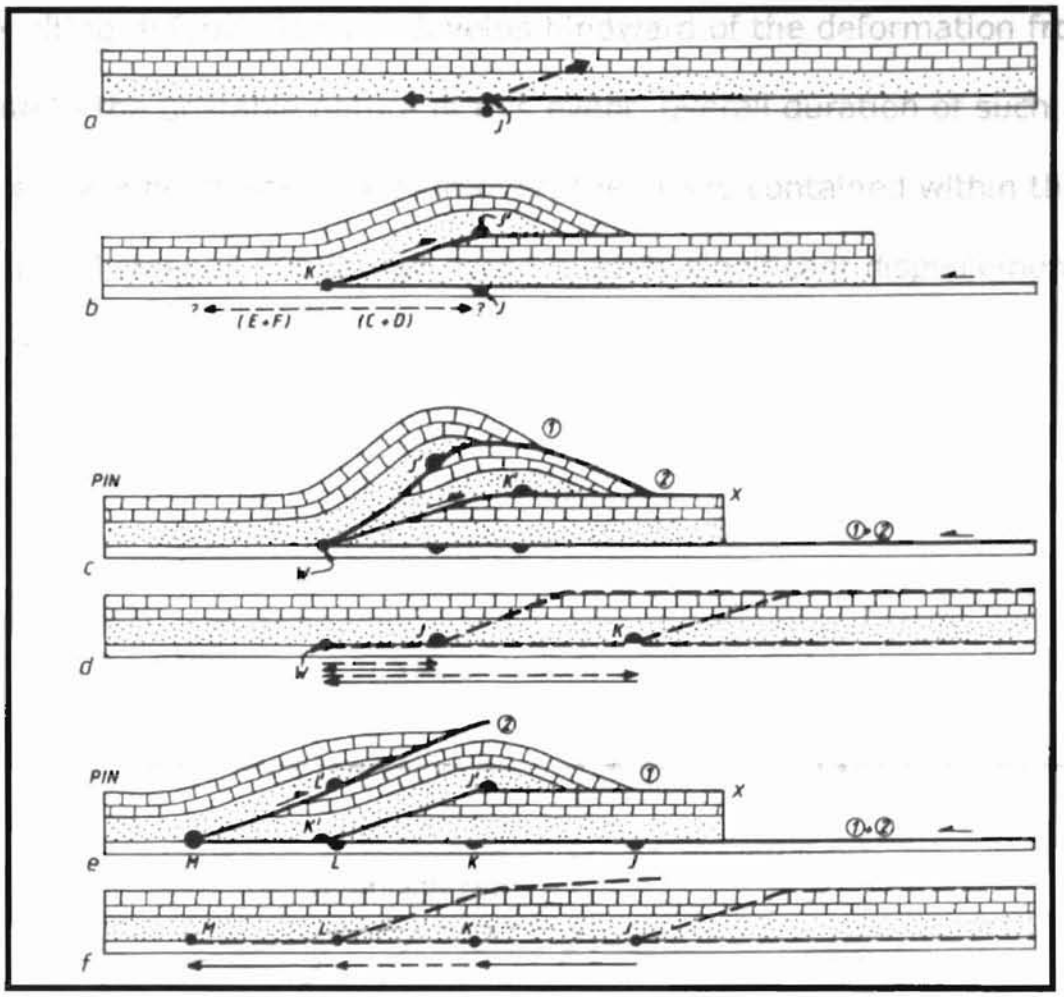

Figure 30. Evolution of a break-backward sequence as proposed by Butler (1987).

opposite the regional movement direction (Butler, 1987). If these back-thrusts are combined with a forward propagating imbricate fan, then a triangle zone can form, creating a triangular wedge of strata bound by both foreland-dipping and hinterland dipping faults (Figure 31).

This type of structure occurs when the forward propagation of the deformation front is inhibited. In a zone of pure shear, the

resulting deformation will develop hindward of the deformation front. Due to the unstable nature of this event, overall duration of such an event will be short-lived. Moreover, the layers contained within the unit will steepen but cannot accommodate significant displacement (Butler, 1987).

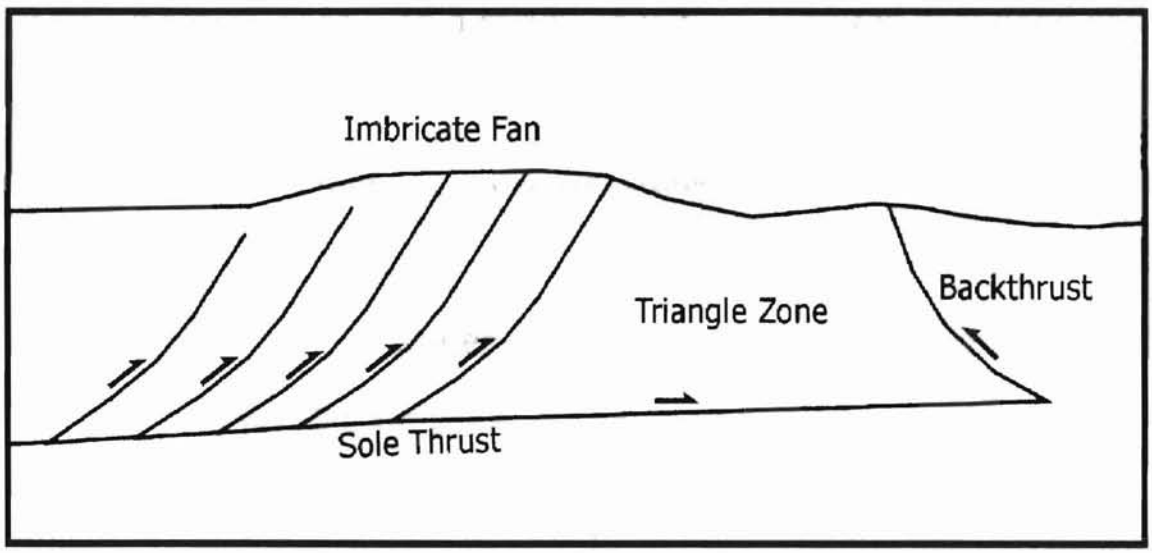

Figure 31. Illustration depicting the formation of a triangle zone between the leading edge of an imbricate fan and a backthrust.

CHAPTER VI

STRUCTURAL GEOLOGY

The goal of this study is to delineate the structural features found within the Summerfield and LeFlore SE Quadrangles. The study area is located in LeFlore County along the Ouachita Mountain-Arkoma Basin transition zone. As a result, structural features contained within this area reflect the deformation styles of both tectonic provinces.

The structural geometry of the transition zone situated between the Ouachita Mountains and the Arkoma Basin has been an area of study and debate for decades. With the advancement and availability of data in the last fifteen years, researchers have been able to depict these trends more accurately. Between 1992 and 1995, an Oklahoma Center of Advancement in Science and Technology (OCAST) project was conducted at Oklahoma State University to study the Spiro Sandstone and associated structural features within the Wilburton gas field and surrounding area. Cemen and others (1994, 1995, 1997 and in press), Al-Shaieb and others (1995), Akthar (1995) and Sagnak (1996) concluded that a triangle zone is present north of the Choctaw

Fault zone. This triangle zone is bound to the north by the northerly-dipping Carbon Fault, to the south by the southerly-dipping Choctaw Fault and underlain by the Lower Atokan Detachment (LAD) (Figure 32).

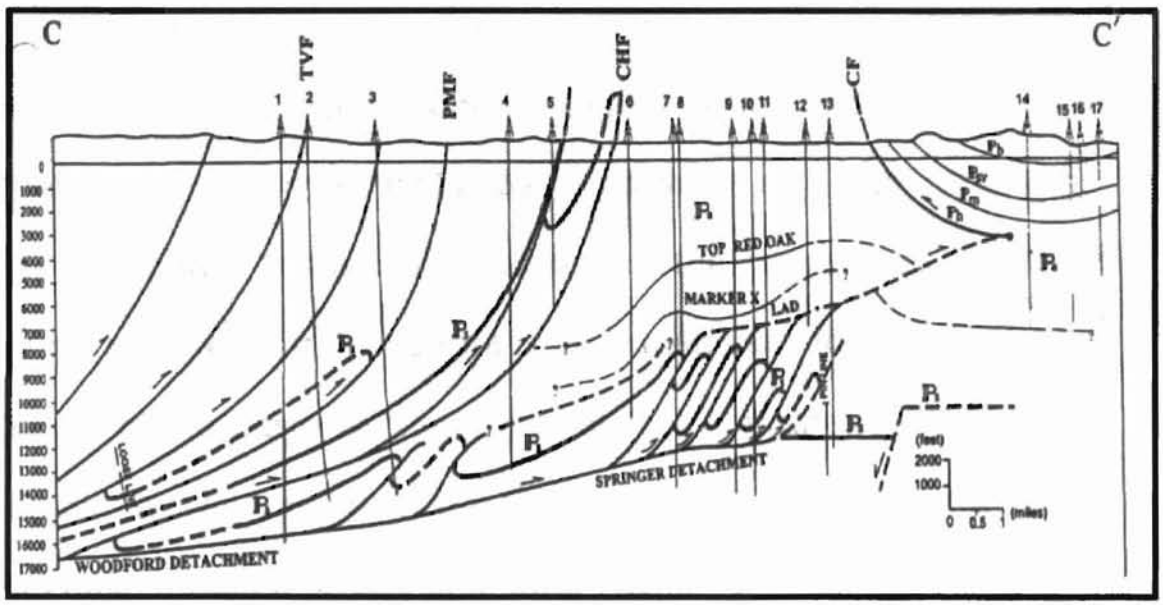

Figure 32. Cross-section showing the presence of the triangle zone, duplex structure, and other structural features in the Wilburton gas-field area. Cross-section located in T3-6N, R18E. (from Cemen, Sagnak and Akthar, 2001).

Following OCAST project, Evans (1997), Ronck (1997) and Mehdi (1998) determined the eastward continuation of the structural features of the Wilburton gas-field area (Figure 33). Within the Summerfield and LeFlore SE Quadrangles, many of the same surface and subsurface structural features described by the previous authors are found. These structural features extend from southwest of the Hartshorne area eastward into Arkansas.

Within the study area, Pennsylvanian rocks are exposed at the surface (Figure 34). Gently dipping Desmoinesian Series strata occur in the north. All of these units have a northerly dip, with increasing dip to the south. Atokan strata dominates the central area. North of the Choctaw Fault, Atokan strata is asymmetrically folded due to the influence of the westerly-plunging Heavener Anticline and Pine Mountain Syncline. South of the Choctaw Fault, a series of imbricate faults have thrusted middle and lower Atokan and Morrowan strata creating numerous tight folds. At the southern margins of the area, overthrusted Morrowan strata is present south of the Ti Valley Fault.

To ascertain information on subsurface geometries within the area, three balanced cross-sections were constructed (Figure 29-31, and Plates 1-3). This task was achieved by the integration of well-log and seismic data. After completion, restoration of the Spiro Sandstone

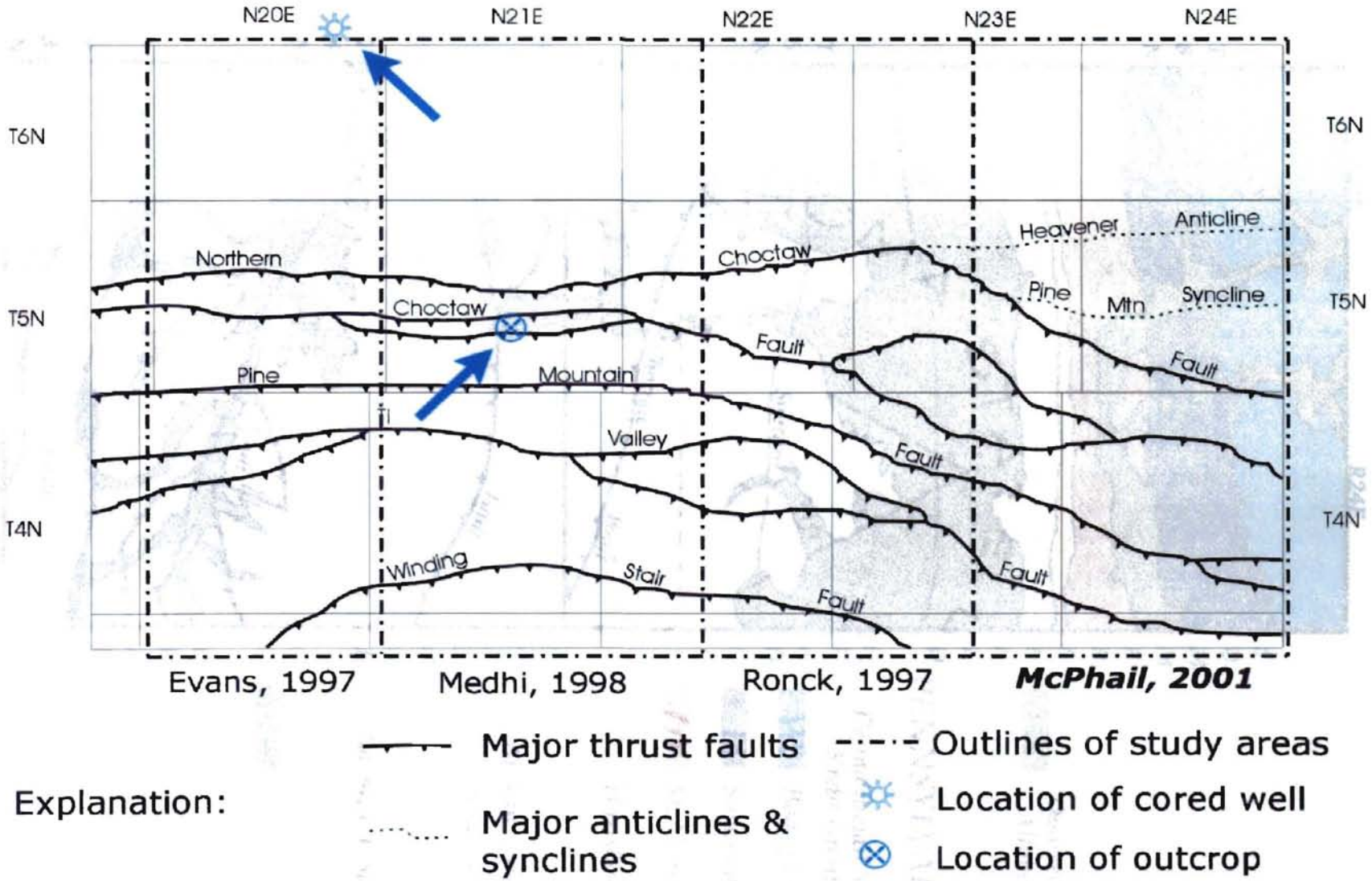

Figure 33. Regional base map depicting core and outcrop locations.

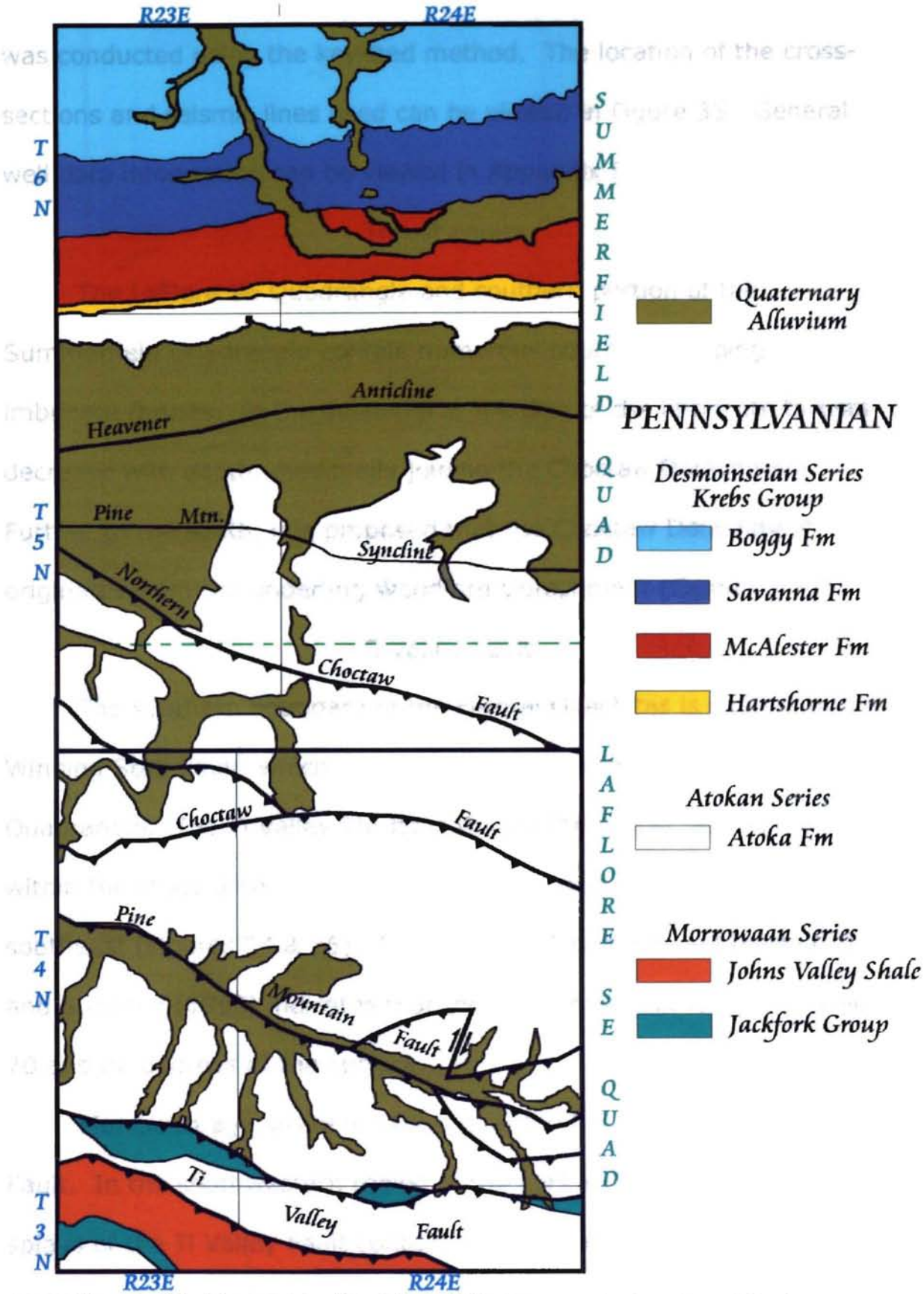

Figure 34. Basemap depicting lithology and structural features.

was conducted using the key-bed method. The location of the cross-sections and seismic lines used can be viewed in Figure 35. General well data information can be viewed in Appendix I.

Thrust Faults

The LeFlore SE Quadrangle and southern portion of the Summerfield Quadrangle contain numerous southerly-dipping imbricate thrusts. In the subsurface, the dips of the imbricate thrusts decrease with depth, eventually joining the Choctaw Detachment. Further to the south, it is proposed that the Choctaw Detachment originates from the underling Woodford Detachment (Cemen, 1995).

Ti Valley Fault

The southern boundary of the Frontal Ouachitas is defined by the Winding Stair Fault, which is not present within the LeFlore SE Quadrangle. The Ti Valley Thrust is the southernmost fault contained within the study area. Its overall trend is west-northwest to east-southeast (Figures 34 & 35). Surface mapping conducted by Hemish and Suneson (1990) indicates that the dip of this fault ranges between 70 and 80 degrees at the surface.

Morrowan age strata is exposed on the hanging wall of Ti Valley Fault. In the southwestern region of the LeFlore SE Quadrangle, splays of the Ti Valley Fault contain steeply dipping sections of Atokan, Jackfork and Johns Valley Shale (Figure 34).

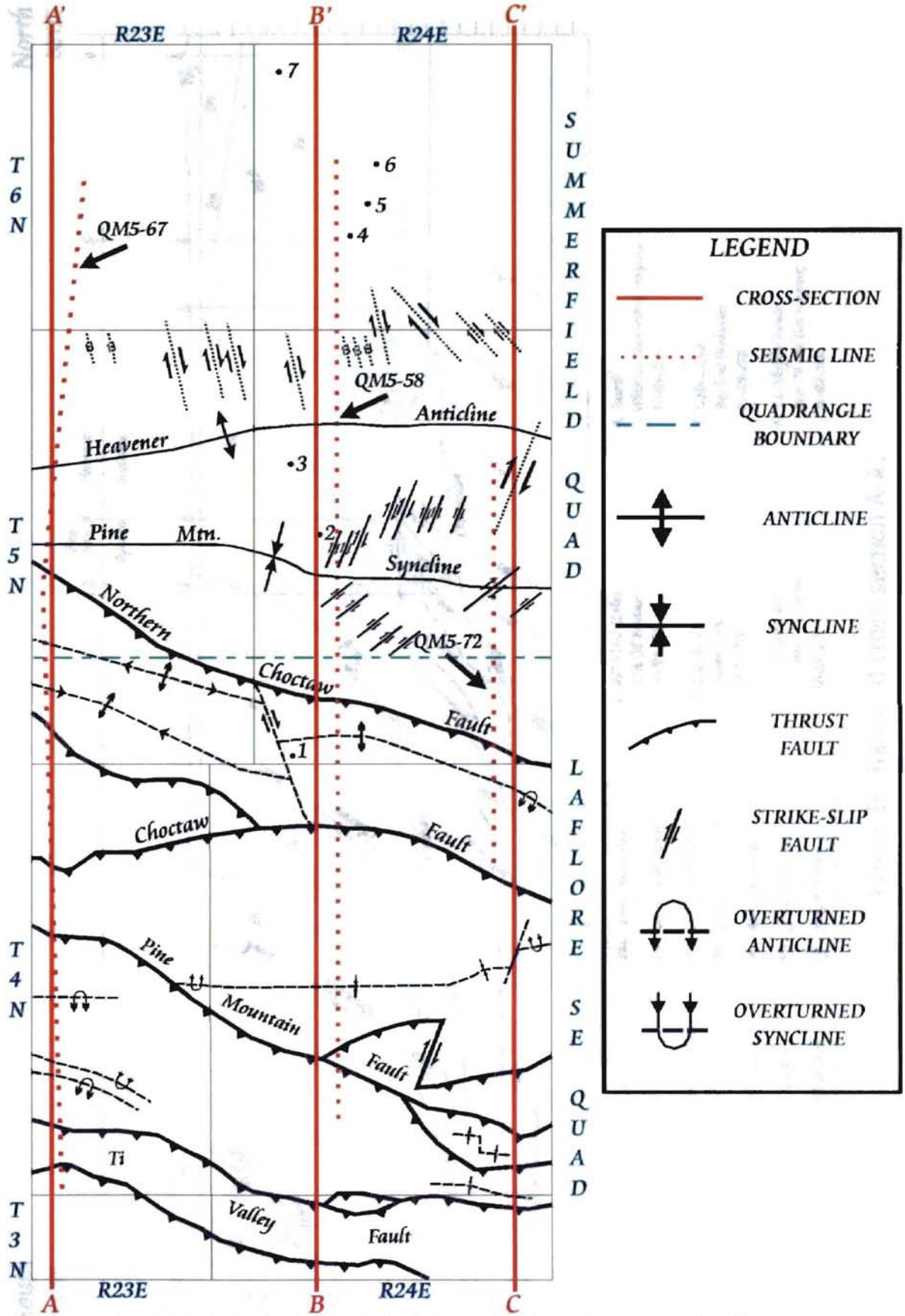

Figure 35. Geologic basemap of area depicting seismic and cross-section lines.

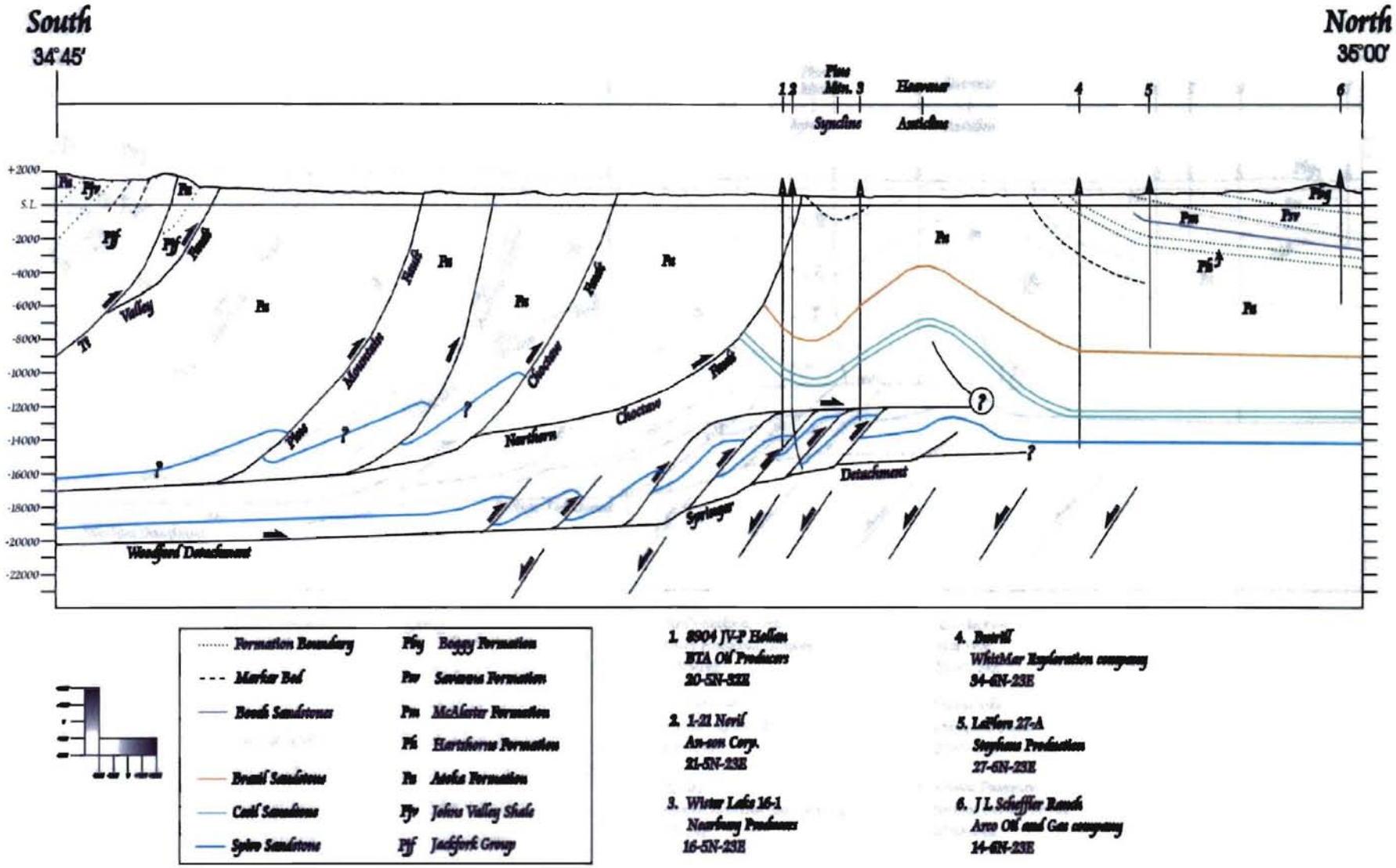

Figure 36. Balanced cross-section A-A'.

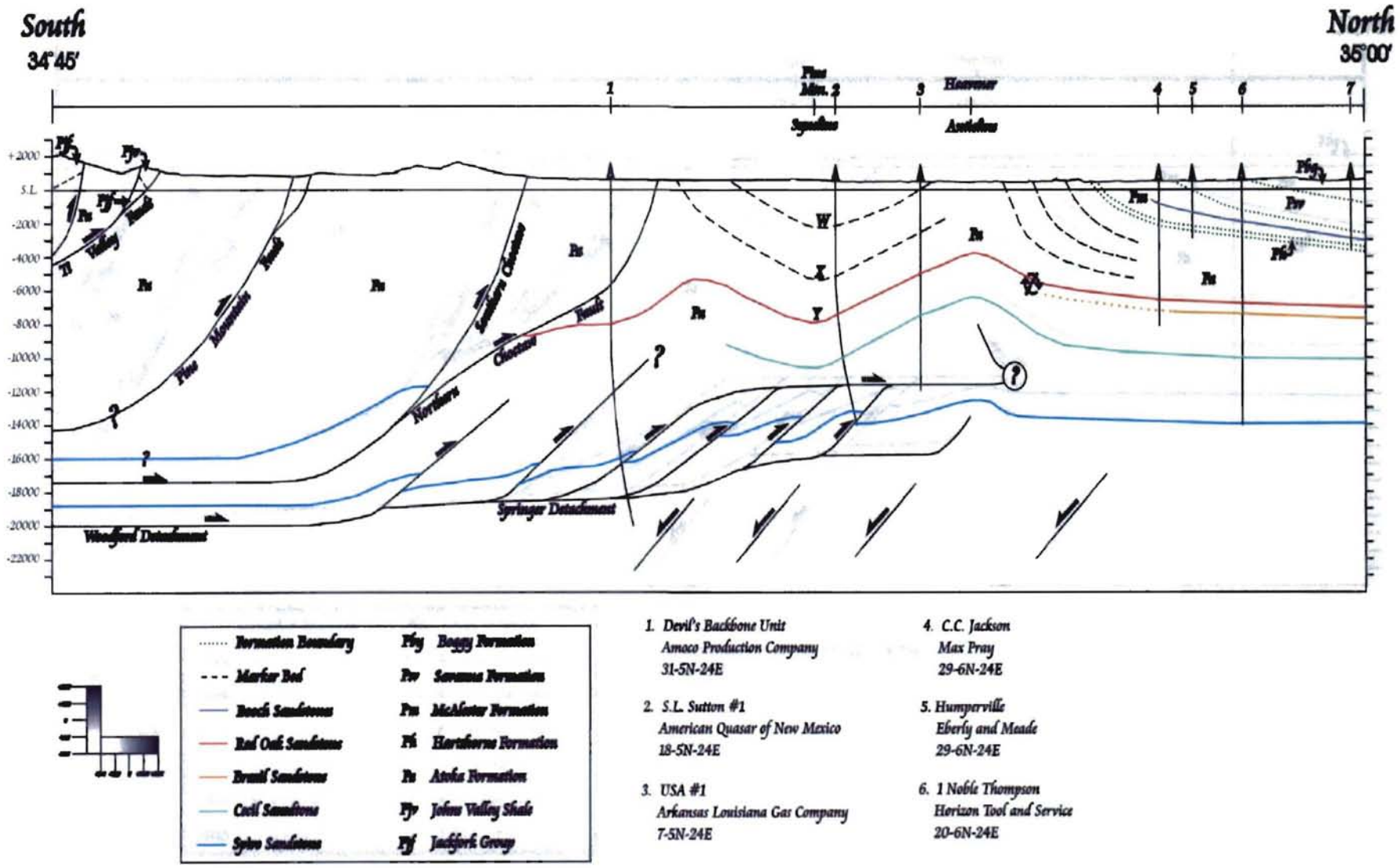

Figure 37. Balanced cross-section B-B′.

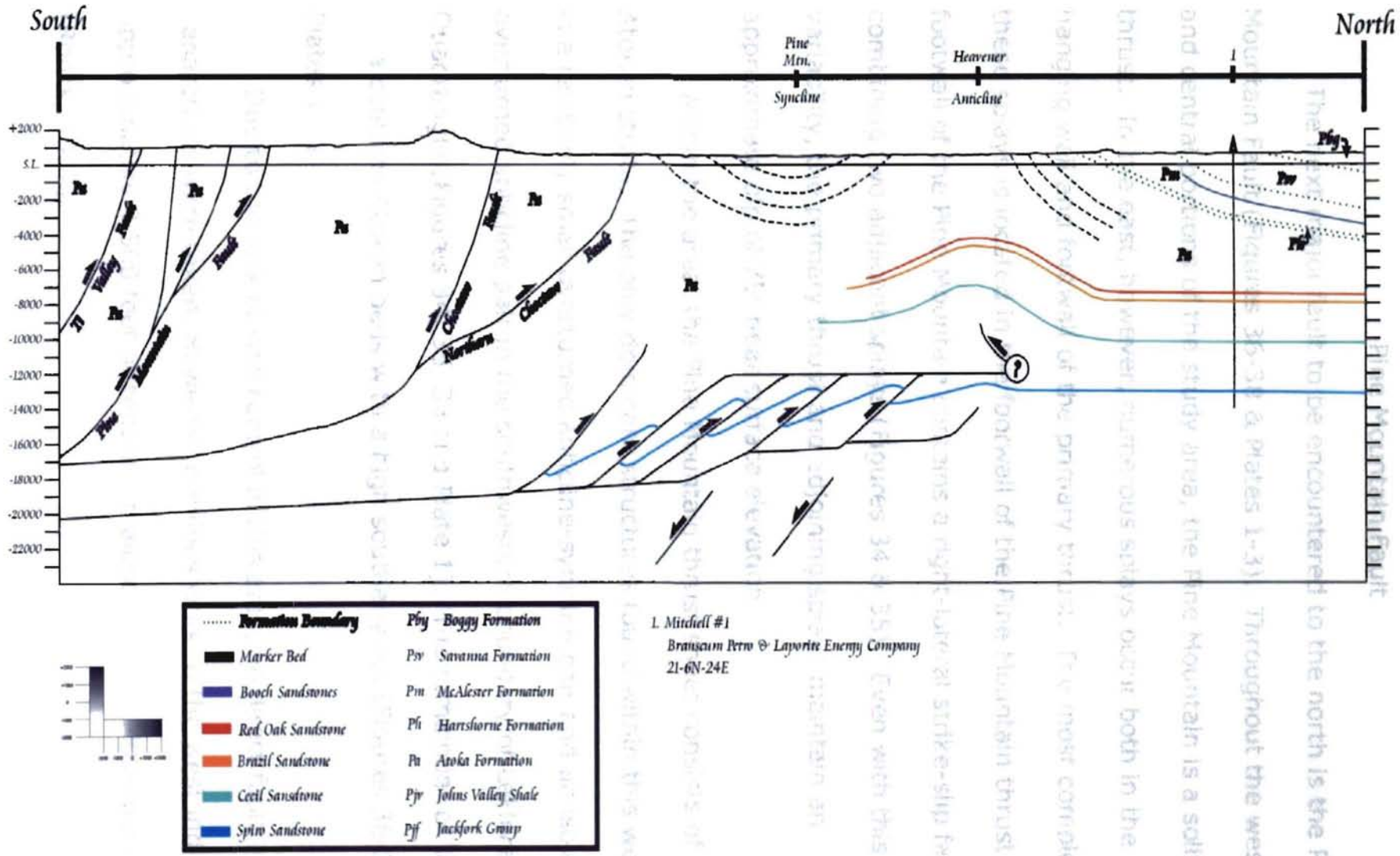

Figure 38. Balanced cross-section C-C′.

Pine Mountain Fault

The next major fault to be encountered to the north is the Pine Mountain Fault (Figures 36-38 & Plates 1-3). Throughout the western and central portions of the study area, the Pine Mountain is a solitary thrust. In the east, however, numerous splays occur both in the hanging wall and footwall of the primary thrust. The most complex of these splays is located in the footwall of the Pine Mountain thrust. The footwall of the Pine Mountain contains a right-lateral strike-slip fault combining two adjacent splays (Figures 34 & 35). Even with this variability, the primary thrust and adjoining splays maintain an approximate dip of 75° near surface elevation.

Within the area, the Pine Mountain thrust sheet consists of Atokan strata. The only dominant structures found within this wedge is a relatively small overturned anticline-syncline pair and an isolated overturned anticline pair in the southwestern boundary of LeFlore SE Quadrangle (Figures 34, 35, 36 and Plate 1). The remainder of the area contains Atokan beds with a high southerly dip (Figures 36-38, Plates 1-3).

Due to the lack of well control in this area, no direct fault separations were taken. However, previous work to the west indicates approximately 3,500 feet of separation along the Pine Mountain Fault (Ronck, 1997).

Choctaw Fault

As discussed previously, the Choctaw fault is the northern boundary of the Frontal Ouachitas. Surface geological mapping of the area by Hemish and Suneson (1990) and Hemish and Mazengarb (1992) show the northernmost fault to be the Choctaw Fault. However, subsurface data from wells within this area and to the west show an absence of Lower Atokan strata, primarily the Spiro Sandstone, in the frontal wedge contained within the two northern most faults. However, Middle Atokan strata is present within this area and areas to the west. Therefore, the northern-most fault occurred after Spiro time, making the primary thrust the southern of the two, or the true Choctaw Fault. Because of this, the northern most fault has been given the name of the Northern Choctaw Fault (Figures 36-38 and Plates 1-3), and must be younger than the Choctaw Fault.

South of the Choctaw fault, the area contains additional splays. Seismic data show that these splays adjoin the main branch of the Choctaw in the subsurface. With this data it can be concluded that the Choctaw Fault is the leading thrust in Frontal Ouachitas, and its orogenic formation occurred as an imbricate fan system with break-forward geometry.

Basal Detachments and Duplex Structure

Underlying the Choctaw Detachment, a different geometry can be observed. The dominant structure seen in all cross-sections is the formation of a duplex structure in the underlying footwall of the Choctaw Fault. This duplex stems from a large scale, major decollement surface. This primary decollement is the Woodford Detachment, named for the shale in which the fault resides. It enters the south part of the area at about 20,000 feet below sea level, and gently rises 1,000 feet over a distance of eight miles.

At this point the basal detachment turns up-section. It effectively leaves the Woodford Shale and rises into the Springer Shale. The Springer Detachment serves as the floor thrust of the duplex structure, whose base lies approximately 16,000 feet below sea level.

In addition to the Springer Detachment, another detachment resides in the footwall of the Choctaw Fault. Branching off from the ramp that forms the Springer Detachment, the Lower Atokan Detachment (LAD) acts as a roof thrust for a large duplex structure. It climbs to a depth of 12,000 feet below sea level, where it continues relatively horizontal for some distance. Evidence to support this location can be seen in seismic lines and well logs within the area.

Due to the nature of roof thrusts, overlying strata is not effected by the deformation below the LAD. The middle Atokan Cecil Sandstone is present above the LAD, and can be seen relatively undisturbed by the underlying deformation. The deformation of Middle Atokan units can be explained by compression stemming from the formation of the Heavener Anticline and Pine Mountain Syncline (Figures 36-38 & Plates 1-3).

Contained within the LAD and Springer Detachment resides numerous southerly dipping faults. These imbricate faults branch from the floor thrust and extend to the roof thrust creating a series of horses. These horses are hinterland-dipping and decrease in size as they propagated forward. Well log analysis shows Atokan strata contained within these individual horses reveal a characteristic anticline-syncline pairing.

Triangle Zone

Within the Summerfield and LeFlore Se Quadrangles, well data and seismic profiles suggests that the triangle zone described in the Wilburton area, in relation to the OCAST project (Cemen and others, 1994, 1995, 1997, 2001; Al-Shaieb and others, 1995; Akthar, 1995 and Sagnak, 1996), continues into this area. However, notable changes have occurred as this zone propagated to the west. As in previous studies, the triangle zone is floored by the LAD, bound to the

south by the Northern Choctaw Fault, and bound to the north by the Carbon Fault.

The nature of the Carbon Fault originates from the LAD. Stress built within the foreland region during the Ouachita Orogeny, eventually obtained enough force in the opposing direction to inhibit further propagation. At this point of zero displacement, a backthrust formed that was foreland-dipping. Within this area, well-log data and seismic profiles Appendices (4, 5 and 6) suggest that the overall displacement of strata by the Carbon Fault is diminishing as it extends east. Even at this diminished level of displacement, the overall effects of the Carbon Fault can be seen via surficial features.

Figures 36 through 38 show that the placement of the Carbon Fault corresponds to the core of the Heavener Anticline. The overall size of the triangle zone increases to the east within the area. This is due to the fact that the Heavener Anticline intersects the Choctaw Fault just west of Summerfield Quadrangle. As the Choctaw Fault extends eastward across the area, it bends in a southeastward direction. The result is an increase in the distance between the boundaries of the triangle zone (Figures 36-38).

Heavener Anticline and Pine Mountain Syncline

Contained within the study area is a prominent anticline-syncline pair. This feature is observable in the landsat image in Figure 39.

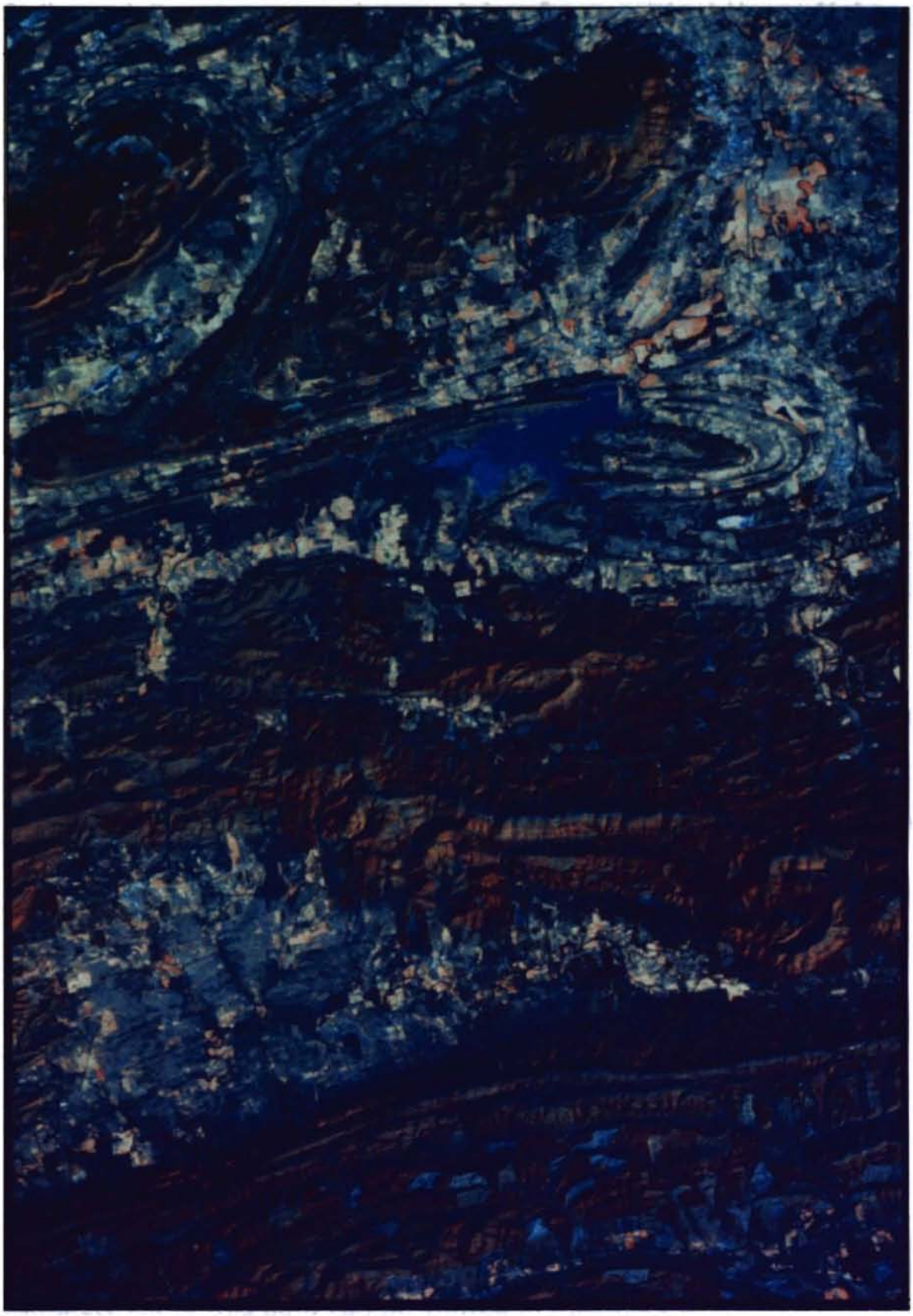

Figure 39. Landsat image of Ouachita Mountains and Arkoma Basin.

Strike and dip measurements were taken from resistant Upper Atokan age sandstone ridges by Hemish and Mazengrab prior to 1992. This raw data was then processed using GeoPlot and RockWorks in order to classify and obtain trends of the features. Forty-eight strike and dip measurements were obtained from both the northern and southern limbs of the Pine Mountain Syncline, and data shows that the Pine Mountain Syncline is an asymmetrically, northwesterly plunging feature. The data is presented in Appendix III. The data was then plotted in order to show placement of the poles on a Lambert Equal Area stereogram and contours assigned in order to graphically represent the data (Figure 40). An S-Pole girdle (π circle) was then placed through the two bedding pole concentrations. This π circle represents the strike and dip of the plane perpendicular to that of the hinge line of the fold (Davis and Reynolds, 1996). With this data, the location of the S-Pole (π-axis) was determined to have a trend of S80°E with a plunge of 12°.

Fault Analysis

In addition to subsurface mapping of faults contained within the area, fault orientations were taken from thrust faults contained within the Summerfield and LeFlore SE Quadrangles. Measurements were taken every 2000 feet on all major thrust faults and splays. A complete list of this data can be viewed in Appendix II.

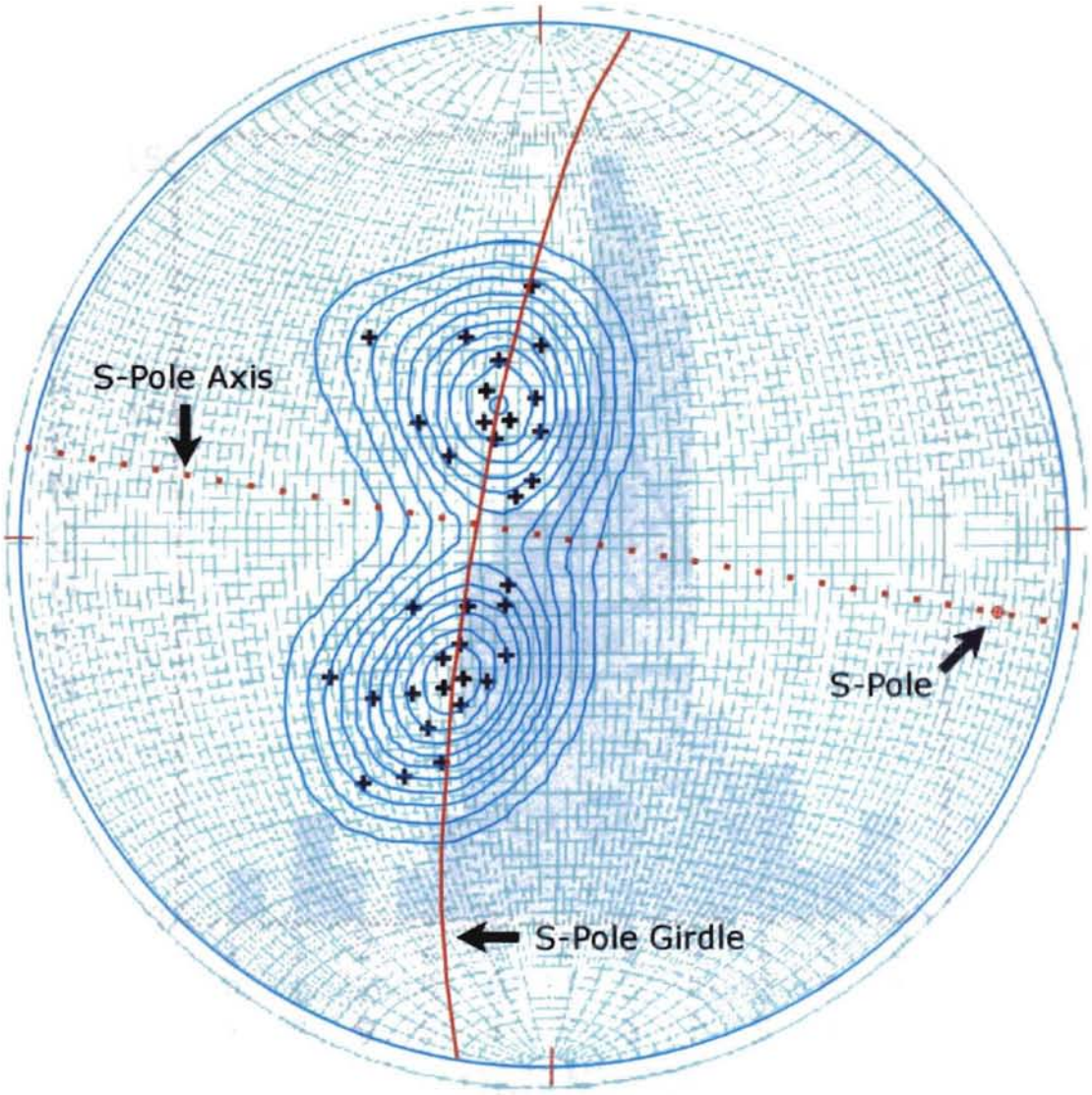

Figure 40. S-Pole diagram depicting trend of the Pine Mountain Syncline within Summerfield Quadrangle.

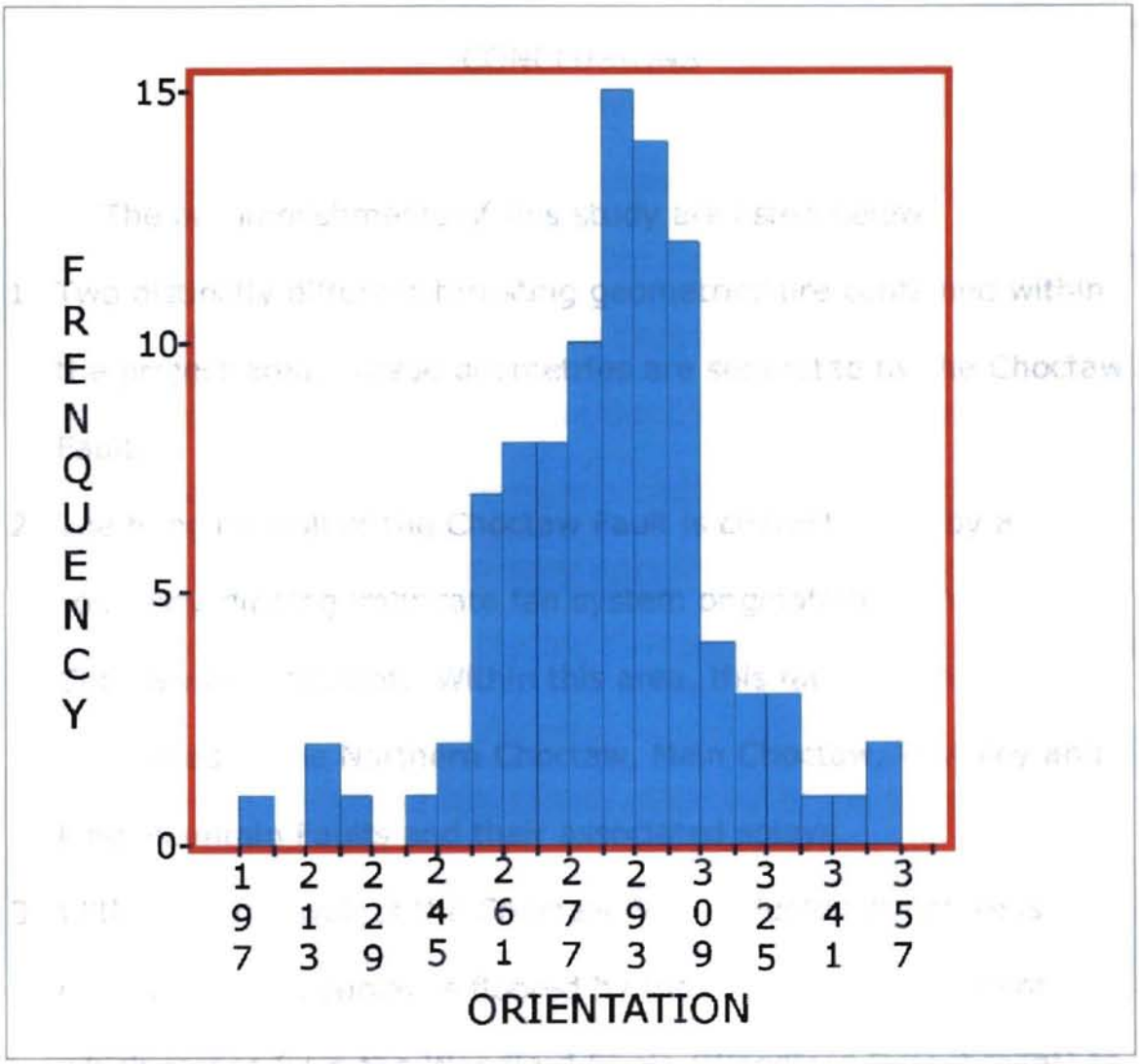

Figure 41. Histogram depicting fault orientation in study area.

CHAPTER VII

CONCLUSIONS

The accomplishments of this study are listed below.

1. Two distinctly different thrusting geometries are contained within the project area. These geometries are separated by the Choctaw Fault.
2. The hanging wall of the Choctaw Fault is characterized by a southerly-dipping imbricate fan system originating from the Choctaw Detachment. Within this area, this fan system is comprised of the Northern Choctaw, Main Choctaw, Ti Valley and Pine Mountain Faults and their associated splays.
3. Within the footwall of the Choctaw Fault a duplex structure is observed. This duplex is floored by the Springer Detachment, which ramps from the Woodford Shale (Woodford Detachment) to the Springer Shale within the central portion of the study area.
4. The roof thrust overlying the duplex structure is called the Lower Atokan Detachment (LAD), and has been delineated from the Wilburton gas-field area. However, the overall orientation and

position of the LAD has changed significantly. Within this area, the overall slope of the LAD has decreased to nearly horizontal and its position is stratigraphically deeper than in the adjoining areas to the west.

5. The leading edge of the Ouachita Fold-Thrust Belt transforms into a triangle zone north of the Northern Choctaw Fault. The triangle zone is underlain by the Lower Atokan Detachment (LAD), bound to the north by the blind, back-thrusted Carbon Fault and to the south by the southerly-dipping Northern Choctaw Fault.
6. The overall area contained within the triangle zone increased from west to east, due to the increase in distance between the Northern Choctaw Fault and the Heavener Anticline. Displacement associated with northerly-dipping Carbon Fault decreases from west to east.
7. The average amount of shortening observed in the Summerfield and LeFlore SE Quadrangles is approximately 43%.
8. The general strike observed of the Heavener Anticline-Pine Mountain Syncline pair is N80°W. Further sterographic analysis of the Pine Mountain Syncline shows the position of the β point to be trending S80°E with a 12° plunge.
9. The lack of hydrocarbons present within the Spiro sandstone can be explained by one of the following: (a) the structural position of the

observed duplex is stratigraphically lower within the area, allowing the hydrocarbons to migrate to the west. (b) The lack of Chamosite (Berthierine) within the subsurface Spiro interval and the presence of glauconite allowed for deterioration of primary porosity. Without the necessary pore space, significant hydrocarbons were unable to accumulate within the area.

WORKS CITED

Akhtar, Saleem, 1995, The Geometry of Thrust Faulting in the Wilburton gas Field and Surrounding, Latimer County, Oklahoma, unpublished M.S. thesis, Oklahoma State University, Stillwater, OK, 97p.

Al-Shaieb, Z., I. Cemen and A. Cleaves, 1995, Overthrusted Natural Gas Reservoirs in the Arkoma Basin, OCAST Project no. AR2-025:4859, OCAST Research and Development Programs Division, 174p.

Al-Shaieb, Z., P. Deyhim, 2000, Chamosite: A key Mineral for Interpretation of the Depositional Environment of the Spiro Sandstone, Oklahoma Geological Survey Circular 103, p. 157-171.

Al-Shaieb, Z., J.W. Shelton, J. Puckette, and D. Boardman, 1995, Sandstone and Carbonate Reservoirs of the Mid-Continent, Oklahoma City Geological Society-Oklahoma State University Core Workshop; Syllabus for Short Coarse, Oklahoma Geological Society, Publishers, p. 59-72.

Boyer, S., and D. Elliot. 1982. Thrust Systems. The American Association of Petroleum Geologists Bulletin: vol. 66, no 9 P. 1196-1230.

Butler, R.W.H. 1987. Thrust Sequences. Journal of the Geological Society, London: vol. 144, p. 619-634.

Cemen, I., Z. Al-Shaieb, A. Sagnak, R. Feller, and S. Akthar, 1994, Preliminary Interpretation of a Seismic Profile and the Spiro Sandstone Reservoir Data in the Vicinity of the Wilburton Gas Field, Oklahoma Geological Society Guidebook 29, p. 249-251.

Cemen, I., Z. Al-Shaieb, A. Sagnak, R. Feller, and S. Akthar, 1997, Triangle Zone Geometry of the Frontal Ouachitas in the

Wilburton Area, Arkoma Basin, Oklahoma: Implications for fault Sealing in the Wilburton Gas Field (Abstract) AAPG Annual Convention Program with Abstracts, p. A-19.

Davis, G.H., and S.J. Reynolds. 1996. Structural Geology, 2nd Edition. John Wiley & Sons, Inc., New York.

Evans, J., 1997, Structural Geometry and Thrust Faulting in the Baker Mountain and Panola Quadrangles, Southeastern Oklahoma: unpublished M.S. thesis, Oklahoma State University, Stillwater, OK, 99p.

Hemish, L.R., 1993, Geology of the Wister State Park Area, LeFlore County, Oklahoma, Oklahoma Geological Survey Guidebook 28, 27p.

Hemish, L.R., and C. Mazengarb, 1992, Geologic Map of the Summerfield Quadrangle, LeFlore County, OK (unpublished): Oklahoma Geological Survey, scale 1:24,000.

Hemish, L.R., and N.H. Suneson, 1989-1990, Geologic Map of the LeFlore SE Quadrangle, LeFlore County, OK (unpublished): Oklahoma Geological Survey, scale 1:24,000.

Hemish, L.R., and N.H. Suneson, 1997, Stratigraphy of the Krebs Group (Desmoinesian), South-Central Arkoma Basin, Oklahoma, Oklahoma Geological Survey Guidebook 30, 84 p.

Houseknecht, D.W., 1986, Evolution of a Passive Margin to a Foreland Basin, south-central U.S.A., in Allen, P.A. and P. Homewood, eds. Foreland Basins: International Association of Sedimentologists Special Publications 8, p. 327-345.

Houseknecht, D.W. and T.A. McGilvery, Red Oak Field, Structural Traps II, Traps Associated with Tectonics, American Association Of Petroleum Geologists Treaties of Petroleum Geology, p. 201-221.

Johnson, K.S. 1988, General Geologic Framework of the field trip area, In Johnson, K.S., ed., Shelf to Basin Geology and Resources of Pennsylvanian strata in the Arkoma Basin and Frontal Ouachita Mountains of Oklahoma: Oklahoma Geological Survey Guidebook 25, p. 1-5.

Jones, P.B., 1984, Triangle Zone Geometry and Terminology (Abstract): Western Canadian and International Expertise, Exploration Update; A Joint Convention of CSEG and CSPG, Calgary, Alberta, 1994, p. 69-70.

Marshak, S. and G. Mitra. 1988. Basic Methods in Structural Geology, Prentice Hall Publishers, Upper Saddle River, NJ.

Meckel, L.D., D.G. Smith and L.A. Wells, 1992, Ouachita Foredeep Basins: Regional Paleogeography and Habitat of Hydrocarbons, in Macqueen, R.W., and D.A. Leckie, ed., Foreland Basins and Fold Belts: AAPG Memoir 55, p. 427-444.

Ronck, J.L., 1997, Structural Geology of Thrust Faulting in the Wister Lake Area of the Frontal Ouachita Mountains, Arkoma Basin, Southeastern Oklahoma, unpublished M.S. Thesis, Oklahoma State University, 111 p.

Sagnak, A., 1997, Geometry of Late Paleozoic Thrust Systems in the Wilburton Area: unpublished M.S. Thesis, Oklahoma State University, 101p.

Suneson, N. H., 1988, The Geology of the Ti Valley Fault in the Oklahoma Ouachita Mountains, in Johnson, K.S., ed., Shelf to Basin Geology and Resources of Pennsylvanian strata in the Arkoma Basin and Frontal Ouachita Mountains of Oklahoma: Oklahoma Geological Survey Guidebook 25, p. 33-48.

Suneson, N. H., 1995, Structural Interpretations of the Arkoma Basin-Ouachita Mountains Transition Zone, Southeastern Oklahoma; A Review: in Johnson, K.S., Editor, Structural Styles in the Mid-continent, 1992 Symposium, Oklahoma Geological Survey Circular 97, p, 259-263.

Suppe, John. 1983, September. Geometry of Kinematics of Fault-Bend Folding. American Journal of Science: vol. 283, p.684-721.

Sutherland, P.K. and W.L. Manger. 1979. Ozark and Ouachita Shelf-to-Basin Transition, Oklahoma-Arkansas, Oklahoma Geological Survey Guidebook 19, 81 p.

Sutherland, P.K., 1982, Lower and Middle Pennsylvanian Stratigraphy, In South-Central Oklahoma, Oklahoma Geological Survey

Guidebook 20, 42 p.

Sutherland, P.K., 1988, Late Mississippian and Pennsylvanian Depositional History in the Arkoma Basin Area, Oklahoma and Arkansas: GSA Bulletin, v. 100, no 11, p. 1787-1802.

Tearpock, D. and R.E. Bischke. 1991. Applied Subsurface Geological Mapping. Prentice Hall Publishers, Upper Saddle River, NJ.

Appendix I

Cross-Section A-A'											
Well No.	**Operator**	**Well Name**	**Loc.**	**Sec.**	**K.B.**	**Total Depth**	**Spiro* 1**	**Spiro* 2**	**Cecil A***	**Cecil B***	**Brazil***
A-1	BTA Oil Producers	8904 JV-P Hollan	5N-23E	20	767'	15117'	13980'	NP	10540'	11350'	8180'
A-2	An-son Corp.	1-21 Nevil	5N-23E	21	603'	16675'	14120'	16275'	10470'	11210'	8390'
A-3	Nearburg Production	1 Wister Lake 16	5N-23E	16	574'	13400'	13100'	NP	9700'	10255'	6120'
A-4	Whitmar Exploration	Buttrill 1-34	6N-23E	34	654'	15216'	15030'	NP	12970'	13610'	9200
A-5	Stephens Production	LeFlore 27-A	6N-23E	27	660'	8861'	NP	NP	NP	NP	NP
A-6	Arco Oil & Gas Co.	J.L. Sheffler Ranch 1	6N-23E	14	798'	6650'	NP	NP	NP	NP	NP

Cross-Section B-B'											
Well No.	**Operator**	**Well Name**	**Loc.**	**Sec.**	**K.B.**	**Total Depth**	**Spiro* 1**	**Spiro* 2**	**Cecil A***	**Cecil B***	**Brazil***
B-1	Amoco Production	Devil's Backbone	5N-24E	31	711'	21019'	16230'	NP	13460'	NP	10990'
B-2	Amer. Quasar of N.M.	S.L. Sutton #1	5N-24E	18	602'	14590'	14430'	NP	?	?	?
B-3	Ark. Louisiana Gas	USA #1	5N-24E	7	510'	12251'	NP	NP	?	?	?
B-4	Max Pray	C.C. Jackson	6N-24E	29	540'	8547'	NP	NP	NP	NP	NP
B-5	Eberly & Meade	Humpervill e	6N-24E	29	545'	3260'	NP	NP	NP	NP	NP
B-6	Horizon Tool & Ser.	1 Noble Thompson	6N-24E	20	598'	14630'	14305'	NP	10730'	NP	8090'
B-7	Mannix Oil Co.	Penelope 1-18	6N-24E	18	627	4220'	NP	NP	NP	NP	NP

Cross-Section C-C'											
Well No.	**Operator**	**Well Name**	**Loc.**	**Sec.**	**K.B.**	**Total Depth**	**Spiro* 1**	**Spiro* 2**	**Cecil A***	**Cecil B***	**Brazil***
C-1	Branscum Petro	Mitchell #1	6N-24E	21	561'	14610'	13500'	NP	10733'	NP	8545'

* denotes top of bed

Appendix II

Number	Fault	Orientation	Direction	Surface_Elevation	Lithologic_Name	Lith_Type
1	a	303	NW	540	Qt	1
2	a	303	NW	570	Qt	1
3	a	303	NW	520	Pa	2
4	a	302	NW	520	Qa	1
5	a	301	NW	525	Qa	1
6	a	299	NW	540	Pa	2
7	a	297	NW	560	Pa	2
8	a	297	NW	580	Pa	2
9	a	282	NW	620	Pa	2
10	a	288	NW	615	Pa	2
11	a	283	NW	605	Pa	2
12	a	280	NW	605	Pa	2
13	a	286	NW	610	Pa	2
14	a	291	NW	640	Pa	2
15	a	290	NW	620	Pa	2
16	a	288	NW	605	Pa	2
17	a	291	NW	560	Pa	2
18	a	291	NW	620	Pa	2
19	a	294	NW	590	Qa	1
20	a	280	NW	600	Qoa	1
21	b	295	NW	680	Pa	2
22	b	226	SW	635	Qa	1
23	b	269	SW	700	Pa	2
24	b	271	SW	595	Pa	2
25	b	255	SW	780	Pa	2
26	b	255	SW	700	Pa	2
27	b	265	SW	700	Pa	2
28	b	266	SW	780	Pa	2
29	b	267	SW	780	Pa	2
30	b	267	SW	750	Qoa	1
31	b	260	SW	740	Pa	2
32	b	275	NW	800	Pa	2
33	b	276	NW	980	Pa	2
34	b	283	NW	1140	Pa	2
35	b	285	NW	850	Pa	2
36	b	300	NW	820	Pa	2
37	b	301	NW	840	Pa	2
38	b	299	NW	900	Pa	2
39	b	295	NW	1010	Pa	2
40	b	302	NW	1020	Pa	2

Appendix II

Number	Fault	Orientation	Direction	Surface_Elevation	Lithologic_Name	Lith_Type
41	c	323	NW	640	Pa	2
42	c	317	NW	650	Pa	2
43	c	300	NW	600	Pa	2
44	c	291	NW	600	Pa	2
45	c	280	NW	555	Qa	1
46	c	271	NW	585	Qoa	1
47	c	279	NW	640	Pa	2
48	c	310	NW	675	Pa	2
49	c	312	NW	700	Pa	2
50	c	309	NW	760	Pa	2
51	c	348	NW	620	Pa	2
52	c	350	NW	685	Qoa	1
53	c	349	NW	640	Pa	2
54	c	340	NW	740	Pa	2
55	c	325	NW	700	Pa	2
56	c	301	NW	740	Pa	2
57	d	286	NW	640	Qa	1
58	d	271	NW	620	Qa	1
59	d	307	NW	640	Qa	1
60	d	308	NW	675	Qa	1
61	d	305	NW	680	Qoa	1
62	d	304	NW	660	Qa	1
63	d	312	NW	690	Qa	1
64	d	299	NW	680	Qa	1
65	d	290	NW	695	Qa	1
66	d	292	NW	700	Qa	1
67	d	290	NW	740	Pa	2
68	d	277	NW	745	Pa	2
69	d	300	NW	735	Qa	1
70	d	292	NW	735	Qa	1
71	d	300	NW	755	Qa	1
72	d	284	NW	790	Qa	1
73	d	284	NW	795	Qoa	1
74	d	294	NW	845	Pa	2
75	d	293	NW	960	Pa	2
76	d	260	SW	950	Pa	2
77	e	240	SW	900	Pa	2
78	e	260	SW	940	Pa	2
79	e	263	SW	1020	Pa	2
80	e	269	SW	980	Pa	2

Appendix II

Number	Fault	Orientation	Direction	Surface_Elevation	Lithologic_Name	Lith_Type
81	e	200	SW	940	Pa	2
82	e	215	SW	840	Pa	2
83	e	218	SW	800	Qa	1
84	e	260	SW	795	Qa	1
85	e	250	SW	840	Pa	2
86	e	261	SW	840	Pa	2
87	e	257	SW	860	Pa	2
88	e	250	SW	900	Pa	2
89	e	326	NW	860	Pa	2
90	e	325	NW	940	Pa	2
91	e	317	NW	1000	Pa	2
92	e	292	NW	1000	Pa	2
93	e	270	NW	900	Pa	2
94	e	268	SW	1010	Pa	2
95	e	267	SW	920	Pa	2

Appendix III

Measurement	Type	Strike	Dip
1	Plane	N75E	20SE
2	Plane	N90E	18S
3	Plane	N60E	20SE
4	Plane	N88E	41SE
5	Plane	N88E	23SE
6	Plane	N90E	30S
7	Plane	N90E	31S
8	Plane	N70E	35SE
9	Plane	N77E	30SE
10	Plane	N70E	35SE
11	Plane	N50E	43SE
12	Plane	N69E	19SE
13	Plane	N50E	42SE
14	Plane	N44E	20SE
15	Plane	N70E	25SE
16	Plane	N45E	27SE
17	Plane	N80E	10SE
18	Plane	N70E	9SE
19	Plane	N65E	21SE
20	Plane	N40W	15NE
21	Plane	N60W	11NE
22	Plane	N48W	8NE
23	Plane	N50W	23NE
24	Plane	N50W	20NE
25	Plane	N32W	40NE
26	Plane	N42W	36NE
27	Plane	N60W	24NE
28	Plane	N25W	22NE
29	Plane	N59W	43NE
30	Plane	N49W	31NE
31	Plane	N62W	35NE
32	Plane	N65W	38NE
33	Plane	N61W	27NE
34	Plane	N59W	34NE
35	Plane	N70W	25NE
36	Plane	N72W	18NE
37	Plane	N68W	23NE
38	Plane	N56W	26NE
39	Plane	N53W	48NE

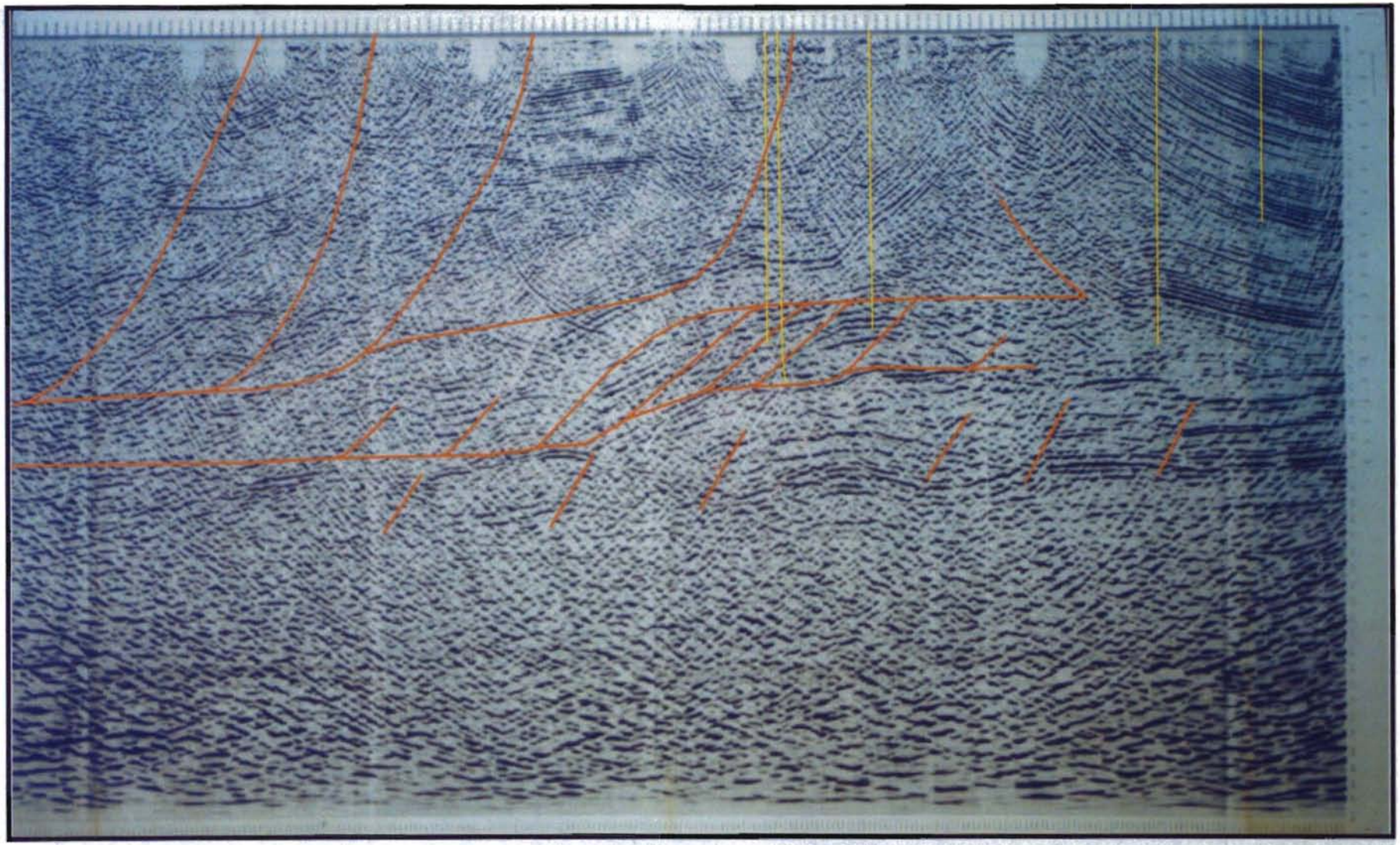

Appendix IV. Interpretation of seismic line QM5-67 for cross-section A-A'.

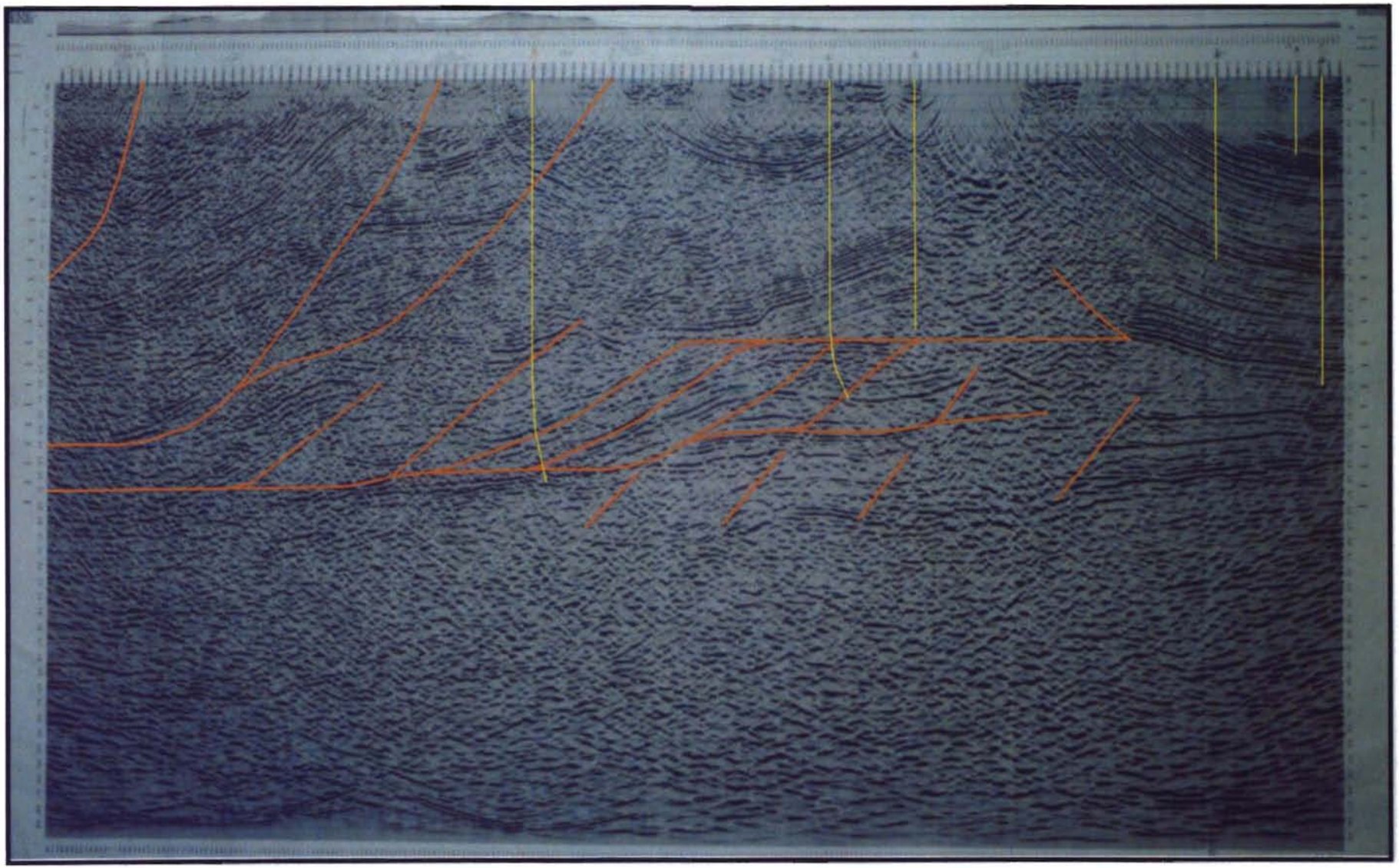

Appendix V. Interpretation of seismic line QM5-58 for cross-section B-B'.

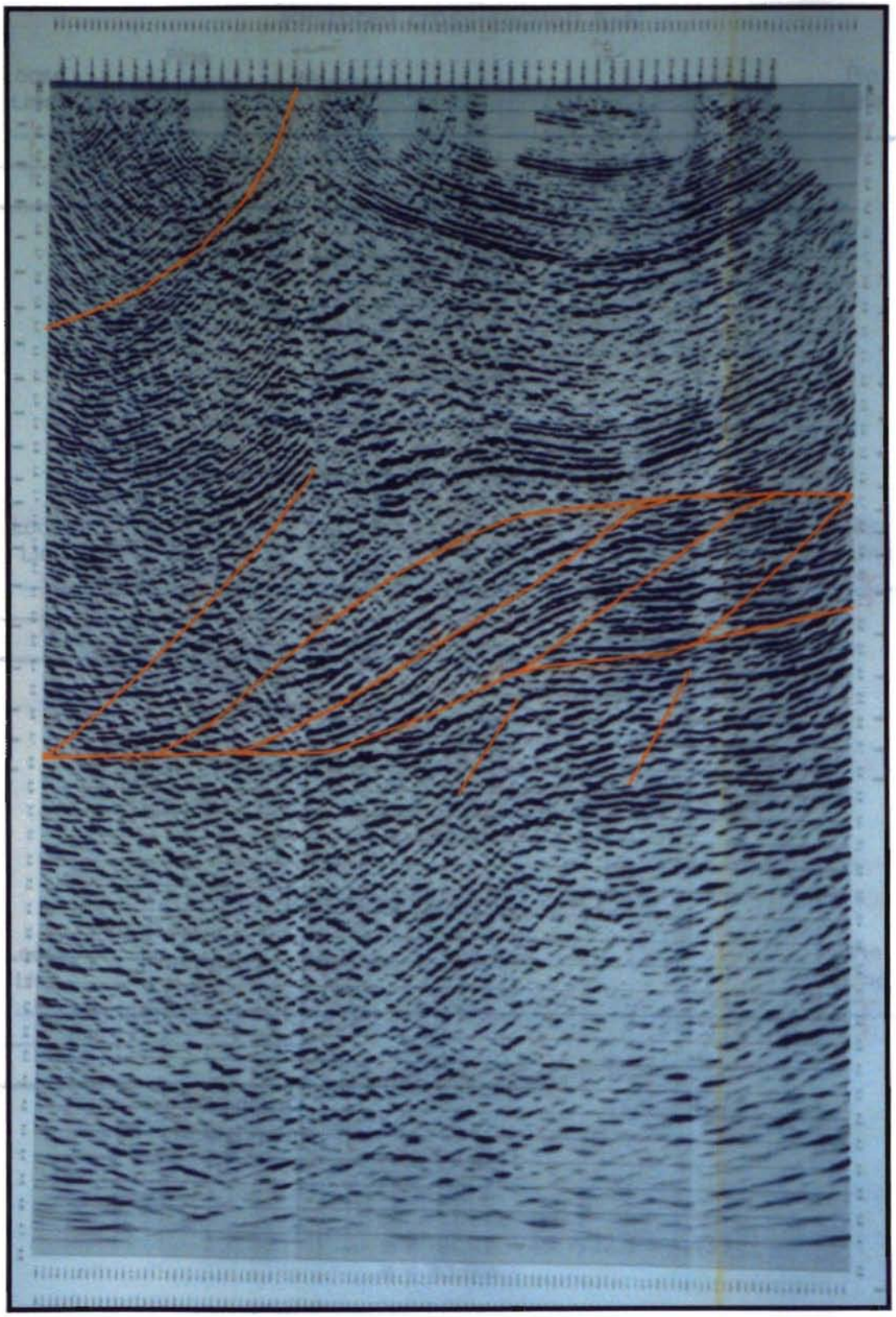

Appendix VI. Interpretation of seismic line QM5-72 for cross-section C-C'.

Restored cross-section A-A'

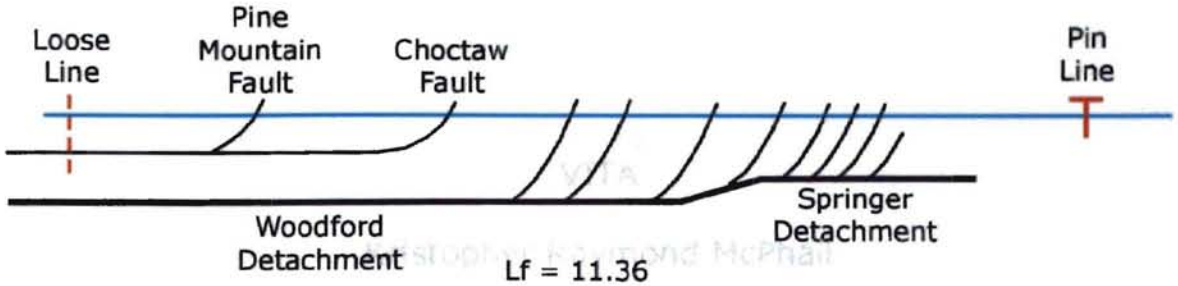

Lf = 11.36
Lo = 19.98
dL = Lf - Lo = -8.62
e = dL/Lo = -8.62/19.98 = -.431
e = 43.1%

Restored cross-section B-B'

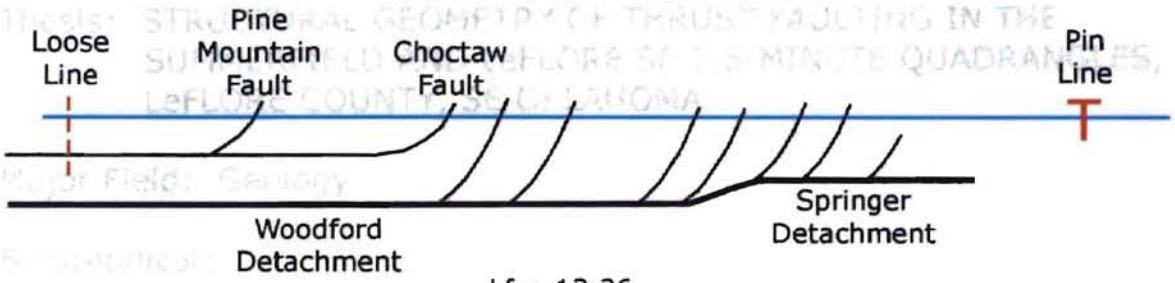

Lf = 13.26
Lo = 23.01
dL = Lf - Lo = -9.75
e = -dL/Lo = -9.75/23.01 = -.424
e = 42.4%

Restored cross-section C-C'

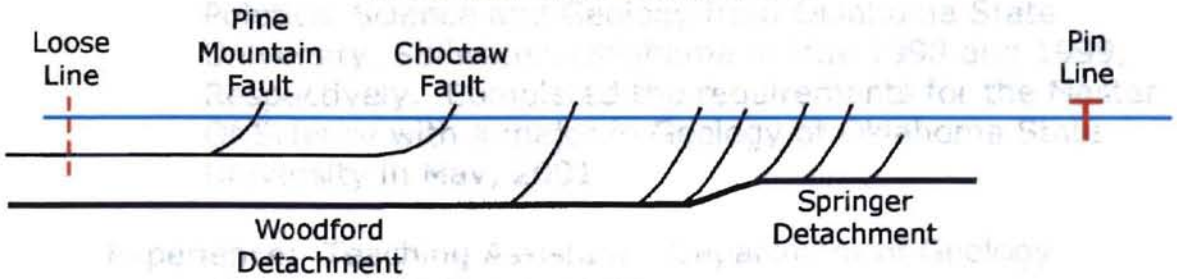

Lf = 12.4
Lo = 22.1
dL = Lf - Lo = -9.7
e = -dL/Lo = -9.7/22.1 = -.439
e = 43.9%

Appendix VII. Restorations of cross-sections A-A', B-B' and C-C'.

PLATES

I, II, and III

Balanced Cross-Section of Seismic Line A- A'

South
34°45′

North
35°00′

1 2 Pine Mtn. 3 Heavener 4 5 6

Syncline Anticline

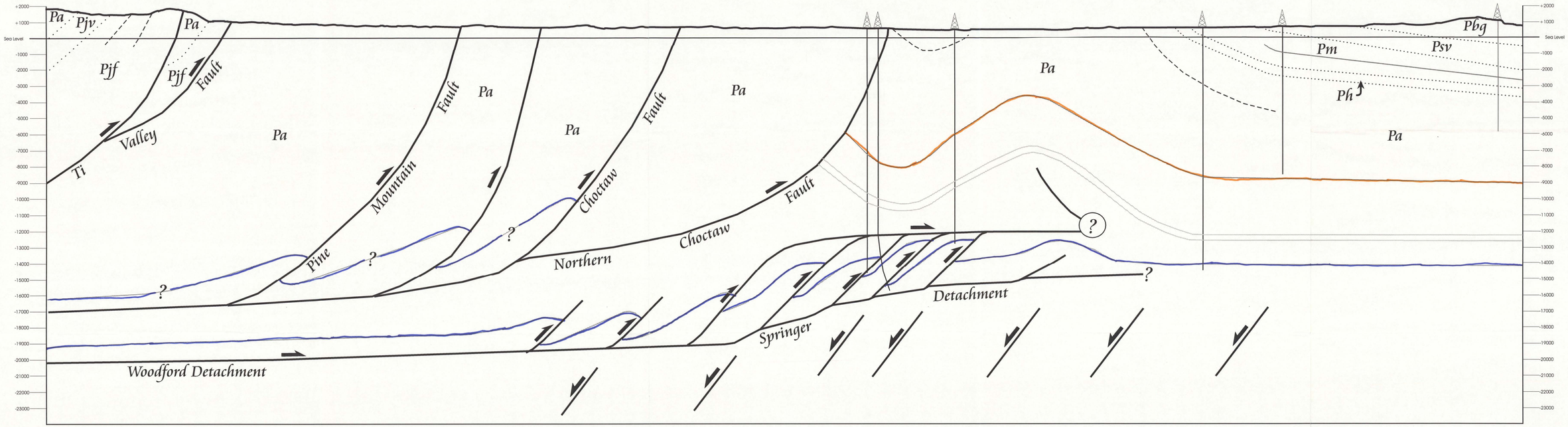

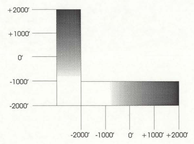

·····	Formation Boundary	Pby Boggy Formation
– –	Marker Bed	Psv Savanna Formation
——	Booch Sandstones	Pm McAlester Formation
		Ph Hartshorne Formation
——	Brazil Sandstone	Pa Atoka Formation
——	Cecil Sandstone	Pjv Johns Valley Shale
——	Spiro Sandstone	Pjf Jackfork Group

1. 8904 JV-P Hollan
   BTA Oil Producers
   20-5N-23E

2. 1-21 Nevil
   An-son Corp.
   21-5N-23E

3. Wister Lake 16-1
   Nearburg Producers
   16-5N-23E

4. Buttrill 1-34
   WhitMar Exploration company
   34-6N-23E

5. LeFlore 27-A
   Stephens Production
   27-6N-23E

6. J L Scheffler Ranch
   Arco Oil and Gas company
   14-6N-23E

PLATE I

Kristopher R. McPhail
School of Geology
Oklahoma State University

Structural Cross-Section of Seismic Interpretation B - B'

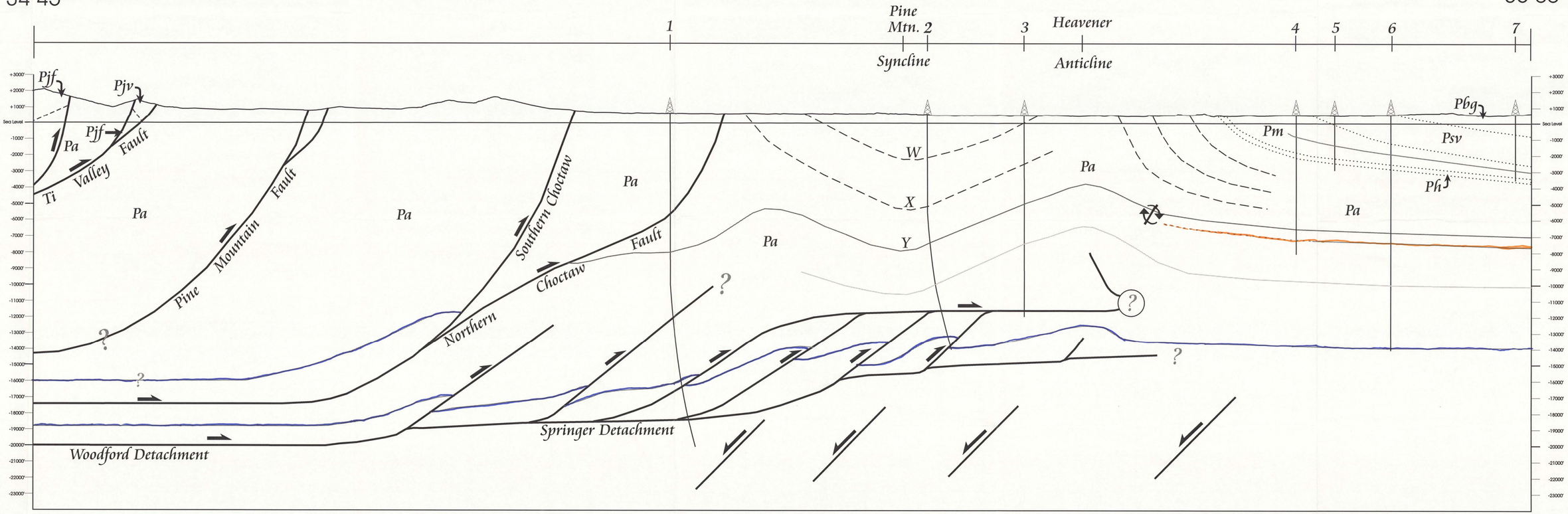

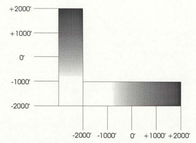

·····	Formation Boundary	Pby	Boggy Formation
– –	Marker Bed	Psv	Savanna Formation
———	Booch Sandstones	Pm	McAlester Formation
———	Marker Y Sandstone	Ph	Hartshorne Formation
———	Brazil Sandstone	Pa	Atoka Formation
———	Cecil Sandstone	Pjv	Johns Valley Shale
———	Spiro Sandstone	Pjf	Jackfork Group

1. Devil's Backbone Unit
   Amoco Production Company
   31-5N-24E

2. S.L. Sutton #1
   American Quasar of New Mexico
   18-5N-24E

3. USA #1
   Arkansas Louisiana Gas Company
   7-5N-24E

4. C.C. Jackson
   Max Pray
   29-6N-24E

5. Humperville
   Eberly and Meade
   29-6N24E

6. 1 Noble Thompson
   Horizon Tool and Service
   20-6N-24E

7. Penelope 1-18
   Mannix Oil Company
   18-6N-24E

PLATE II

Kristopher R. McPhail
School of Geology
Oklahoma State University

Balanced Cross-Section of Seismic Line C - C'

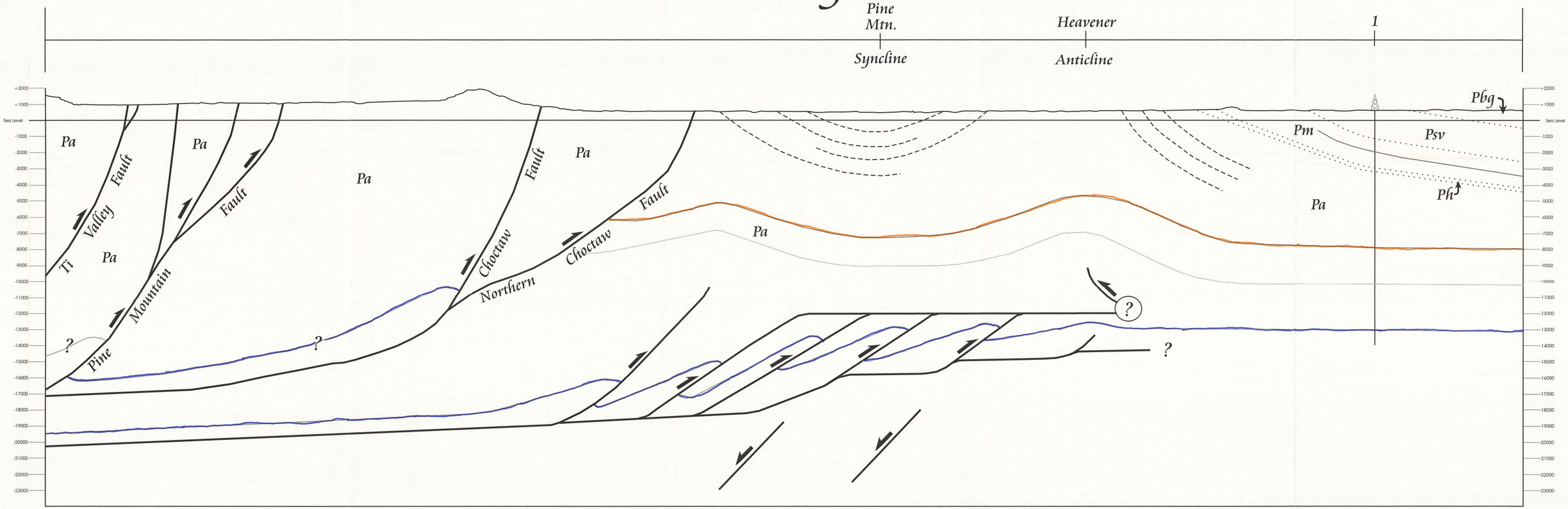

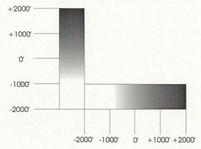

·····	Formation Boundary	Pby Boggy Formation
– –	Marker Bed	Psv Savanna Formation
——	Booch Sandstones	Pm McAlester Formation
		Ph Hartshorne Formation
——	Brazil Sandstone	Pa Atoka Formation
——	Cecil Sandstone	Pjv Johns Valley Shale
——	Spiro Sandstone	Pjf Jackfork Group

1. Mitchell #1
   Branscum Petro
   21-6N-24E

PLATE III

Kristopher R. McPhail
School of Geology
Oklahoma State University

VITA

Kristopher Raymond McPhail

Candidate for the Degree of

Master of Science

Thesis: STRUCTURAL GEOMETRY OF THRUST FAULTING IN THE SUMMERFIELD AND LeFLORE SE 7.5-MINUTE QUADRANGLES, LeFLORE COUNTY, SE OKLAHOMA

Major Field: Geology

Biographical:

Personal Data: Born in Little Rock, Arkansas on April 25, 1973, the son of Treva and Ken McPhail.

Education: Graduated from Bartlesville High School, Bartlesville, Oklahoma in May of 1991; receved Bachelor of Science in Polotical Science and Geology from Oklahoma State University, Stillwater, Oklahoma in May 1998 and 1999, Respectively. Completed the requirements for the Master Of Science with a major in Geology at Oklahoma State University in May, 2001.

Experience: Teaching Assistant: Department of Geology, Oklahoma State University
Summer Internship: Department of the Interior, United States Geological Survey (USGS) Menlo Park, California

Professional Memberships: American Association of Petroleum Geologists (AAPG)